INORGANIC CHEMISTRY
FRONTIERS

REVIEW

View Article Online
View Journal | View Issue

Cite this: *Inorg. Chem. Front.*, 2020, **7**, 3282

Low-temperature wet chemistry synthetic approaches towards ferrites†

Stefano Diodati,[a] Richard I. Walton,[b] Simone Mascotto[c] and Silvia Gross *[a]

Received 9th March 2020,
Accepted 11th May 2020

DOI: 10.1039/d0qi00294a

rsc.li/frontiers-inorganic

Ferrites are a broad class of iron-containing oxides that includes spinel ferrites MFe_2O_4, perovskites $MFeO_3$, and hexagonal ferrites (hexaferrites) such as $BaFe_{12}O_{19}$. These materials have a wide array of applications owing to their diverse properties: notable instances include catalysis, piezoelectric components, magnetic components, biomedical applications, heterogeneous catalysis and photocatalysis. Given the growing importance of environmentally friendly, low-temperature methodologies to obtain functional materials, there is a growing interest in synthetic approaches which are compatible with the principles of "green chemistry". In this context, wet chemistry represents an attractive choice, and furthermore offers the possibility of scale-up for manufacture of materials in volumes for practical application. Though there is a sizeable amount of literature on the synthesis of ferrites, the most common approaches require treatments at temperatures above 200 °C, either as the main synthetic procedure itself (thermal decomposition), or as a post-synthetic step (for example, calcination after sol–gel autocombustion). This review aims at summarising, categorising, classifying and critically discussing the different low-temperature (<200 °C), wet chemistry approaches employed in recent years for the synthesis of ferrites. This will include hydrothermal, solvothermal, sonochemical, and microwave methods, with examples taken from literature making reference to the various sub-classes of ferrites.

Ferrites: a useful and multifaceted class of compounds

Ferrites are a broad class of oxides containing iron which in general include spinel ferrites MFe_2O_4, perovskites, ilmenite ($FeTiO_3$) and hexagonal ferrites (or hexaferrites). These materials have a wide array of applications owing to their diverse properties.[1–10] Notable examples include catalysis,[11–15] piezoelectric components,[16,17] magnetic components,[18–21] biomedical applications[22,23] and photocatalysis,[24–29] photoanodes[30] and photocathodes.[31] In particular, their magnetic properties make them convenient materials for heterogeneous catalysis as they greatly simplify catalyst isolation and recovery operations. In general, the nature of ferrites as iron-containing oxides endows them with important magnetic properties, which vary depending on the specific structure and nature of non-iron metals involved.[32,33] Spinels in particular (due to their specific structure – *vide infra*) have been shown to display both hard ($CoFe_2O_4$)[6] and soft[33] magnetic behaviour, making them very attractive materials in applications ranging from magnetic recording to magnetic resonance imaging (MRI).[6,34,35]

Given the importance of ferrites in a wide variety of fields, numerous works have been dedicated to the synthesis and study of these materials.[1,3,18,33,34,36–46] The present review will, however, focus specifically on wet chemistry methods which not only afford the desired materials, but also comply with the principles of Green Chemistry[47] and can be achieved whilst maintaining low temperatures (≤200 °C) of synthesis, due to the importance for industry to steadily move towards greener and more environmentally friendly approaches (*vide infra* "Green chemistry: the need for low-temperature wet synthesis approaches").

Spinels

In general, spinel ferrites can be described as ferrites having the formula MFe_2O_4, where M is a divalent metal species (such as Fe, Co, Zn, Ni Cu or others).[32,48–51] From a crystallographic point of view, spinel ferrites crystallise in a cubic close-packed structure[32,34] having $Fd\bar{3}m$ symmetry with a unit cell containing 8 formula units ($M_8Fe_{16}O_{32}$).[21,34] In particular, metal ions within this structure occupy 1/8 of the tetrahedral and 1/2 of the octahedral sites.[32,48–50,52] Spinel structures are divided

[a]*Dipartimento di Scienze Chimiche – Università degli Studi di Padova, Via Marzolo 1, 35131 Padova, Italy. E-mail: silvia.gross@unipd.it*
[b]*Department of Chemistry, University of Warwick, Gibbet Hill Road, Coventry, CV4 7AL, UK*
[c]*Institut für Anorganische und Angewandte Chemie, Universität Hamburg, Martin-Luther-King-Platz 6, 20146 Hamburg, Germany*

†Electronic supplementary information (ESI) available: Table summarising examples of hydrothermal syntheses of $BiFeO_3$. See DOI: 10.1039/d0qi00294a

between normal, inverse and partially inverse spinels. In normal spinel ferrites (such as for instance $ZnFe_2O_4$)[53] the trivalent metal (*i.e.* Fe) occupies octahedral sites, whereas the divalent metal ions (Zn) lie in tetrahedral sites (Fig. 1). A second class of spinels are known as inverse spinels (such as $NiFe_2O_4$);[52] in inverse ferrites the iron cations are equally split between tetrahedral and octahedral sites, whereas the divalent atoms occupy in turn the octahedral sites vacated by iron.

A third (much broader) subset of spinels exists where the structure is intermediate between normal and inverse, these are known as partially inverse spinels. In general, therefore, the chemical formula for a spinel ferrite may be written as $[M_{1-i}Fe_i]^{TET}(M_iFe_{2-i})^{OCT}O_4$ where the square and curved brackets labelled TET and OCT represent the tetrahedral and octahedral environments of the ions, respectively and i (where $0 \leq i \leq 1$) is known as degree of inversion (with 0 indicating a normal and 1 indicating an inverse spinel ferrite structure).[52]

This distinction is very important because many of the particular properties which make spinel ferrites such interesting functional materials arise directly from this distribution of metal species over crystal sites.[52,54–58] Many studies have been carried out on how to control the cation distribution in spinels to affect the final properties of the resulting material.[52,54–56,58] While bulk ferrites have a typical degree of inversion, depending on the nature of the M metal, the value of i in nanosized ferrites may vary based upon the synthetic history of the material; in particular, low temperature synthesis may allow access to a different distribution of cations than can be accessed at high temperatures.[54,58–60]

A subclass of spinel ferrites includes more than one metal. These "doped" or "quaternary" ferrites $M_xM'_{1-x}Fe_2O_4$ can therefore take advantage of the properties of both "parent ferrites" (MFe_2O_4 and $M'Fe_2O_4$).[19,42,61–67] Because each M species has its own characteristic electronic structure, the oxides may feature novel or enhanced properties.[68–71]

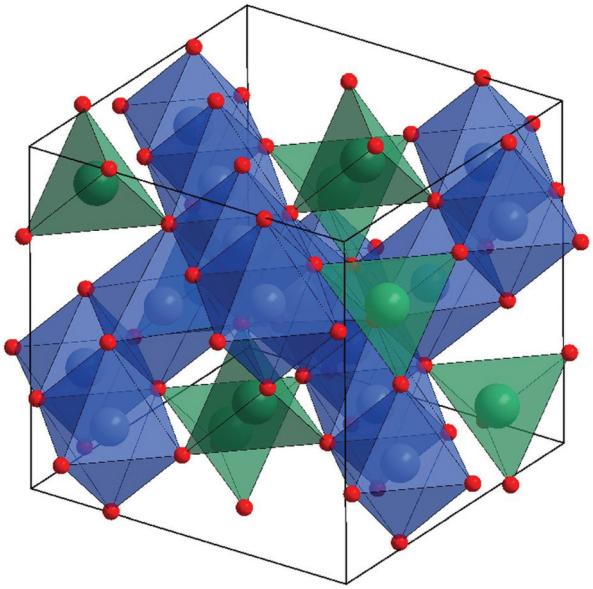

Fig. 1 Crystal structure of normal spinel ferrite $ZnFe_2O_4$ highlighting the octahedral Fe (blue) and tetrahedral Zn sites (green) with red oxide anions.

This great variety of structural and compositional possibilities endows spinel ferrites with a very broad spectrum of magnetic, electric and functional properties,[6,55,56,72–75] making them materials of great interest in a high number of applicative avenues. Nickel and magnesium ferrites have been reported as potential catalysts for water splitting and CO_2 decomposition.[25,76] The magnetic properties of spinel ferrites have furthermore attracted interest in the fields of spintro-

Stefano Diodati

Stefano Diodati is a postdoc fellow in the workgroup of Prof. Silvia Gross. His field of research concerns the synthesis of crystalline inorganic nanostructures (ferrites, oxides, sulphides) through wet chemistry methodologies, with a particular focus on low temperature, green methods such as subcritical hydrothermal synthesis. A further focus of his research is the characterisation of inorganic materials from the compositional (XPS, ICP-MS), structural (powder XRD) and morphological (SEM, AFM) point of view. Most recently he worked on the statistical characterisation of coffee extracts through comparative NMR and other complementary techniques.

Richard I. Walton

Richard Walton is Professor of Chemistry at the University of Warwick and his research group is working in the field of inorganic materials, focussed on the use of innovative synthesis methods for functional solids. This spans zeotypes and metal–organic frameworks through to condensed oxides, with an emphasis on solution-based synthesis routes and characterisation using diffraction and spectroscopy including at synchrotron and neutron facilities. Practical applications are explored and exploited through various industrial collaborations including in areas such as heterogeneous catalysis and ionic conductors. He is presently an editor of the Inorganic Materials Series *published by the Royal Society of Chemistry.*

nics[77] and biomedicine,[78–81] where they can act as either drug carriers or as *foci* for hyperthermia treatments. Spinels have further found applications in the fields of sensors,[82,83] magnetic adsorbers,[21,84] antiparasitic agents[85] and as components for magnetic devices.[86–88]

Perovskites

The ABX_3 perovskite structure is one of the most familiar and versatile found in solid-state inorganic materials.[89] Named for the mineral $CaTiO_3$, the perovskite structure is adopted by many possible combinations of cations (A and B) and anions (X). The A cation adopts coordination number 12 in the ideal cubic perovskite, while the smaller B cation adopts octahedral coordination, such that a three-dimensional network of corner-shared $[BX_6]$ octahedra form a network in which the larger A cations reside, Fig. 2. The versatility in the structure lies in its structurally flexibility: distortions of the structure are possible to accommodate a range of relative ionic sizes, the most common of which are concerted rotations of the corner-shared octahedral to maintain their connectivity, while lowering the coordination number of the A-site cations, Fig. 2b. Another often found distortion is displacement of the B-site cations within their octahedra. This can give rise to polar properties, exploited in ferroelectric devices. For ABO_3 oxides, various combinations of differently charged cations are possible to ensure neutrality: commonly $A^{3+}B^{3+}O_3$, $A^{2+}B^{4+}O_3$ and $A^{+}B^{5+}O_3$. Thus for iron in ferrites, the composition $A^{3+}Fe^{3+}O_3$ is expected to be prevalent, with the expectation that replacement of A^{3+} by A^{2+} may permit partial oxidation of the Fe to the higher +4 oxidation state.

Ferrite perovskites have attracted interest for their various properties and continue to be heavily researched. Magnetic properties have long been studied in this family, in particular

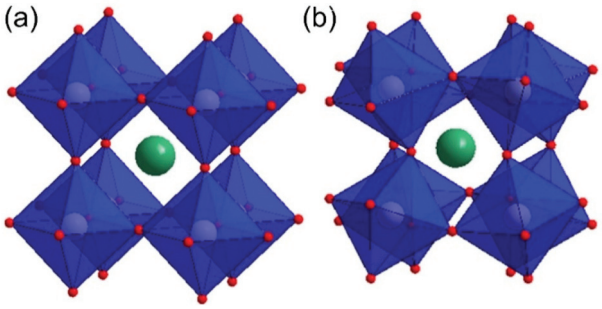

Fig. 2 The ABX_3 perovskite structure (a) view of ideal cubic unit cell with blue $[BX_6]$ octahedral and green 12-coordinate A sites and (b) the distorted orthorhombic unit cell as found for $GdFeO_3$ where the octahedral are tilted with respect to each other.

in the rare-earth ferrites (so-called orthoferrites), where A is a lanthanide or Y^{3+} and B is Fe^{3+}.[90] Depending on the rare-earth cation the materials show complex magnetic behaviour associated with orientation of spins of each of the lanthanide and Fe^{3+} sub-lattices. More recently the interplay of magnetism and polar properties has emerged of being importance.[91] Such multiferroicity and enhanced magnetoelectric coupling in ferrites is exemplified by $BiFeO_3$ that has been the focus of intense investigation in this respect.[92–94] The coexistence of coexistence of ferroelectricity, ferroelasticity, and ferromagnetism in a single phase is of relevance for the development of electronic devices such as in next generation data storage and $BiFeO_3$ shows antiferromagnetism, ferroelectricity and ferroelasticity over a wide temperature range above room temperature. Photocatalysis by $BiFeO_3$ has also been widely studied, due to its band gap being appropriate for solar light activation, and it has been thoroughly investigated for the degradation of organics in solution.[95] The hexagonal ferrite perovskites of the

Simone Mascotto

Simone Mascotto (1981, Trento, Italy) is Assistant Professor of Inorganic Chemistry at the University of Hamburg, Germany. He received a MSc degree in Industrial Chemistry from the University of Padua (2006) and a PhD in Physical Chemistry from the Justus-Liebig-University of Giessen (2009). In 2010–2013 he was a Marie Curie postdoctoral fellow at the University of Trento, Italy and research associate at the Helmholtz-Zentrum Berlin, Germany. His research group focuses on the design of metal oxides with tailored surface properties and on the investigation of surface-related phenomena in nanomaterials by scattering methods at large scale facilities.

Silvia Gross

Silvia Gross is Professor of Inorganic and Colloid Chemistry at the University of Padova and her research group is working in the field of wet-chemistry and colloidal synthesis of different inorganic materials (oxides, sulphides, metal nanoparticles), with particular focus on low temperature and sustainable routes. A relevant part of the activity is devoted to the thorough structural, morphological and chemico-physical characterisation of the materials, also by time-resolved and/or in situ *experiments performed at synchrotron radiation sources. She is DFG Mercator Fellow and regularly visiting professor at the Justus-Liebig University of Giessen. She has authored about 160 ISI papers.*

smaller rare earths (Y, Dy–Lu) have also been recently studied for their multiferroic properties.[96]

Ferrite perovskites have shown promise as heterogeneous catalysts for oxidation reactions, and have been investigated for many years,[97] in applications such as methanol oxidation.[98,99] With an increasing interest and awareness of environmental concerns and the need for effective catalysts for clean combustion and pollution abatement, the materials continue to be developed and optimised for applications. $La_{1-x}Ca_xFeO_3$ materials have been shown to be effective for activation of the combustion of propane and ethanol, which was ascribed to the presence of Fe^{4+}.[100] A systematic study of $AFeO_3$ (A = La, Nd, Sm) and $LaFe_{1-x}Mg_xO_3$ found that the materials gave complete conversion of methane and CO, with a correlation between structural chemistry, chemical composition and activity.[101] More detailed studies of non-stoichiometry in $La_{1-x}FeO_{3-\delta}$ showed that composition dictates activity for hydrocarbon oxidation,[102,103] while others have also suggested that the synthesis method is also important.[104] Wet chemical approaches have been shown to give higher surface area for $LaFeO_3$.[105] This enables $LaFeO_3$ to be used as a support for precious metals to perform effective oxidations.[106,107]

Other recent examples of catalysis applications include $LaFeO_3$ for activating H_2O_2 to oxidise methyl orange,[108] in three-way catalysis for automotive exhausts,[109] for the conversion of CO and NO to dinitrogen,[110] and a titanium-doped $LaFeO_3$ has been used for catalytic wet peroxide oxidation.[111] Electrocatalytic activity towards oxygen evolution in alkaline media has been long studied with ferrites since systematic work on $La_{1-x}Sr_xFeO_{3-\delta}$,[112,113] and has been tuned by exploring structure–property relationships in much more complex solid-solutions.[114] This is of tremendous importance in contemporary applications in rechargeable batteries, fuel cells, and hydrogen production from water splitting.

Other important applications of orthoferrites are as cathode materials in solid-oxide fuel cells: here mixed ionic-electronic conductors are needed, along with catalytic activity for oxygen reduction and thermal expansion that is matched to a solid electrolyte.[115,116] To meet this combination of criteria, substitutions into the parent $LaFeO_3$ perovskite has been extensively studied to tune the electronic structure and to induce oxide-ion vacancies to provide anion conduction pathways. This includes materials co-doped with Sr and Ni, or Co.[117,118] The material $Nd_{0.5}Ba_{0.5}FeO_{3-\delta}$ when doped at the B-site with Cu, Ni or Co has proved to be compatible with proton-conducting electrolytes.[119] Related to this, is recent work that shows how the oxygen non-stoichiometry in ferrites can be used for thermochemical air separation, making use of their intrinsic oxygen storage capacity, such as in $SrFe_{0.95}Cu_{0.05}O_{3-\delta}$,[120] or the parent $SrFeO_{3-\delta}$.[121]

Hexagonal ferrites

The ABX_3 composition is found in other structure types, which are often labelled as perovskites, but these do not have the essential feature of solely corner-shared octahedral $[BX_6]$ units. For example, Fig. 3a and b shows the structure of an example of a so-called 'hexagonal perovskite' that contains layers of corner-linked $[BX_6]$ trigonal bipyramids, separated by layers of A cations.[122] This structure is found for some ferrites, notably ferrites of the small rare-earth cations, as will be discussed below.

A second important type of hexagonal ferrite are the 'hexaferrites' exemplified by the barium iron oxide $BaFe_{12}O_{19}$. This phase, known as the M-type hexaferrite, has a structure containing iron in three distinct coordination environments, octahedral, tetrahedral and pyramidal, Fig. 3c. More complex hexaferrite structures are known, such as the Y-type $Ba_2Me_2Fe_{12}O_{22}$, where Me is a divalent metal cation, and the family is further diversified by stacking of M-type, Y-type and spinel motifs.[36]

The hexaferrites have long been studied for their magnetism, which find widespread technological used in hard permanent magnets in applications such as magnetic recording and data storage materials, but they are also now used as components for mobile and wireless communications at microwave per GHz frequencies, and in electromagnetic wave absorbers.[1] Recent interest has been focussed on the formation of composite materials based on hexaferrites, such as with polymer matrices, and for this purpose fine powders of the oxides are needed that can be suitably surface modified.[123]

Green chemistry: the need for low-temperature wet synthesis approaches to ferrites

From a functional and applicative point of view, ferrites are becoming increasingly relevant. As outlined at the beginning of this review, new application avenues have been disclosed in an endeavour to enhance both the economic and the environ-

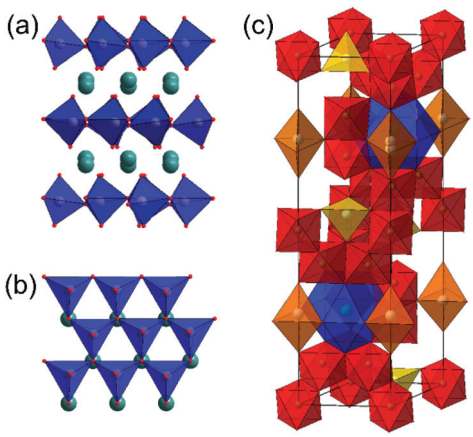

Fig. 3 Example of hexagonal ferrites (a) and (b) shows the ABO_3 hexagonal layered perovskite structure as found for $YbFeO_3$ ($YMnO_3$ type), where $[BX_5]$ trigonal bipyramids are shown in blue and layers of A cations are the green spheres: (a) view showing stacking of layers and (b) a view perpendicular to the layers. (c) shows the unit cell of the hexaferrite $BaFe_{12}O_{19}$ with three distinct iron environments: octahedral (red), tetrahedral (yellow) and pyramidal (orange) and 12-fold coordination sites for Ba (blue).

mental sustainability of synthetic approaches, thus also complying with one of the most relevant out of the 12 paradigms of Green Chemistry:[47] lowering processing time and temperature, which would allow to pursue the goal of reducing energy consumption, a goal which in turn represents one of the major targets in designing future sustainable syntheses of materials.

Lowering temperatures necessarily requires a turn to wet chemistry and solution-based routes, since temperatures below 200 °C are not sufficient to reach the activation energy required for solid state reactions, grain coalescence and coarsening, and eventually the initiation of crystallisation in solid state. In wet-chemistry routes, the limit imposed by the boiling point of the used medium or solvent inherently helps maintain milder synthesis conditions. Despite some exceptions (*e.g.* polyol synthesis[124] and the Pechini[125] method), most of the currently used wet chemistry routes affording the crystallisation of inorganic nanostructures are carried out at temperatures ranging from room temperature (*e.g.* mini- and microemulsion, biogenic synthesis, radiolysis, sonolysis, laser ablation, microfluidics) to 150–200 °C (sol–gel, hydro- and solvothermal, coprecipitation), only rarely exceeding them. There is still space for improvement: the experimental set-up can be optimised to increase the efficiency of the heat and mass transfer during the synthesis, as well as to reduce heat losses, making the overall process more energy efficient.

It should however be pointed out that lowering the synthesis temperature, is not the only relevant aspect involved in reducing the energy consumption: decreasing the processing time, *i.e.* the time for which energy must be provided to the reaction system, is also of paramount important. A systematic optimisation of the experimental landscape is needed for this aspect as well. A recent work by some of us[126] has shown how the crystallisation of ferrites by an already established hydrothermal approach,[127] relying on heating a suspension of oxalates at 135 °C for 24 h, could be also achieved by heating for only 1 to 3 hours (depending on the nature of the involved divalent metal cation), which implies a reduction in energy consumption, all other conditions being equal, by a factor of 24 to 8. In this work, the crystallisation of the targeted ferrites was followed, in a time-resolved fashion, by using different analytical tools sensitive to different range orders, from local/atomic (XAS, XPS) to long range (XRD, SAXS) to macroscopic scale (TEM, SEM). It could furthermore be pointed out that the nucleation and growth of the final nanostructures occurs within a very limited time frame, and no further growth occurs by increasing the heating period.

Hydro/solvothermal approaches to ferrites

The term hydrothermal refers to the use of water as a reaction medium when heated to above its boiling point in a sealed vessel. Under these conditions, autogeneous pressure is produced, and the combined role of increased temperature and pressure in the synthesis and crystallisation of solids has been long studied.[128,129] It is already known how under these conditions, physical properties of water, such as viscosity, ionic product and dielectric constant, change significantly at high pressure and temperature thus enabling solubilisations, crystallisations and, possibly, chemical reactions that would not occur under normal conditions. This is particularly the case once the supercritical point is exceeded (for water T_c = 647.14 K and p_c = 22.06 MPa), but even so most hydrothermal reactions currently reported use milder conditions. The term solvothermal, later coined by Demazeau,[130–132] encompasses all possible solvents, with their differing boiling points, viscosities and dielectric constants, and this method widened the use of solution chemistry to allow access to a larger range of materials. These solution-based routes to solids originally developed from studies of the formation of minerals in the Earth's crust and led to synthetic silicates, exemplified by the zeolites.[133] The growth of large crystals of a range of materials has benefitted from hydrothermal chemistry,[134] and more recently attention has turned to the formation of polycrystalline powders of condensed solids that would usually be prepared using the high temperatures associated with solid-state chemistry.[135–141] The ongoing use of hydrothermal chemistry is also driven by the discovery of new materials, with compositions and structure types not seen by other preparative routes, and that may be metastable under conventional synthesis conditions,[142] as well as control over crystal form over length-scale from nanometres upwards.[143] The key feature of the hydro/solvothermal method is that synthesis and crystallisation of a materials occurs in a single reaction, directly from solution, with no second step of annealing or calcination need to induce the formation of the desired phase. This then means that intricate crystal forms can be isolated, or metastable atomic-scale structure and polymorphs, that would otherwise transform or collapse at elevated temperature. Most solvothermal chemistry for materials synthesis is performed under rather mild conditions, with maximum temperature of around 250 °C, so the pressure generated is not high (typically ten times atmospheric pressure) and arguably not an important synthetic parameter, but under these conditions reagents that would otherwise be insoluble are solubilised to some extent (often with the aid of a mineraliser) to bring about crystallisation from homogeneous solution or to mediate heterogeneous reactions. While some authors report the use of solvothermal chemistry as a processing step, which is followed by a high temperature annealing rather like sol–gel chemistry, in the following sections we will focus on true solvothermal synthesis, where the advantages outlined above are at play. We have chosen examples of materials to show the versatility of the hydrothermal method: this includes a range of chemical compositions and also materials whose properties have been characterised for practical applications.

Solvothermal routes to perovskites

In this section we will review the solvothermal crystallisation of $AFeO_3$ materials, where A = a large trivalent cation. In terms

of ferrite perovskites, much work has been done on the hydrothermal crystallisation of $BiFeO_3$, which has been the focus of attention for its multiferroicity and, more recently, its photocatalytic properties.[95] There are numerous published reports of the one-step hydrothermal crystallisation of the solid in the past 12 years, and many examples are summarised in Table S1 (ESI),† which contains selected examples of the published work on this chemistry. Chen *et al.* in 2006 pioneered this work, reporting the phase-pure synthesis of $BiFeO_3$ as submicron crystallites from aqueous 4 M KOH.[144] The same year, Han *et al.* reported that, along with $BiFeO_3$, two further bismuth ferrites could be selectively synthesised as phase-pure powders: the sillenite-structured $Bi_{12}Fe_{0.63}O_{18.945}$ (close to the ideal composition $Bi_{25}FeO_{40}$) and $Bi_2Fe_4O_9$.[145] As well as phase selectivity the crystal morphology could be adjusted by temperature and/or pH as shown in Fig. 4. This illustrates the complexity in hydrothermal synthesis if competing phases form from a given set of reagents and shows how optimisation of conditions may be necessary to obtain a desired phase as a pure material.

Li *et al.* later tuned the crystal form of $BiFeO_3$ on the micron-scale by choice of pH and introduction of a polymer (polyethylene glycol) to the synthesis, as shown in Fig. 5.[146]

Table S1 in ESI† shows the frequent observation of competing sillenite $Bi_{25}FeO_{40}$ and $Bi_2Fe_4O_9$ materials in the hydrothermal synthesis of $BiFeO_3$. The formation of these may depend on the Bi : Fe ratio used in the synthesis, but Cai *et al.* proposed that $Bi_{25}FeO_{40}$ is formed early in the hydrothermal

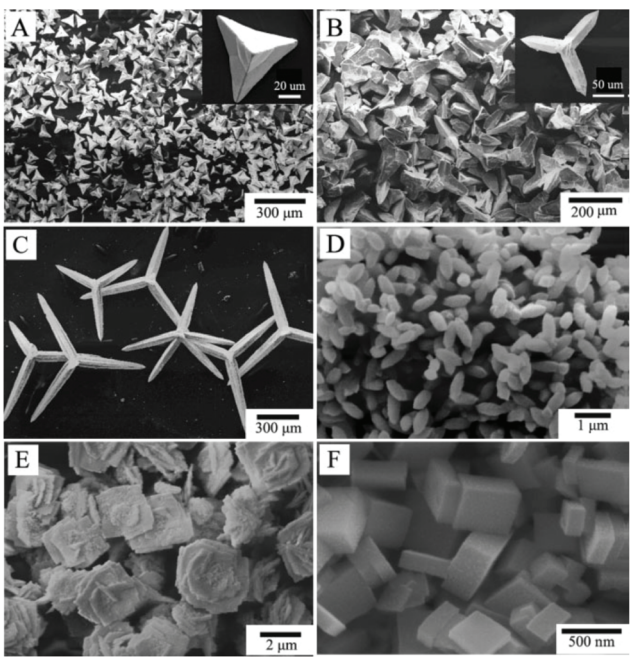

Fig. 4 SEM images of bismuth ferrites prepared by hydrothermal synthesis (A) $Bi_{12}Fe_{0.63}O_{18.945}$ (pH ~ 12, heating temperature, 180 °C); (B) $Bi_{12}Fe_{0.63}O_{18.945}$ (pH ~ 10, 180 °C); (C) $Bi_{12}Fe_{0.63}O_{18.945}$ (pH ~ 8, 180 °C); (D) $BiFeO_3$ (200 °C); (E) $Bi_2Fe_4O_9$ (180 °C); (F) $Bi_2Fe_4O_9$ (270 °C). Reprinted with permission from Han *et al.*[145]

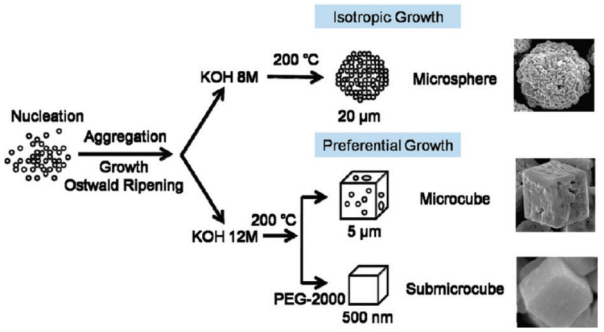

Fig. 5 Crystal morphology control of $BiFeO_3$ proposed by Li *et al.* and reproduced with permission.[146]

reaction and reacts further to give the perovskite product; in their case, the stabilisation of the sillenite was aided using polyvinylalcohol as an additive in solution.[147] Lopes *et al.* performed a detailed study that supported this view, showing that $Bi_{25}FeO_{40}$ could be formed at room temperature, and then under hydrothermal conditions was formed at short reactions times before the emergence of $BiFeO_3$.[148]

While most of the work on $BiFeO_3$ has used hydrothermal conditions (*i.e.* water as solvent) there is some evidence how the presence of a secondary solvent can influence the crystallisation and hence form of the products. For example, Chen *et al.* found that the addition of acetone lowered the synthesis temperature,[149] while Zhang *et al.* found that addition of polyvinylpyrrolidone in ethanol lead to the assembly of primary crystallites into a hierarchical structure of micron diameter rods.[150]

Hou *et al.* performed hydrothermal synthesis of $BiFeO_3$ in an applied magnetic field and found that with increasing field strength up to 12 T the crystallite size decreased from 40 μm to 20 μm and at 12 T chain-link agglomerates of the primary particles were formed, Fig. 6.[151] The subsequent magnetic response of the materials was improved for the samples pre-

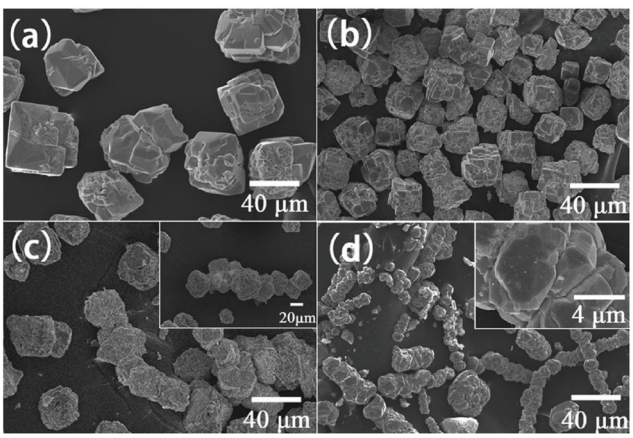

Fig. 6 SEM images of $BiFeO_3$ obtained by hydrothermal synthesis at 200 °C with 8 M KOH for 6 h in various magnetic fields: (a) 0 T; (b) 4 T; (c) 8 T and (d) 12 T. Reproduced with permission from Hou *et al.*[151]

pared in-field: magnetisation measured under a 1.8 T magnetic field was enhanced from 0.1003 emu g^{-1} (0 T) to 0.2067 emu g^{-1} (12 T).

The hydrothermal method can be used to crystallise films of oxides on suitable substrates and in the case of $BiFeO_3$, Huang *et al.* showed how epitaxial growth of the material on orientated surfaces of $SrTiO_3$ was possible to give micron-thick films with favourable dielectric properties.[152] This is important for the fabrication of electronic devices, but annealing is necessary to remove and achieve the dielectric properties expected for the material.

Substitutional chemistry of $BiFeO_3$ using hydrothermal crystallisation is also possible in one-step hydrothermal reactions, and this has been done to tune dielectric and ferromagnetic properties. The advantage of the solution mediated reaction is a high homogeneity of atomic mixing, which by solid-state synthesis often requires repetitive cycles of grinding and heating to achieve. Lanthanum-doped $BiFeO_3$ materials, $Bi_{1-x}La_xFeO_3$ with x up to 0.3 have been reported from hydrothermal reactions, with enhanced ferromagnetic and dielectric properties over the parent material,[153,154] whilst using microwaves as the heating source allowed rapid synthesis of materials with even higher lanthanum content.[155] Replacement of Bi^{3+} by Ba^{2+} is also possible,[156] while co-doping with both Ca^{2+} and Sm^{3+}, leads to oxide-ion vacancies as seen by XPS, which may be responsible for the high temperature dielectric anomalies observed in the material.[157]

The extensive work on the hydrothermal synthesis of $BiFeO_3$, clearly illustrates its ease of implementation over a range of pH, temperature, reaction time, with some choices of reagents possible. In contrast, hydrothermal synthesis of rare-earth (lanthanide, yttrium or scandium) ferrites has received comparatively less attention. Yoshimura and co-workers reported in the 1980s that the hydrothermal synthesis of $LaFeO_3$ required temperatures above 300 °C from lanthanum oxide and hydrated iron oxide in KOH solution, with optimum temperature 450–500 °C.[158] This has been verified by Adschiri and co-workers.[159] More recent work has shown how additives in solution can bring about hydrothermal crystallisation of $LaFeO_3$ from nitrate precursors KOH solution at around 250 °C. The additives include sodium carbonate,[160] urea,[161,162] and while others have used citric acid, although a second step of calcination at 800 °C is needed in those cases to crystallise the materials, so these are not strictly hydrothermal reactions but more akin to a co-precipitation.[163,164] Interestingly, the rare-earth ferrites of other lanthanides are more readily synthesised: this includes those of all of the elements Pr–Lu (except Pm) that crystallise at 240 °C from KOH in 24 hours without any need for extra mineralisers or additives; the materials are highly crystalline and have magnetic properties that match those prepared by conventional solid-state synthesis.[165–169] In the case of $YbFeO_3$, the choice of mineraliser, KOH, NaOH, or mixtures of, was shown to influence crystal morphology, which was rationalised by considering the interaction of solution cations with the growing phases of the crystallites: as shown in Fig. 7, one effect is to adjust the aspect ratio of the cuboid crystals that are formed.[170] B-Site doping has also proved possible in the series $LaFe_{1-x}Cr_xO_3$ ($0 \leq x \leq 1$)[171] and $REFe_{0.5}Cr_{0.5}O_3$ (RE = La, Tb, Ho, Er, Yb, Lu and Y)[172] prepared directly from hydrothermal solutions at 240 °C in aqueous KOH and their magnetic and ferroelectric properties shown to be highly dependent on composition. Similarly, the series $GdFe_{1-x}Cr_xO_3$ ($0.1 \leq x \leq 0.9$) has been prepared and characterised.[173]

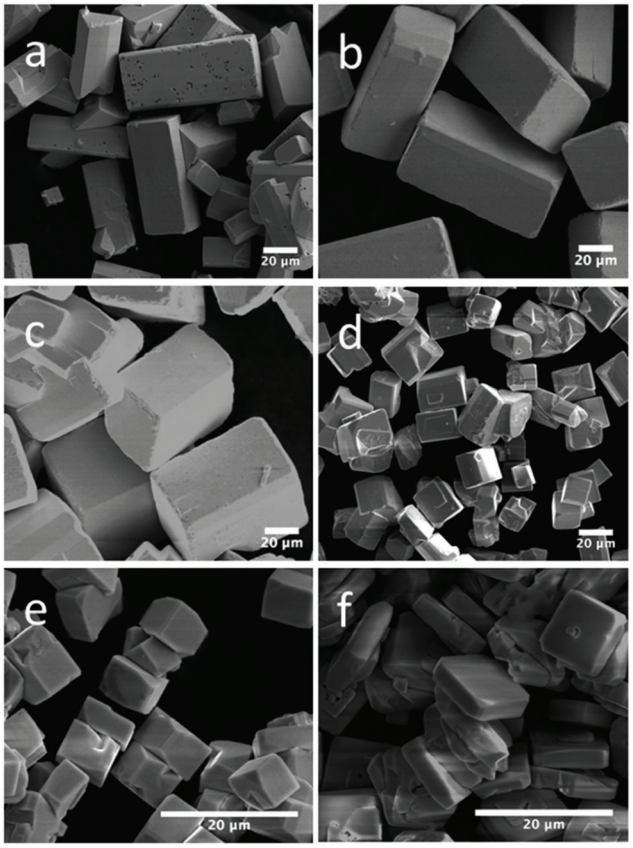

Fig. 7 SEM images of orthorhombic $YbFeO_3$ with NaOH/KOH mixed mineraliser: (a) 25 M/0 M; (b) 20 M/5 M; (c) 15 M/10 M; (d) 10 M/15 M; (e) 5 M/20 M; and (f) 0 M/25 M. Reproduced with permission from Zhang *et al.*[170]

The rare-earth ferrite $YFeO_3$ also crystallises directly from solution and although some groups have reported that higher temperatures of 300 °C are needed,[174–176] others have used 240 °C and concentrated KOH.[177] The fact the some of the rare-earth orthoferrites require high temperature (supercritical) hydrothermal conditions or the use of additives is not understood at present. Feng and co-workers proposed that the role of urea as additive was to release NH_4^+ into solution where it interacted with the growing faces of the perovskite crystals.[161,178,179] Further work is needed to prove this hypothesis and to understand properly the kinetics and mechanism of crystal growth of perovskites from hydrothermal solutions.

For the smaller rare-earth cations, a hexagonal perovskite structure is also possible (see Fig. 3 above) and this may be accessed using solvothermal synthesis selectively over the

orthorhombic polymorph. For example, the reaction between rare-earth (RE) acetates (RE = Tm–Lu) and iron acetylacetonate in 1,4-butanediol at 300 °C gave hexagonal $REFeO_3$ materials consisting of submicron particles.[180] Upon subsequent calcination, the hexagonal phases irreversibly transformed into the perovskite phase at around 980 °C. This is an important example of how the use of mild synthesis conditions allows accessible to a metastable polymorph that cannot be stabilised at high temperature by classical solid-state synthesis. In the case of $YbFeO_3$, the solvothermal reaction between Yb chlorides and iron acetylacetonate in 1,4-butanediol in the presence of 1,6-hexanediamine yielded the orthorhombic perovskite $YbFeO_3$, in contrast to the hexagonal polymorph prepared using the prior method.[181,182]

As well as the perovskites, it is here worth mentioning that $FeTiO_3$, the mineral ilmenite, can be prepared *via* hydrothermal synthesis. Although having a perovskite-like composition, this material has a trigonal corundum structure with alternating layers of octahedral Fe^{2+} and Ti^{4+}. Guan *et al.* prepared hexagonal plates of $FeTiO_3$ hydrothermally and tested their electrochemical and catalytic properties,[183] Zhang *et al.* prepared various morphologies at 180 °C, depending on reaction time and solution pH, and demonstrated shape-dependent photocatalysis for the degradation of an organic dye,[184] Aparna and Sivasubramanian used a urea-aided hydrothermal method to prepare hexagonal plates (300 nm diameter) that could be as electrochemical sensors for dopamine,[185] and Palanisamy *et al.*, prepared nanoflower-shaped particles that were tested as a catalyst for electrochemical CO_2 reduction.[186] Tao *et al.* used a different approach for preparing $FeTiO_3$ nanostructures, by ball milling commercially available $FeTiO_3$ followed by hydrothermal treatment.[187,188]

Hydro/solvothermal approaches to spinels

In this section we will consider spinels consisting of divalent cations in combination with trivalent Fe. The spinels MFe_2O_4 (M = Mn, Co, Ni, Cu, Zn, Mg) are the most widely studied and form readily under hydrothermal conditions. Early work in the 1970s by Swaddle and co-workers used hydroxides and oxides as precursors in alkali solutions up to 350 °C.[189] Milder condition are in fact needed when metal salts are used and these can give fine powders directly from solution at 150 °C, or lower.[190] There are many examples of hydrothermal formation of such spinels and some selected examples will be chosen to illustrate the control that can be achieved in synthesis. Rath *et al.* prepared nanoparticles 9–12 nm in size of $Mn_{0.65}Zn_{0.35}Fe_2O_4$ from chloride precursors in ammonia solution at 180 °C: pH above 10 was optimum and the precipitation of an iron hydroxide before reaction with the other metal salts was found to be necessary to isolate the quaternary oxide.[191] The work was extended to other compositions $Mn_{1-x}Zn_xFe_2O_4$ ($0 \leq x \leq 1$), and the nano-sized materials were found to have a different distribution of cations over tetrahedral and octahedral sites than after annealing, as evidenced by irreversible changes in magnetic response after heating above 300 °C;[192] this illustrates how the hydrothermal synthesis can allow access to metastable polymorphs of materials, not accessible by high temperature synthesis. Xia *et al.* prepared similar materials from nitrate salts in NaOH solution and found that only with higher Zn content could Fe_2O_3 impurities be avoided,[193] while Nalbandian *et al.* used careful pH control to prepare homogeneous nanocrystalline powders, Fig. 8, that had low sintering temperatures to allow the formation of dense, fine-grained microstructures for practical application.[194] $Ni_{0.5}Zn_{0.5}Fe_2O_4$ can also be prepared at a low temperature of 120 °C.[195]

Nanorods of $MnFe_2O_4$ were prepared using pre-made nanorods of Mn_2O_3, demonstrating how the form of solid-state precursors might be used to direct the formation of desired morphology of multi-metal oxide *via* hydrothermal chemistry.[196] It should be noted that $MnFe_2O_4$ could also be prepared as nanorods directly from metal chlorides treated hydrothermally in sodium hydroxides solution,[197] suggesting that further work is needed to understand crystal growth mechanism.

The use of microwave heating for the hydrothermal synthesis of the spinels $Co_{1-x}Zn_xFe_2O_4$ and $Ni_{1-x}Zn_xFe_2O_4$ (x = 0, 0.3, 0.5, 0.7, 1) was shown to be an effective way to give 10 nm diameter crystallites in reactions as short as 10 minutes.[64]

Nanocrystalline $Cu_{1-x}Co_xFe_2O_4$ ($0 \leq x \leq 1$) samples were prepared hydrothermally, aided by the surfactant cetyltrimethylammonium bromide (CTAB), and studied for catalysis of the nitration of toluene: the materials with equal amounts of Cu and Co were most active and allowed the regioselective formation of 1,4-dinitrotoluene.[198]

Tiano *et al.* developed a general hydrothermal approach to MFe_2O_4 for M = Mg, Fe, Co, Ni, Cu, and Zn, from simple metal salt precursors in NaOH solution from which crystallite size and shape could be controlled by addition of surfactants.[199] This allowed access to materials with crystallite sizes of just a

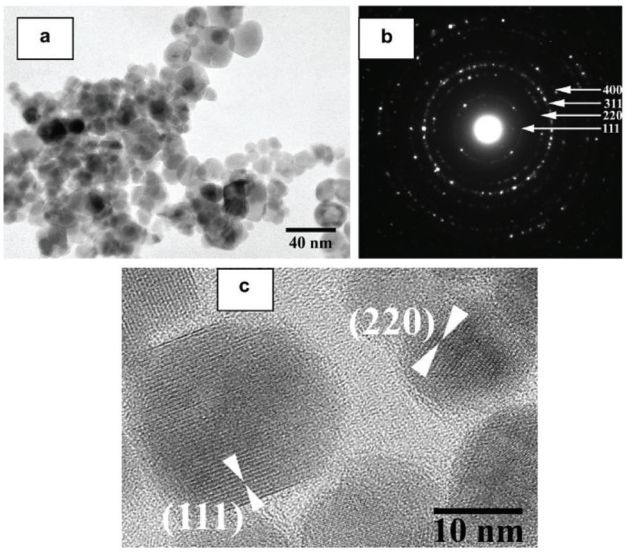

Fig. 8 (a) Bright field TEM micrograph, (b) selected area diffraction and (c) HRTEM image of hydrothermally prepared nanocrystalline $Mn_{0.8}Zn_{0.2}Fe_2O_4$. Reprinted with permission from Nalbandian *et al.*[194]

few nanometres up to 10s of nanometres, and a comprehensive set of characterisation measurements allowed structure/property relationships to be established: this included application as magnetically-recoverable photocatalysts and as mimics of the enzymatic activity of peroxidases, where enhanced activity over pure iron oxides was proven. MFe_2O_4 with M = Co, Ni, Cu, Zn were also studied as magnetically-separable catalysts, for epoxide ring opening reactions, and hydrothermally-prepared nanoparticulate $CeFe_2O_4$ was found to be the active catalyst.[200]

Aside from magnetic and catalysis properties, other applications of hydrothermally prepared ferrite spinels include $NiFe_2O_4$ for the detection of liquefied petroleum gas in air,[201] magneto-dielectric properties of $Ni_{0.54}Zn_{0.48}Fe_{1.98}O_4$,[202] microwave absorbing materials $Co_x(Cu_{0.5}Zn_{0.5})_{1-x}Fe_2O_4$,[203] and the absorption of dye molecules for depollution.[204] The spinel β-$LiFe_5O_8$ was prepared as a nanocrystalline powder at 140 °C from $FeCl_3{\cdot}6H_2O$, in equimolar amounts of $LiOH{\cdot}H_2O$ and NaOH at 140 °C and their electrochemical capacity was found to be superior to other lithium ferrites.[205]

Diodati *et al.* explored a very easy, low-temperature (T = 135 °C), route based on the coprecipitation of metal precursors from an aqueous suspension containing oxalates combined with a low-temperature hydrothermal treatment.[54,127]

As outlined in the above section concerning green chemistry, time-resolved experiments showed that the formation of crystalline ferrites could be achieved after only 1 to 3 hours of hydrothermal processing,[126] thus disclosing the possibility to implement an energy effective route to the up-scaling of these materials.

This route was further also implemented for the synthesis of quaternary spinel ferrites containing both zinc and either nickel ($Ni_xZn_{1-x}Fe_2O_4$) or cobalt ($Co_xZn_{1-x}Fe_2O_4$).[59]

Precursors/additives in solvothermal spinel synthesis

Further versatility can be brought to solvothermal synthesis by inclusion of dissolved species, such as salts, surfactants and co–solvents and, in this section, we will consider their benefits for the formation of spinel ferrites. The use of solution additives in solvothermal reactions provides a means to adjust crystal size and shape in the resultant product. Polyethylene glycols, available in a range of molecular weights, are convenient water-compatible solution additives that have been widely studied to control the hydrothermal crystallisation of ferrite spinels: this includes the synthesis of nanocrystalline forms of $CoFe_2O_4$,[84,206] $Zn_xNi_{1-x}Fe_2O_4$,[207] $Co_xZn_{1-x}Fe_2O_4$,[208] $Mn_{0.2}Ni_{0.8}Fe_2O_4$,[209] $Ni_{0.5}Zn_{0.5}Fe_{1.5}Cr_{0.5}O_4$[210] $MnxCo_{1-x}Fe_2O_4$,[211] $MnFe_2O_4$,[212] $CoCr_xFe_{2-x}O_4$[213] $Mn_xNi_{1-x}Fe_2O_4$[214] and $NiFe_2O_4$.[215] The synthesis of magnetic nickel spinel ferrite $NiFe_2O_4$ nanospheres by a reverse emulsion-assisted hydrothermal process proved possible, using ethyltrimethylammonium bromide, polyoxyethylene(10)nonylphenyl ether, iso-amyl alcohol and hexane, in an aqueous medium at 120 °C.[216] This lead to the formation of nanorods of oxyhydroxides and layered hydroxides at short reaction times, prior to the formation of nanospheres of the ferrite spinel.

The use of oleate complexes as reagents in solvothermal ferrite preparation has been studied and the role of the oleate can be as a surface capping agent on the resulting crystallites so to control the crystallite size and shape. A set of the ferrites MFe_2O_4 (M = Co, Ni, Mn, Zn) were prepared from mixed-metal (M,Fe)-oleate complexes upon solvothermal treatment in heptane at 140–180 °C: this yielded 5–6 nm crystallites coated with oleic acid.[217] For $CoFe_2O_4$ the choice of solvent mixture and temperature could be used to tune the crystallite size between 5 and 12 mn.[218] In the case of $NiFe_2O_4$, various alcohols and urea were investigated as solution additives to control the crystallite size and shape.[219] Repko *et al.* prepared a precursor solution of $Fe(oleate)_3$ and $Co(oleate)_2$ and used this as a reagent for the solvothermal formation of nanoparticles of $CoFe_2O_4$ in water–pentanol mixtures at 180 °C, or in pentanol and 1-octanol (or toluene) at 220 °C.[220] The particles could subsequently be surface modified with citrate, or with TiO_2, *via* hydrolysis of titanium isopropoxide leading to different dispersions and separations of the nanocrystals, Fig. 9.

Angotzi *et al.* have recently extended the solvothermal oleate route to prepare nanoscale heterostructures that consist of $CoFe_2O_4$ and $MnFe_2O_4$ cores with shells of either spinel iron oxide (maghemite/magnetite) or manganese ferrite, added in a second solvothermal reaction, Fig. 10.[221] These complex structures contain an intimate intergrowth between hard (cobalt ferrite) and soft magnetic materials with a hydrophobic coating, and provide a possible means to tune magnetic properties for practical applications.

Acetylacetonates provide convenient precursors for solvothermal synthesis that are soluble in organic solvents. Fe

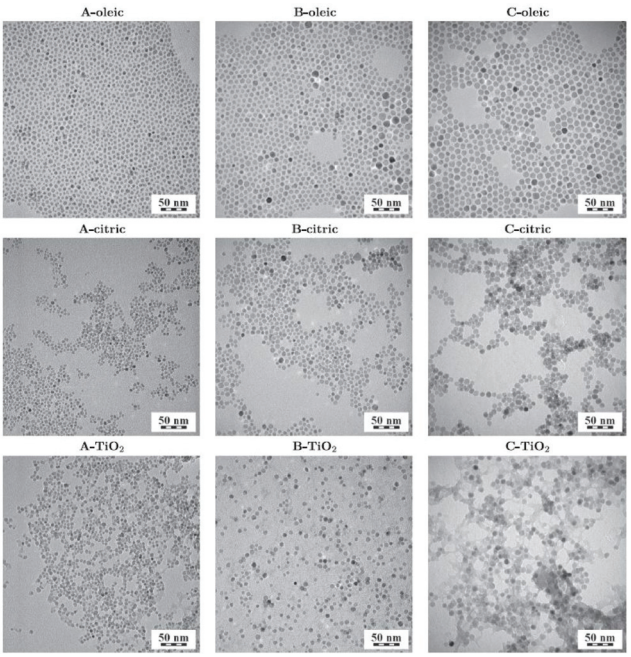

Fig. 9 $CoFe_2O_4$ crystallites of three different sizes (A, B and C) coated with oleic acid, citric acid and TiO_2. Reproduced with permission from Repko *et al.*[220]

$(acac)_3$ and $M(acac)_2$ (M = Ni, Co, Mn, Mg, Zn) treated in water in aloe-vera extract at 200 °C for 2 hours gave agglomerated nanocrystals ranging from 8–45 nm in diameter, depending on the divalent metal.[222] $Fe(acac)_3$ has also been used as a precursor to other ferrites under solvothermal conditions, including manganese ferrites in oleylamine and phenyl ether.[223] and gallium ferrites using 1,4-butanediol as solvent.[224] $Mn_xFe_{3-x}O_4$ nanoparticles were prepared in various polyols from trivalent manganese and iron acetylacetonates directly from solution at 200 °C: this lead to organic coated particles that were soluble in water.[225]

Jolley *et al.* produced Mn–Fe spinels in hydrothermal reactions in the presence of proteins and found protein-encapsulated Mn-ferrites showed different crystal chemistry compared to the pristine materials: in the absence of proteins a solid-solution between γ-Fe_2O_3 (maghemite) and Mn_3O_4 (hausmannite) was found, but within proteins the Mn end-member was a chalcophanite-like layered Mn oxide.[226]

Heterometallic cluster species provide versatile precursors to mixed-metal oxides since the ratio of metals in the precursors can be pre-defined and intimately mixed prior to the crystal growth of the mixed oxide product. The trinuclear heterometallic acetate clusters $[MFe_2O(CH_3CO_2)_6(H_2O)_3]\cdot nH_2O$ 120 °C (M = Ni, Co, Mn, and Zn) provide a good example and these can be hydrothermally decomposed at 120 °C in water, or various alcohols to yield uniform spinel ferrite nanoparticles.[227] Monodispersed iron cobalt oxide (Fe_2CoO_4) and iron manganese oxide ($Mn_{0.43}Fe_{2.57}O_4$) nanoparticles were prepared using bimetallic pivalate clusters of $[Fe_2CoO(O_2CtBu)_6(HO_2CtBu)_3]$, $[Co_4Fe_2O_2(O_2CtBu)_{10}(MeCN)_2]$, and $[Fe_2MnO(O_2CtBu)_6(HO_2CtBu)_3]$ using a mixture of oleylamine and oleic acid with either diphenyl ether or benzyl ether as solvent at their respective boiling points of 260 and 300 °C.[228] A similar approach was adopted for the synthesis of $ZnFe_2O_4$ and $NiFe_2O_4$ from appropriate heterometallic pivalates.[229]

The use of non-aqueous solvents provides a way of modifying crystal growth conditions, by adjusting the solubility of reagents, adjusting diffusion, as well as modifying the pressure at a given temperature. The solvent itself may be reactive, for example, providing reducing or oxidising conditions. Deng *et al.* pioneered the synthesis of $MnFe_2O_4$ ferrites in non-aqueous solvothermal reactions, reporting the formation of monodisperse microspheres for M = Co, Mn, Zn from ethylene glycol with addition of sodium acetate and polyethylene glycol.[230] The sodium acetate was proposed to provide electrostatic stabilisation, while the polyethylene glycol acted as a surfactant to further prevent particle agglomeration. Ethylene glycol as solvent with PEG additive allows access to some intricate and hierarchical crystal morphologies: for example, 100 nm spherical mesocrystals of $Co_{0.5}Zn_{0.5}Fe_2O_4$ constructed from agglomerates of primary nanocrystals.[231] Wang *et al.* prepared hollow $CoFe_2O_4$ nanospheres using ethylene glycol as solvent and with urea as an additive, Fig. 11, and the materials were shown to have favourable properties an anodes for lithium-ion batteries.[232]

Otero-Lorenzo *et al.* recently described a comprehensive investigation of colloidal nanocrystal clusters of Fe_3O_4 and $Mn_xFe_{3-x}O_4$ formed in ethylene glycol using polyethylene glycol and sodium acetate as solution additives.[233] This led to the conclusion that the spinel oxides formed *via* a series of poorly crystalline intermediates followed by the assembly of nanocrystals of spinels into the final colloidal clusters.

Continuous routes to ferrite spinels

One advantage of solvothermal routes to oxide materials is the possibility of development of continuous flow methods where solutions of reagents can be pumped through heated pipework that at controlled mixing points gives an industrially-viable production method for the production of nanomaterials at scale.[234,235] In the case of ferrites, this approach has been adopted for several compositions. Cabañas and Poliakoff used

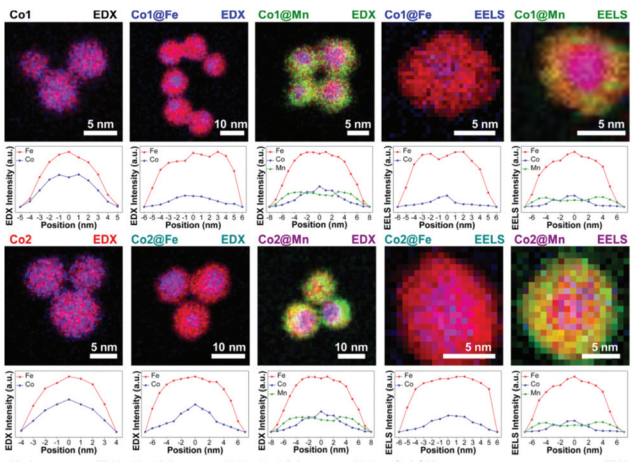

Fig. 10 Energy-dispersive X-ray maps of metal cation concentration in core–shell nanocrystals of cobalt ferrite and manganese ferrite coated with a second spinel oxide, with line-scans below each map. Reproduced with permission from Angotzi *et al.*[221]

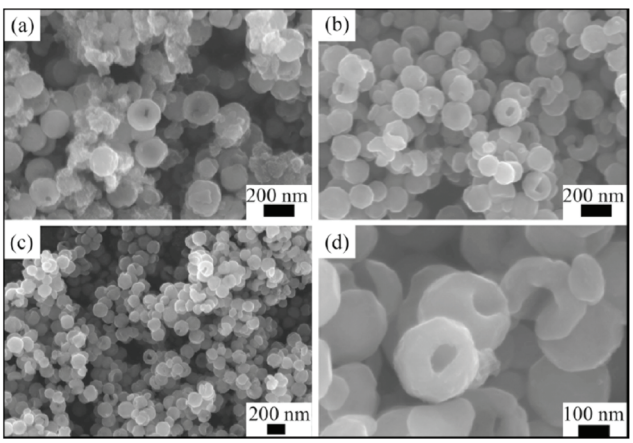

Fig. 11 Scanning electron microscopy images of $CoFe_2O_4$ nanospheres prepare *via* hydrothermal synthesis in the presence of ethylene glycol at reaction times of (a) 6 hours, (b) and (d) 12 hours and (c) 24 hours. Reproduced with permission from Wang *et al.*[232]

a continuous hydrothermal reactor to produce various spinel ferrites including Fe_3O_4, MFe_2O_4 (M = Co, Ni, Zn) and $Ni_xCo_{1-x}Fe_2O_4$ from mixtures of Fe(II) acetate and M(II) acetates.[236] Electron microscopy TEM showed a bimodal particle size distribution with small particles of ~10 nm and larger particles up to 100 nm, and possible reaction mechanisms were discussed, to account for the solution redox chemistry. $MeFe_2O_4$ (M = Ni, Cu, Zn) and their solid solution with γ-Fe_2O_3 were prepared in continuous flow at 400 °C, 30 MPa with a particle size that increased with increasing residence time.[237] The particles were proposed to form *via* rapid formation of low-crystallinity γ-Fe_2O_3 followed by secondary nucleation of the solid solution on its surface with surface dissolution of the primary particles. Stingaciu *et al.* compared $CoFe_2O_4$ samples prepared in a continuous flow reactor with those made in batch reactors and a custom-made spiral reactor; the material made in continuous flow had the narrowest particle size distribution, while magnetic measurements showed a strong interparticle interaction.[238] $Co_{1-x}Ni_xFe_2O_4$ (x = 0–0.8) nanoparticles were prepared from nitrate precursors in sodium hydroxide solution at 390 °C and 30 MPa: this gave 12–20 nm crystallite with high surface areas and their catalytic properties for CO oxidation and the oxygen evolution reaction were studied.[239]

Recently, some of us have used a continuous hydrothermal flow synthesis (CHFS) approach[59] to prepare crystalline spinel quaternary ferrites $M_xZn_{1-x}Fe_2O_4$ (M = Co, Ni; x = 0.2, 0.35, 0.5, 0.65, 0.8). In particular, the same materials were synthesised both through conventional batch hydrothermal synthesis (HT – as described above) at 135 °C as well as *via* CHFS. The as prepared compounds were thoroughly characterised from a compositional (ICP-MS, XPS) and structural (XRD) point of view in order to compare the two synthetic approaches and achieve a detailed understanding of how the chosen approach influences the characteristics of the resulting spinel. It could be concluded that CHFS requires higher temperatures and a more complex setup, but is capable of continuous synthesis, and thus can afford a greater quantity of materials over time. In contrast, the simpler HT synthesis was far easier and less time consuming to implement, despite, as a batch method, only being able to yield a limited mass of products in a given time span. Interesting differences were pointed out as far as material composition was concerned: analyses *via* ICP-MS evidenced that the HT protocol was more successful in affording a good stoichiometric control over the final product by simple adjustment of the nominal stoichiometric ratios between the metal precursors.

Hydro/solvothermal approaches to other ferrites

Hexagonal barium hexaferrite, $BaFe_{12}O_{19}$, is a material well studied as a hard ferrite used in magnetic recording devices, and hydrothermal routes to the material have been reported, where the aim has been to produce fine powders that can be sintered into magnetic solids.[240–244] Liu *et al.* developed a synthesis route from Fe^{2+} and Fe^{3+} precursors, with the former being oxidised *in situ* but yielding samples free of Fe_2O_3 and $BaFe_2O_4$ impurities.[245] Related hexagonal ferrites have been reported *via* hydrothermal routes including $SrFe_{12}O_{19}$,[246] $Sr_{1-x}Nd_xFe_{12}O_{19}$ [247] and $Sr_{1-x}Sm_xFe_{12}O_{19}$.[248] It should be noted that many of the reported hydrothermal routes to the hexaferrite family involve a second step of calcination to induce crystallinity and to optimise magnetic properties, and hence these are best thought of as processing rather than synthesis routes. For example, although $BaFe_{12}O_{19}$ forms from solution at sufficiently high hydroxide ion concentration, annealing at 1000 °C is needed to improve saturation magnetisation and intrinsic coercivity.[239] Recent work has examined how the particle morphology of the hexaferrites may be controlled by hydrothermal synthesis: for example, Jing *et al.* produced M-type $SrFe_{12}O_{19}$ directly at 220 °C as flake-like particles with magnetic behaviour that depended on grain size.[249] Soria *et al.* studied $SrFe_{12}O_{19}$ plates formed by a similar method using a comprehensive set of characterisation methods and found a greater proportion of tetrahedral iron than in reference bulk materials.[250] Dong *et al.* found a large magnetocrystalline anisotropy in $SrFe_{12}O_{19}$ nanosheets and measured favourable microwave absorbing properties.[251]

Other multinary iron oxides that have been prepared hydrothermally include the garnet phase $Sm_3Fe_5O_{12}$ [252] and the sillenite-structured $Bi_{12}Fe_{0.63}O_{18.945}$ (close to the ideal composition $Bi_{25}FeO_{40}$) and $Bi_2Fe_4O_9$.[145]

Sonochemistry

A relatively little-known approach, which has nevertheless gained significantly more interest in the last five years, is the sonochemical approach. Sonochemistry is based on the formation, growth and collapse of bubbles in a liquid medium (cavitation) by exposure of the system to ultrasonic waves.[2,253–255] Within this context, the act of the bubbles collapsing can cause significant, as well as extremely localised, temperature increases (to around 4750 °C) with equally swift cooling (in excess of 10^{10} °C s^{-1})[253] This can be taken advantage of in several ways: it can be used for instance to instantaneously decompose volatile metallorganic compounds to obtain individual metal atoms, agglomerate them and obtain nanoparticles.[253] In other cases (such as many of those examined herein) the localised high temperatures can be used to effectively locally calcine a synthesised material to yield crystalline products without actually needing to bring the entire system to high temperatures;[258] this locally confined calcination" provides the additional benefit that, as an extremely localised phenomenon, it does not give rise to agglomeration or coalescence phenomena in the system (unlike more conventional calcination approaches).[258] Interested readers are referred to more specific works on the approach, such as those by Thompson and Doraiswamy[254] or Mason and Lorimal.[255]

Despite requiring dedicated equipment to suitably generate the cavitation effects necessary for the reactions to take place,[259] the sonochemical approach is, perhaps surprisingly, eminently scalable, able to be employed from the laboratory scale (where a simple ultrasonic rig apparatus may be

sufficient)[260] to high scale flow reactors;[259] The technical and engineering aspects of this issue have been the subject of a work by Gogate *et al.*[261]

In general, the reports available in the literature on sonochemistry mainly cover spinel ferrites, with the cobalt, zinc and nickel spinels being the most common. Some reports exist concerning perovskite ferrites (namely $BiFeO_3$), but in those cases a conventional calcination step was always involved to achieve crystalline materials.[262,263]

Concerning successful and actually low-temperature syntheses, Abbas *et al.*[256,264] were not only able to achieve the synthesis of shape-controlled cobalt spinel ferrite (obtaining both nanocubes and nanospheres – Fig. 12), but also expanded the scope of their research to quaternary ferrites, achieving a mixed Ni/Zn spinel ferrite with controlled stoichiometry. Both these syntheses were carried out at room temperature in deionised water: the metal precursors (chlorides) were dissolved in the aqueous medium and sonicated (Vibra Cell-VCF 1500, Sonics and Materials; 5 cm^2 titanium horn; 20 kHz), before adding 3 M NaOH.

The effect of the confined calcination mentioned above was the subject of a study by Choudhury *et al.*[258] whereby the chemical intermediate reactions for the formation of $ZnFe_2O_4$ from acetate precursors were hypothesised and compared to the obtained experimental results. Reactions were carried out in a conical flask and an ultrasound bath (capacity: 2.5 L, frequency: 35 kHz, Power: 35 W) was employed for sonication, generating a 1.5 bar ultrasound wave. The study concluded that transient cavitation in the reaction medium provides the energy to promote the *in situ* calcination of oxide particles to yield the ferrite product, with the added benefit of generating smaller size of ferrite crystals compared to conventional calcination. An earlier study by Reddy *et al.*[265] took a more theoretical approach, by coupling experimental results of $ZnFe_2O_4$ sonochemical synthesis with simulations of the radial motion of cavitation bubbles. In particular, they concluded that the resulting particle size was mainly governed by the rate of production of $OH^{\bullet}$ radicals.

In a more recent work,[257] Chen *et al.* employed sonochemistry to prepare $ZnFe_2O_4$ nanocubes embellished with reduced graphene oxide for use in electrochemical sensing of biomarkers (specifically 4-nitroquinoline-*N*-oxide) (Fig. 13). Syntheses were carried out at room temperature in deionised water by reacting the nitrate metal precursors with ammonium hydroxide (final pH 8.0) in a 100 W, 40 kHz ultrasonic bath. The graphene oxide was then added by drop-casting.

In work by Harzali *et al.*,[266] the synthesis of the quinary $Ni_{0.4}Cu_{0.2}Zn_{0.4}Fe_2O_4$ spinel through a combination of coprecipitation and ultrasound irradiation was described (Fig. 14). The compound was prepared from sulfate metal precursors in

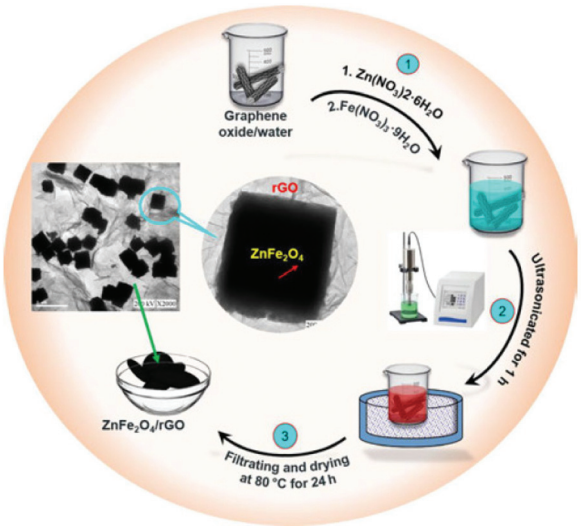

Fig. 13 Reaction scheme for formation of $ZnFe_2O_4$/graphene oxide nanocomposite using sonochemistry. Reproduced with permission from Chen *et al.*[257]

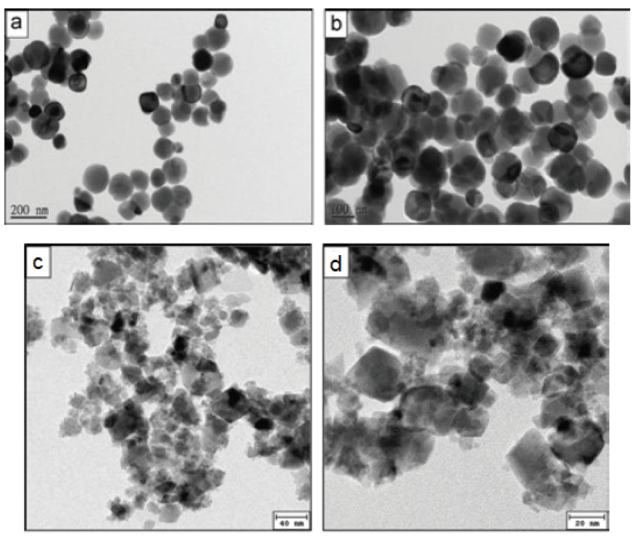

Fig. 12 $CoFe_2O_4$ nanospheres (a and b) and nanocubes (c and d) synthesised in water through controlled sonochemistry at room temperature. Reproduced with permission from Abbas *et al.*[256]

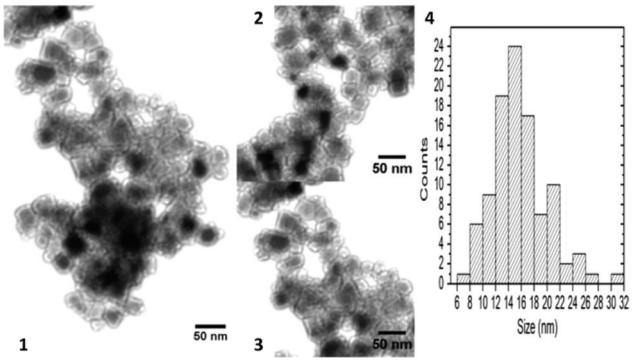

Fig. 14 TEM micrographs and size histogram of $Ni_{0.4}Cu_{0.2}Zn_{0.4}Fe_2O_4$ synthesised at T = 90 °C, t = 2 h and for P_{diss} = 46.27 W (1, 2, and 3 represent different areas of the sample; 4 the size histogram). Reproduced with permission from Harzali *et al.*[266]

deionised water by adjusting the pH to 12 with NaOH and sonicating at 28.03, 38.23 or 46.27 W (equivalent to bulk reaction temperatures of 70, 90 and 100 °C, respectively). The resulting powders were crystalline after drying and required no further high temperature annealing steps.

Yadav *et al.*[267] were able to prepare $CoFe_{2-x}Gd_xO_4$ with controlled gadolinium doping levels (x = 0.00, 0.05, 0.10, 0.15 and 0.20). The synthesis was carried out in deionised water at room temperature and the nitrate precursors were sonicated at 20 kHz, 70 W after basification with NaOH. It was shown that doped materials with controlled stoichiometry were afforded by the protocol and the influence of Gd content on structural, magnetic, dielectric, electrical, impedance and modulus spectroscopic features was investigated. The obtained spinels showed potential for applications in microwave and magnetic recording devices and, perhaps more importantly, the method was found to be promising for future synthesis research in the field of rare earth-doped spinel ferrites. Furthermore, the economic and environmental advantages featured by the method make it attractive for possible scaling-up at the industrial level.

Other notable works on the subject include those by Senapati *et al.* ($CoFe_2O_4$),[268] Shafi *et al.* (crystalline $CoFe_2O_4$ and amorphous $NiFe_2O_4$)[269,270] and Wu *et al.* (Fe_3O_4).[271]

Microemulsion and miniemulsion synthesis

A very convenient, albeit not easily implemented at the industrial scale, approach to pursue the crystallisation of nanoscale inorganic materials, with a certain control on size, size distribution and shape, relies on carrying out a reaction within the confined environment of micro- and miniemulsion droplets, which act as "nanoreactors".[272] This class of methods, typically based on the precipitation of the targeted oxide within the confined space of water droplets dispersed in a continuous apolar phase, as described extensively in the following, cannot be classified as fully "green" methods because of the use of organic solvents such as cyclohexane. Nevertheless, they present unique features, such as the exploration of unconventional crystallisation pathways[272] and the possibility to pursue the crystallisation of the targeted oxides already at room temperature.[273–275] Indeed, also in this case, as in the above described solvo- and hydrothermal routes, formation of phases which would not be affordable by high temperature routes. Micro- and miniemulsions differ not only because of their different typical droplet size, but also regarding their thermodynamics *viz.* kinetic stability. Microemulsions[276] are thermodynamically stable colloidal dispersions, characterised by droplets with an average hydrodynamic diameter of 5–50 nm, that are spontaneously formed by mechanical stirring,[277,278] whereas miniemulsions[279–282] are kinetically stable systems, consisting of droplets with an average size of 30–300 nm, generated by using high shear forces.[279–282] Since the synthesis of oxides is typically performed through precipitation reactions in a water medium, the formation of oxides within droplets is generally carried out in inverse (water-in-oil) emulsions (also referred to as "reverse micelles"), by mixing an emulsion containing an aqueous metal salt precursor solution with a second one containing a precipitating agent (acid/base). Whereas, in the case of microemulsions, the droplet collisions result in the fusion and mixing of the reactants, with slower characteristic exchange times compared to the diffusion of reactants in bulk conditions,[283] miniemulsion droplets can instead be considered as independent nanoreactors, in which reactions run in parallel. Miniemulsion droplets are stable against diffusional degradation processes and collisions are hindered. As a consequence, in order to promote the collision and fusion of the droplets and consequently the mixing of the reactants, ultrasounds, providing the high shear forces needed for disrupting the droplets, are necessary.[284] For the synthesis of ferrites, microemulsions have been broadly used, whereas only few examples concerning the use of miniemulsion to achieve ferrites have been reported. In the following section, the state-of-the-art in the micro- and miniemulsion synthesis of ferrites is summarised. It is worth highlighting that, in many cases, oxo/hydroxo metal compounds were achieved as a first product of microemulsion synthesis, which in turn needed a further thermal treatment to be converted into crystalline ferrites. Most of these examples, have deliberately not been reported in this contribution, as it is focussed on low temperature routes to ferrites.

Microemulsion and miniemulsion routes to perovskite and spinel ferrites

A very comprehensive review on the use of microemulsion for the synthesis of ferrites was authored by Mathew,[34] summarising different protocol examples, typically relying on water-in-oil emulsions, based on a CTAB/1-hexanol/water system. In these routes CTAB acts as the surfactant. Different examples of the microemulsion-based synthesis of various spinel ferrites, such as zinc ferrite, nickel–zinc ferrite, manganese–zinc ferrite and cobalt ferrite, are provided. In some cases, different oil/surfactants formulations were used, as exemplified in Fig. 15.

Very recently, Scano *et al.*[285] have also published a comprehensive review on the preparation of ferrites by microemulsions, presenting a series of advantages with respect to other methods, due to the possibility of confining reactions in nanosized reactors, allowing the preparation in mild synthesis conditions of a wide variety of nanostructured ferrites with controlled composition, particle size and shape.

In a more general work,[286,287] the potential of reverse micelles as nanosized aqueous droplets, existing at certain compositions of water-in-oil microemulsions, is presented for the controlled synthesis of nanoparticles, among which also ferrites. The review firstly presents to the reader the basic concepts in the field of reverse micellar synthesis of materials; then the typical synthesis pathways and the correlations between the properties of the microemulsion reaction media (*e.g.* reagent concentrations, ionic strength, temperature, aging time) and the prepared materials are presented.

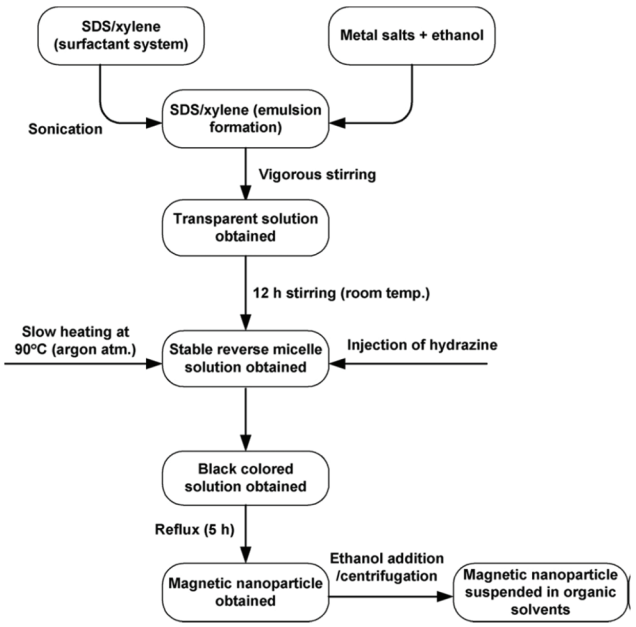

Fig. 15 Flow chart of the typical experimental procedure for the microemulsion synthesis of ferrite nanoparticles (adapted with permission from Mathew *et al.*).[34] SDS: sodium dodecyl sulphate.

A further pivotal report in this regard is the work by Aubery *et al.*,[288] which thoroughly discusses the phase behaviour, dynamics, and structure of water-in-oil (w/o) microemulsions of the aqueous solution/1-hexanol/isooctane system with the goal of determining their effect on Mn–Zn ferrite nanoparticle formation, kinetics and characteristics. The same authors,[289] carried out a further fundamental systematic study devoted to investigate the formation of w/o microemulsions with high aqueous phase uptake in a non-ionic surfactant system as a reaction medium for the synthesis of Mn–Zn ferrite nanoparticles. In particular, a comprehensive study, based on the phase behaviour of systems containing precursor salts and the precipitating agent, was carried out to correlate the phase diagrams with the internal structure and dynamics of microemulsions, which in turn could be related to the final features of the resulting Mn–Zn spinel and superparamagnetic ferrites. This study must be considered relevant in this context, since it sets the knowledge base for a deeper understanding of the relationship between the final characteristics of the obtained materials with the properties of the reaction medium, *i.e.* the microemulsion.

The unusual conditions achieved by using microemulsions as reaction media was the topic of a further investigation by Bellusci *et al.*[290] The authors, through a comprehensive approach, pointed out that the physico-chemical equilibria that influence the precipitation of spinel manganese ferrites from an aqueous solution can be substantially altered when the process is carried out in a microemulsion system consisting of a toluene/water/sodium dodecylbenzenesulfonate system. However, prior to the unavoidable final calcination step, only the presence of nanosized mixed hydroxide compounds could be ascertained, a result which was ascribed to a low metal content and a limited matter exchange among aqueous nanodroplets, likely inhibiting the hydroxide to oxide transformation inside the selected micellar system.

In a further work,[291] $MgFe_2O_4$ was obtained using a tertiary heptane/Igepal CO 520/H_2O, system and the effect of the water-to-surfactant ratio on particle size and magnetic properties was studied, whereas a similar investigation by the same authors[292] focussed on the effects which changing the continuous phase had on the particle size and the magnetic properties of the resulting Mg spinel. The same compound was addressed by Holec *et al.*[293]

The effect of the experimental parameters on the final features of the resulting ferrites was also the topic of a thorough investigation by Pemartin *et al.*[66] An oil-in-water (o/w) microemulsion was used for the preparation of Mn–Zn ferrite magnetic nanoparticles (NPs). By variating the precipitating agent and the oil phase concentration, Mn–Zn ferrite nanoparticles with different characteristics could be obtained and it could be shown that, at a fixed microemulsion composition (surfactant : water weight ratio (S : W) 25 : 75, 12 wt% oil phase), the use of NaOH as precipitating agent resulted in smaller nanoparticles compared to when tetramethylammonium hydroxide was used (2.4 nm *vs* 5.2 nm, respectively). Additionally, particle size was shown to increase with higher oil content (9.4 nm for 20 wt% oil), a result which was ascribed to the higher concentration of precursor in the microemulsion. In conclusion, crystallite size varied depending on microemulsion composition and precipitating agent; consequently the magnetic characteristics (blocking temperature and saturation magnetization) also changed as a function of the precipitating agent and microemulsion composition.

Different spinel ferrites, ranging from $CoFe_2O_4$,[294–296] to Ni and Zn ferrites,[297,298] to $Li_{0.5}Fe_{2.5}O_4$,[299] to Mn^{3+} substituted $MnFe_{2-x}Mn_xO_4$ ferrite,[300] to $Ni_{1-x}Zn_xFe_2O_4$ (x = 1, 0.8, 0.6, 0.5, 0.4, 0.2, 0.0),[301,302] to $Co_{0.3}Cd_{0.7}Zn_{1.5x}Fe_{2-x}O_4$ (x = 0.0, 0.1, 0.2, 0.3, 0.4, 0.5),[303] to $Ni_xCo_{(1-x)}Fe_2O_4$ (x = 0.0, 0.2, 0.4, 0.6, 0.8, 1.0),[304] to $CoCrFeO_4$,[305] to MFe_2O_4 (M = Co, Fe, Mg, Mn, Cr, Zn) have been prepared by these routes.[306]

By the microemulsion route, doped spinel ferrites could also be easily achieved, as reported by Baig *et al.*[307] for the rare earth Dy^{3+} substituted $MnFe_2O_4$ nanoparticles, though in this case a final heating step at 400 °C in vacuum was needed to achieve a crystalline nanomaterial.

In an interesting example of combining different synthetic routes, Antonello *et al.*,[15] reported the synthesis of several crystalline first-row-transition-metal (Mn, Fe, Co, Ni, Cu, and Zn) ferrites prepared by a combination of miniemulsion synthesis and solvothermal treatment, pursuing unconventional conditions in terms of space confinement, temperature, and pressure. This synergy allowed to obtain the crystalline ferrites at a much lower temperature (*i.e.*, 80 °C) than usually required and without any post-synthesis thermal treatment. X-ray diffraction revealed that analogous ferrites synthesised by miniemulsion at ambient pressure or in bulk (*i.e.*, from an aqueous macroscopic solution and not in the confined space of the

miniemulsion droplets) either at ambient pressure or under solvothermal conditions did not result in similarly highly crystalline products. Concerning their functional behaviour, the synthesised ferrites were superparamagnetic and were found to be active oxidation catalysts, as demonstrated for the oxidation of styrene, which was taken as a model reaction. Thanks to their magnetic properties, the catalysts could be recovered from the reaction medium by magnetic separation and reused for several cycles without loss in activity.

A further combination of approaches was presented by Tajik *et al.*,[308] who prepared $CuFe_2O_4$ nanoparticles with an average particle size of 22.3 nm by a combined microemulsion and homogenous precipitation method.

In a report by Ahmad,[72] the microemulsion synthesis of spinel nanoferrites having a nominal composition of $Sr_{1-x}Nd_xFe_{2-y}Cd_yO_4$ ($0.0 \leq x \leq 0.1$, $0.0 \leq y \leq 1.0$) and an average crystallite size in the 23–35 nm range is described. Quaternary ferrites were also prepared by using the microemulsion route. Ali *et al.*[309] prepared nanosized Zr–Co doped nickel ferrites with a nominal composition, of $NiZr_xCo_xFe_{2-2x}O_4$ (x = 0.0, 0.2, 0.4, 0.6, 0.8) by using this method.

Microemulsion and miniemulsion routes to hexaferrites and further ferrites

Ali[310] reported a series of complex transition metal/rare earth-based Y-type hexaferrites synthesised by the microemulsion method. Interestingly, the microemulsion route allowed controlled doping, and the effect of doping with manganese (at the tetrahedral site) and with terbium (at octahedral site) could be investigated. It was observed that changes occurred in magnetic properties (such as saturation magnetisation, coercivity, remanence and magnetic moment) due to the cationic stoichiometry and their occupancy in the specific sites.

Differences in the structural and magnetic properties of nanosized barium hexaferrite powders, prepared by single and double microemulsion techniques, were the topic of a study by Koutzarova *et al.*[311,312] In detail, barium hexaferrite powders, featuring nanometric particle sizes, were prepared by either single or double microemulsion (water-in-oil reverse microemulsion system with cetyltrimethylammonium bromide (CTAB) as a cationic surfactant, *n*-butanol as a co-surfactant, *n*-hexanol as a continuous oil phase, and an aqueous phase) and the influence of the type of microemulsion technique on the microstructure and on the magnetic properties of the barium hexaferrite powders was studied. The type of microemulsion adopted was shown to affect, *inter alia*, the average particle size, the shape and the functional properties: ferrites obtained by single microemulsion featured better magnetic characteristics than those obtained by double microemulsion. It should be also pointed out that barium ferries had already been prepared by microemulsion by further authors.[313]

Murtaza *et al.*[314] further employed the microemulsion approach to prepare different Nd–Mn-substituted hexaferrites having general formula $Sr_{2-x}Nd_xNi_{0.5}Co_{1.5}Fe_{12-y}Mn_yO_{22}$ (x = 0.0, 0.02, 0.04, 0.06, 0.08, 0.10, 0.20, 0.30, y = 0.0, 0.25, 0.50, 0.75, 1.00, 1.25, 1.50, 1.75).

Microwave-assisted synthesis of ferrites

The liquid phase synthesis of nanomaterials using microwave-assisted heating has received considerable attention from the scientific community in the last years because it allows rapid volumetric heating, thus enabling remarkable increase of reaction rate, selectivity and yield compared to conventional approaches. This scenario offers attractive perspectives in the fabrication of materials at low cost, improving energy savings and process efficiency.

Microwaves are electromagnetic radiation with frequencies between 0.3 and 300 GHz and wavelengths ranging from 1 mm to 1 m, positioned between infrared and radio wave in the electromagnetic spectrum. For laboratory and domestic application, the usual frequency for microwave heating is 2.45 GHz, corresponding to a wavelength of 12.24 cm. In general, any material containing mobile electric charges such as polar solvents or electrolytes, can be heated by microwaves. Heat is generated by rotation, friction and collision of polar molecules such as water, which try to orientate towards the oscillating electric field (Fig. 16a). In conventional heating systems the thermal energy needs to be transferred from the heating source to the reactor, to the solvent and ultimately to the reactants, which requires large amount of time and of energy dissipation. In contrast, in microwave-based setups the heating occurs directly at the target system, thus making the use of energy sources and energy transfer media (*e.g.* oil bath) superfluous and remarkably improving the time and energy savings (Fig. 16b). There is an extensive number of reports in the literature showing that microwave heating largely increases the rate of chemical reactions. In order to explain the rapid temperature increase promoted by the microwave irradiation, the existence of effects called "specific microwave effects" and "non-thermal microwave effects" was postulated.[315–317] "Specific microwave effects" consider that the thermal heating effect does not have repercussions on the mechanism of the chemical reaction but only influences the reaction time through the formation of hot spots in the reactor. In contrast, "non-

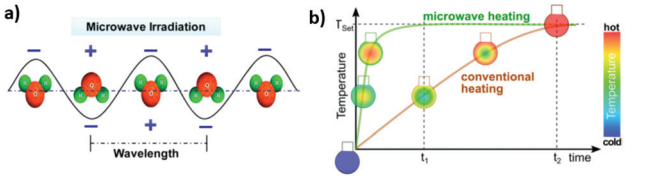

Fig. 16 (a) Water molecules in an alternating electrical field under microwave irradiation (from ref. 323) (b) Time–temperature correlation of conventional and MW-heated reaction vessels as well as the temperature distribution inside the reaction mixture. Reproduced with permission from Schütz *et al.*[324]

thermal microwave effects" predict direct interactions between the molecules and the microwaves in the solution reaction. Possible implications may regard the reaction activation energy or excitement of rotational/vibrational molecular transitions.[318–320]

The heating generated by microwave radiation in a solvent or material is determined by the loss tangent $\tan\delta = \delta''/\delta'$, where δ'' is the dielectric loss, *i.e.* the amount of radiation converted into heat, and δ' represents the dielectric constant, which gives the polarisability of molecules in the electric field.[315,321] To understand the microwave-matter interaction the penetration depth of the radiation should be also considered. This denotes the depth where the incoming microwave power is reduced to the 37%. The penetration depth is inversely proportional to the loss tangent: it grows with increasing material temperature and decreases by enhancing the radiation frequency.[322] For water, which is one the most used solvent in liquid phase syntheses, due to its large availability and environmental-friendly character, the penetration depth at room temperature conditions is approx. 2 cm. Even though this value doubles at 80 °C its dielectric loss drops remarkably, complicating the microwave heating at high temperatures. However, as water is a polar solvent, is considered also a good microwave absorber. When microwave irradiated, the polarised water molecules tend to orientated following the alternating electric field (Fig. 16a). Heat is consequently produced by the rotation, friction, and collision of the molecules. The amount of time required for the molecules to relax is directly correlated to their volume and the extent of the hydrogen-bonding network. As the relaxation time depends on the loss tangent of the solvent, the denser is hydrogen-bonding network, the higher will be the heat developed by irradiation. When electrolyte solutions are considered, the relaxation time decreases at low salt concentrations and then increases again. This behaviour is explained by the initial rupture of the hydrogen bonding network. Even if some molecules are coordinated to the ions, the majority of them do not experience strong intermolecular forces and possess lower relaxation time. At high salt concentration, greater ordering of the water molecules presumably sets in, thus inducing even larger relaxation times than for pure water.[321]

Owing to the manifold advantages offered by water in the synthesis of nanostructured materials, numerous scientific publications have dealt with the employment of microwave radiation in combination with wet chemistry processes. In the following sections the main progress on the microwave-assisted synthesis of ferrites with spinel and perovskite structures in aqueous and other solvents will be highlighted.

Ferrites with spinel structure

The microwave heating has been combined with diverse wet chemistry procedures for the synthesis of spinel ferrites. These comprise hydrothermal, solvothermal, sol–gel and polyol methods.

Among these routes, the hydrothermal approach was the first procedure to be coupled with such electromagnetic fields. Komarneni *et al.*[325] showed more than two decades ago how MFe_2O_4 with M = Mn, Co, Ni, and Zn powders could be obtained from the basic solution of the nitrate salt precursors in few minutes at 164 °C, increasing the reaction kinetics by almost two order of magnitudes with respect to conventional routes. Interestingly, the prepared materials exhibited also high porosity and specific surface areas from 72 to 247 $m^2\ g^{-1}$, most probably due to nanoparticle aggregation during the synthesis. A few years later Kim and co-workers[64] implemented the work of Komarneni *et al.* for the preparation of Co–Zn and Ni–Zn ferrite powders from chloride precursors at 100 °C within 30 min. The incorporation of Zn in the lattice positions of Ni and Co was verified by the lattice parameter increase proportional to the Zn amount. In the past years, the use of additives in the hydrothermal process has become common to control finely the properties of the synthesised materials. The addition of ionic liquids to the water-based reaction mixture and the subsequent microwave heating has had a remarkable influence on the crystal structure of the final products. A transition from $ZnFe_2O_4$ and α-Fe_2O_3 mixed phases, to pure $ZnFe_2O_4$ and pure β-FeOOH was observed by increasing amount of ionic liquid.[326] The spinel structures obtained in such way exhibited also encouraging photocatalytic activity for phenol degradation. $ZnFe_2O_4$ nanoparticles were employed as catalyst precursor by Choi *et al.*[327] for the synthesis of hydrocarbons by reducing CO_2. The microwave-assisted hydrothermal synthesis produced spinel nanoparticles agglomerates with high surface area (119 $m^2\ g^{-1}$) and improved morphology stability under reduction conditions at 400 °C. Microwave heating offers an unconventional way to prepare materials, which usually require elevated temperatures and prolonged reaction time. This is the case of layered metal oxides as sodium/potassium iron oxide nanosheets,[328] prepared by microwave-assisted hydrothermal method at 180 °C within 5 minutes. The layered compounds consist of two-dimensional iron oxide building blocks separated by intercalated alkali ions (Fig. 17). Such nanosheets exhibit ferromagnetic properties due to the magnetic anisotropy of the iron oxide layers. Moreover, the lamellar structure enables high ion diffusion

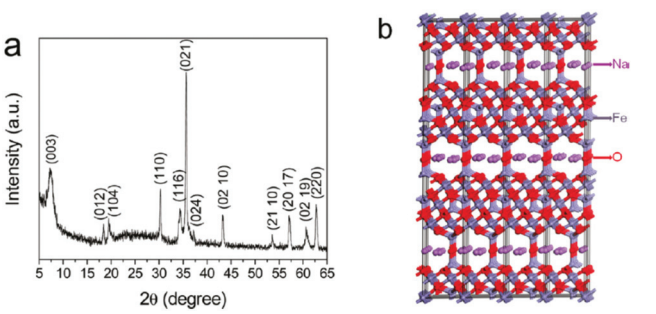

Fig. 17 (a) XRD pattern of sodium iron oxide nanosheets synthesised under microwave irradiation at 180 °C for 5 min. (b) Crystal structure of $Na_{2.4}Fe_{10.99}O_{16.03}$ viewed perpendicular to the *c* axis. The pink, red, and grey spheres correspond to Na, O, and Fe atoms, respectively. Reproduced with permission from Wu *et al.*[328]

and thus promising application in high performance lithium-ion batteries.

The application of microwave radiation for the hydrothermal synthesis of spinel ferrites resulted also in improving the materials' magnetic properties and their applications as magnetic resonance contrast agents. Thus, Williams and co-workers[329] showed that microwave heating induced the formation of small and highly uniform polyelectrolyte functionalized Fe_3O_4 particles with much larger magnetic saturation than materials prepared by conventional hydrothermal methods. The application of electromagnetic fields allows therefore greater control over the final functionality of the ferrites for magnetic resonance applications.

One of the first examples in exploiting the benefits of the microwave radiation within solvothermal synthesis was reported by Caillot *et al.* in 2002 [330] for the preparation of magnetite nanoparticles. Using a home-made microwave autoclave the authors succeeded in the preparation of Fe_3O_4 nanoparticles of 20 nm size within 10 minutes starting from ferrous chloride solution in ethanol. Compared to conventional solvothermal procedures the materials were obtained 10 times faster and with lower grain size. The use of surfactants has been implemented in solvothermal synthesis to enable better control of particle growth and morphology. The introduction of cetyltrimethylammonium bromide in an ethanol solution of iron and zinc metalorganic precursors, lead to the rapid synthesis of $ZnFe_2O_4$ at temperature below 100 °C with crystallites ranging between 8 and 20 nm, even if in the final material significant organic contaminations originated from the solvent or surfactant molecules were present.[332] Diols and in general polyols are in general preferred to surfactants because their bifunctional character to act both as solvent and capping agent, limits the organic content in the reaction mixture. The 1,2-propandiol-based solvothermal synthesis of $CoFe_2O_4$ was employed to generate nanoparticles of average size of about 5 nm.[333] Also in this case the materials presented organic surface contamination from the solvent, however they showed interesting magnetic behaviour. With respect to bulk and conventionally prepared systems, ferrites prepared through this microwave-assisted method possessed much larger magnetic saturation at 10 K.

The microwave-assisted synthesis of metal ferrites using other polyols, such ethylene glycol, offered an interesting tool to further control nanoparticle microstructure and morphology. Giri *et al.*[334] were among the first to develop a microwave refluxing approach for the preparation of metal ferrites. The bifunctional role of ethylene glycol as solvent and capping agent led to phase pure $Co_{1-x}Zn_xFe_2O_4$ ($0 \leq x \leq 0.8$) nanoparticles within few minutes, the crystallinity of which could be improved by increasing the pH of the starting solution. The group of Kozakova[335] showed later how the combination of ethylene glycol and water could be beneficial for directing the structural properties of ferrite materials. They showed that the addition of small portions of water to ethylene glycol in a microwave-assisted environment, lead to Fe_3O_4 particle size reduction up to one third of the original size and to the formation of nanoparticles in superparamagnetic and ferromagnetic states.

Further works made use of larger polyols as triethylene glycol (TREG)[331,336–339] as solvent. The high stabilising properties of TREG enables high dispersion of the nanoparticles without the need of further additives. Solano *et al.*[338] compared the synthesis of MFe_2O_4 (M = Fe, Co, Mn, Ni, and Zn) through solvothermal and microwave-assisted routes in TREG. With both methods, particles of similar size were obtained. However, the use of microwave heating, besides shortening the reaction time, significantly influenced nanoparticle nucleation, leading to monodisperse size distribution and absence of nanoparticle aggregation (Fig. 18).

In order to better highlight whether microwaves influence the ferrite synthesis, the same authors performed a structural comparison with the solvothermal synthetic route on the same systems prepared in ref.[338] using X-ray and neutron diffraction methods.[331] With the only exception of $ZnFe_2O_4$, for which the microwave synthesis induced much higher inversion degree than the thermal approach, the cationic distribution microstructure and magnetic properties of the materials were very similar independent of the synthesis method used. In particular, neutron diffraction studies demonstrated the absence of H atoms and related organic matter coming from the TREG capping ligand, pointing out the improved dispersion of microwave-assisted materials. Schneider and co-workers demonstrated how the TREG-based microwave synthesis is also suitable for upscaling magnetite nanoparticles from milligram to grams.[339] Even though the scalability of the nanoparticles increased their size polydispersity, most likely due temperature gradient issues in the reaction vessel, the materials were produced below 1 h and still possessed high saturation of magnetization.

Besides hydrothermal and solvothermal approaches, which represent the majority of the synthesis processes, the microwave heating for the preparation of spinel ferrites has been combined also with combustion[340,341] and sol–gel methods.[342–344]

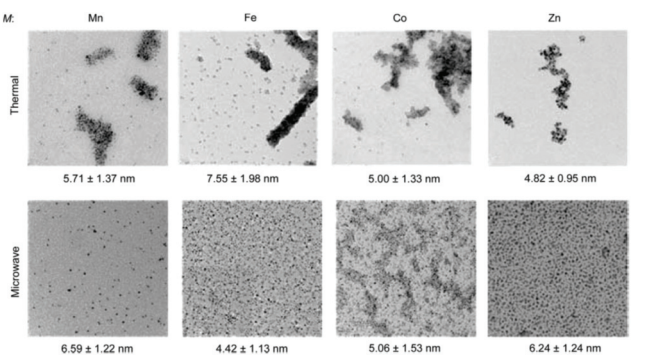

Fig. 18 TEM images of MFe_2O_4 nanoparticles synthesized by the thermal and microwave synthetic routes. For all the investigated cases, the microwave synthesis produces highly homogeneously dispersed nanoparticles. The numbers below each image display the average nanoparticle size with its deviation. Reproduced with permission from Solano *et al.*[331]

The magnetic properties and antimicrobial performance of $NiFe_2O_4$ nanopowders prepared with microwave-assisted combustion method were compare to those obtained *via* conventional approaches.[340] The faster synthesis induced by the electromagnetic fields engendered nanoparticles with almost half of the size of those obtained by standard procedures. As a result, the materials possessed improved magnetic properties and antimicrobial character. In another work, conventional and microwave methods were compared using urea and citric acid fuels for the synthesis of $CoFe_2O_4$ nanopowders.[341] The weaker chelating power of urea with respect to citric acid failed to deliver phase pure ferrites for both approaches. Using citric acid, microwave ignition engendered larger sphere-like ferrite particles with higher inversion degree than those obtained with the conventional approach. For these reasons, and despite small impurities of CoO and CoFe, the microwave-assisted materials also showed better magnetic properties.

The combination of microwave heating with non-aqueous sol–gels offers an intriguing chance for the rational design of spinel ferrite materials beyond the simple synthesis of nanoparticles. Niederberger and co-workers showed how the reaction of metal acetate or acetylacetonates with benzyl alcohol in presence of microwave irradiation yielded Fe_3O_4, $CoFe_2O_4$, $MnFe_2O_4$, and $NiFe_2O_4$ nanoparticles within 12 minutes at 170 °C.[342] The introduction into the reaction mixture of glass substrates or metal nanoparticles enabled the preparation of ferrite thin films and core–shell systems, respectively (Fig. 19).

This route was implemented by Suchomski *et al.*[343] for the synthesis of monodispersed $ZnFe_2O_4$ nanoparticles of spherical shape. Detailed structural and magnetic characterization evidenced an inversion degree of 68% and the presence of a superspin glass state with freezing temperature of about 22 K. In addition, the materials exhibited promising performance as anode material for Li-ion battery with little capacity fading after hundreds of cycles.

Furthermore, the coating capability of the microwave-assisted sol–gel approach has been used for the preparation of ordered macroporous magnetic $MnFe_2O_4$ architectures through nanoparticle deposition on sacrificial colloidal crystals.[344] The control of synthesis parameters such reaction time enabled tuning of the coating thickness and layer homogeneity.

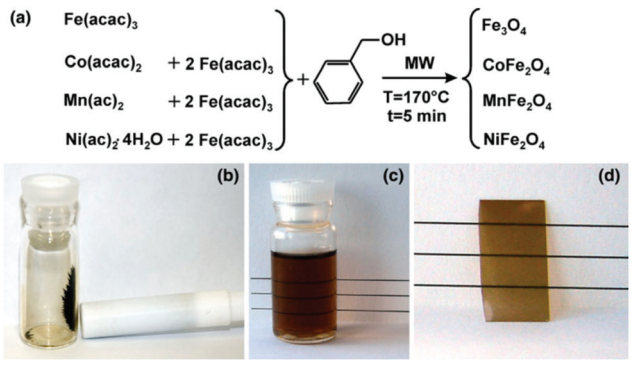

Fig. 19 (a) General reaction scheme displaying the metal oxide precursors employed in the sol–gel synthesis, the solvent, the experimental conditions, and the final composition of the nanoparticles. Photographs of (b) magnetite nanopowder under the influence of a permanent magnet, (c) $CoFe_2O_4$ dispersion in ethanol, and (d) $CoFe_2O_4$ film on a glass substrate. Reproduced with permission from Bilecka *et al.*[342]

Ferrites with perovskite structure

In contrast to the spinel structure, perovskites are characterised by large size difference between the A and B cations. This has strong repercussions on their synthesis conditions, such that perovskite systems tend to require higher temperatures for their formation compared to spinels.[346] Therefore, the low temperature synthesis of ferrites with the perovskite structure is less common. The main contributions in the literature on this field regard mainly $BiFeO_3$. In combination with microwave irradiation, the hydrothermal method represents the principal low temperature synthetic approach. To ensure homogeneous cationic intermixing, avoid the formation of multiphase impurities, and control the particle morphology, polyelectrolytes or surfactants are generally employed in the reaction mixture. Chybczynska and co-workers showed how the petal size and crystallinity of $BiFeO_3$ flower-like particles increased with the amount of polyethylene glycol used in the microwave-assisted hydrothermal synthesis, which was directly correlated with a decrease of the magnetic properties.[347] Besides its interesting magnetic properties, $BiFeO_3$ is a well-known photocatalyst. With respect to conventional hydrothermal method, the preparation of bismuth ferrite with the assistance of microwave heating resulted in materials with higher crystallinity and specific surface area, ascribed to non-thermal effects of microwave during the synthesis.[348] As a result, the materials possessed better photocatalytic properties for the photodegradation of organic dyes. Similar photocatalytic tests were performed by Huang *et al.*[349] on $BiFeO_3$ materials prepared by a microwave-assisted hydrothermal approach using different surfactants molecules as capping agents. The employment of polyvinylpirrolidone instead of EDTA engendered materials with almost four times higher specific surface area, which lead to a significant improvement of the material's photocatalytic performance.

The perovskite structure is well-known for its structural flexibility enabling the incorporation of substitutional metal ions. However, there are very few examples of doped perovskite ferrites in literature obtained by low temperature approaches with the assistance of electromagnetic heating. Ultrathin (~2.5 nm) Cr-doped $BiFeO_3$ ferroelectric films were obtained by hydrothermal approach without any use of mineralizer.[350] Due to the microwave-assisted approach, after only 2 cycles irradiation, atomic step terraces were observed on the films indicating the high ordered growth of the film. The resistive switching behaviour of the films was confirmed by electrical characterization and thermoionic emission was demonstrated to be the dominating charge transport behaviour. Ponzoni *et al.*[155] showed how the preparation of A-site substituted $Bi_{1-x}La_xFeO_3$ up to x = 0.45 could be remarkably accelerated using microwave-assisted hydrothermal synthesis with respect

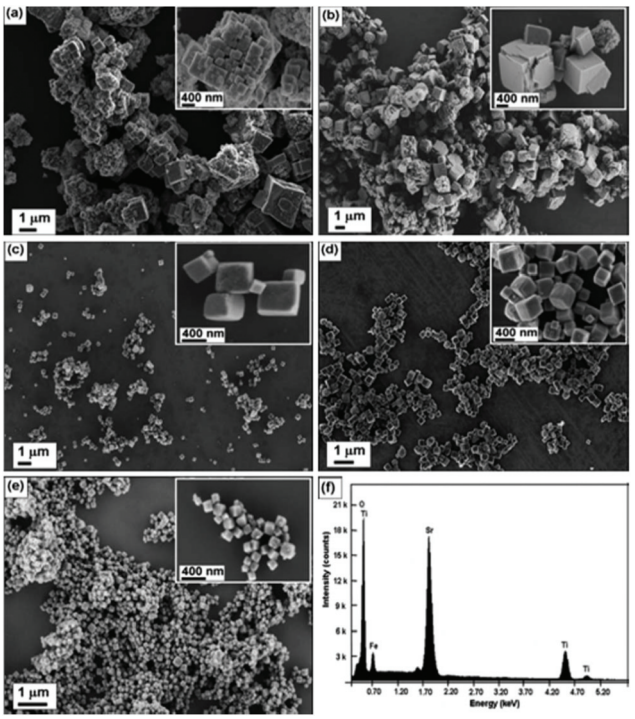

Fig. 20 SEM images of $SrTi_{1-x}Fe_xO_3$ samples prepared *via* microwave-assisted hydrothermal method: x = 0.0 (a), 0.05 (b), 0.1 (c), 0.25 (d), 0.4 (e); (f) EDX spectrum of the x = 0.25 sample Reproduced with permission from da Silva *et al.*[345]

to the conventional method. In a further, report solid solutions of $SrFeO_3$ and $SrTiO_3$ in form of nanocubes could be prepared at 140 °C and a constant pressure of 3 bar by a microwave heated hydrothermal approach (Fig. 20).[345] X-ray and UV spectroscopies revealed that the Fe^{2+}/Fe^{3+} ions occupy the Ti^{4+} sites and that the band gap progressively decreases with the iron amount. In the same work, this synthetic route was also used to prepare films by the tape casting or the suspension methodology.

Other approaches

In this section we will provide examples of synthesis approaches that are not sufficiently featured in the literature to merit their own section. Broadly, they belong to one of two subsets: (i) methods that are not particularly popular (generally because other, more widespread approaches are considered preferable and/or less complex) and (ii) methods that generally involve a high-temperature calcination step and therefore only feature very few examples that may qualify as low-temperature (coprecipitation[353] is one of these latter approaches).

Biosynthesis, includes syntheses where the chemical reactions are aided by biological systems (*e.g.* by having bacteria reduce metal cations through anaerobic respiration).[351] Byrne *et al.*[351] synthesised zinc-substituted magnetite $Zn_xFe_{3-x}O_4$ (x = 0.00, 0.16, 0.42, 0.56, 0.92) through bacterially-assisted synthesis whereby zinc and iron oxyhydroxides were initially coprecipitated from an aqueous solution and then were inoculated with a culture of *Geobacter sulfurreducens* (0.2 mg mL^{-1} protein) and acetate (acting as electron donor for the reduction) and incubated in the dark at 30 °C. Crystalline nanoparticles (Fig. 21) with enhanced magnetic properties were thus obtained.

Similarly Céspedes *et al.*[61] employed bacterial synthesis to prepare several different Zn- or Co-doped ferrite spinel nanoparticles with citric acid coating for applications in magnetic hyperthermia therapy $M_xFe_{3-x}O_4$ (M = Co, Zn; x = 0.00, 0.16, 0.42, 0.71). As described by Byrne *et al.*, Fe and M oxohydroxide mixtures were coprecipitated from an aqueous medium and then treated with a *Geobacter sulfurreducens* culture. It was found that the stoichiometry of M in the final ferrite could be controlled by varying the concentration of M in the M–Fe^{III}-oxyhydroxide intermediate species.

Whereas ball-milling is a well-known top-down dry synthesis method for ferrites,[354–357] Chen *et al.*[358,359] combined ball-milling and ultrasound technology in an aqueous suspension to obtain nickel and manganese spinel ferrite nanoparticles. In both cases the M precursors (either MnO_2 or $NiCO_3{\cdot}2Ni(OH)_2{\cdot}4H_2O$) were milled at room temperature in 1000 ml of ultrapure water together with the iron precursor (either metallic iron powder or iron coming directly from pure iron milling balls). The diameter of the milling balls was 1.0–1.5 mm and a ball to powder mass ratio was 100 : 1. The rotation speed of stirrer was 235 rpm, and the ultrasonic intensity and power were 40 kHz and 200 W, respectively.

The sol–gel auto-combustion approach (and the citrate method in particular), is widely known and applied in the field of ferrite synthesis,[360–363] but in most cases either the auto-combustion process must be triggered at high temperatures, or a calcination step is then employed to reach crystallisation. By contrast, Xiao *et al.*[352] achieved the cobalt spinel

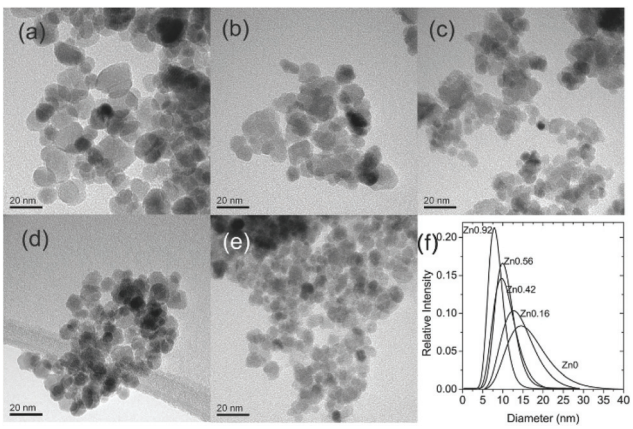

Fig. 21 TEM images showing (a) Zn_0, (b) $Zn_{0.16}$, (c) $Zn_{0.42}$, (d) $Zn_{0.56}$, (e) $Zn_{0.92}$, and (f) size distributions of all samples prepared through bacterially-assisted synthesis. Data obtained by measurement of n = 200 particle diameters per sample. Reproduced from Byrne *et al.*[351]

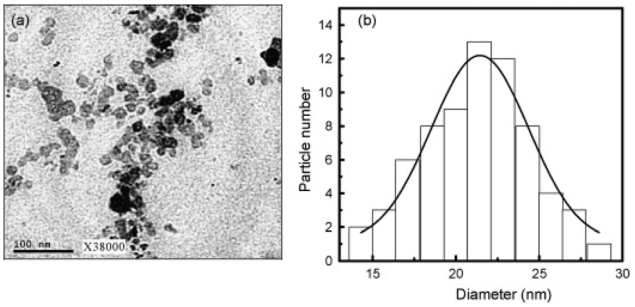

Fig. 22 Cobalt spinel $CoFe_2O_4$ synthesised by a modified citrate sol–gel approach: TEM morphology of the as-burnt powder (a) and corresponding grain size histogram obtained by statistical method (b). Reproduced with permission from Gass *et al.*[352]

$CoFe_2O_4$ by a modified citrate sol–gel approach, affording auto-combustion and formation of crystalline cobalt ferrite powder already at 200 °C (Fig. 22). The synthesis, from an aqueous mixture of citric acid and metal nitrates was stirred at pH 6 until a sol formed. This sol was changed to a gel at 80 °C and into a xerogel at 120 °C. Finally, auto-combustion was triggered at 200 °C yielding the ferrite powder. The combustion was proven to be a thermally induced anionic redox reaction, with carboxyl group as reductant and nitrate ions as oxidant.

Conclusions

We have collected and reviewed recent contributions concerning different wet-chemistry routes, having as common factor the use of low temperature, for the synthesis of different classes of ferrites, focussing largely on materials belonging to the spinel, perovskite and hexaferrite families. The discussion of the different examples reported illustrates that this relevant family of functional materials can be also addressed by relatively environmentally friendly and, in many cases, simple to implement solution- or suspension-based synthesis approaches. As well as complying with the principles of 'green chemistry' the solution-mediated synthetic methods that we have surveyed offer the prospect of industrially-scalable manufacture of materials, as illustrated by the implementation of continuous flow reactors that can feasibly allow efficient production of suitable volumes of powdered ferrites. From the fundamental chemistry point of view, an advantage of the solution synthesis of mixed-metal oxides can lie in the control of distributions of substituent metal cations in solid solutions or during isomorphous replacement. This may allow formation of atomically homogeneous materials, or, on the other hand, the intentional construction of core–shell particles, thus allowing tuning of properties beyond chemical composition and crystal structure. A second benefit of solution crystallisation lies in the possibility of control of crystal morphology with size from the nanoscale to the micron-scale and shape from isotropic spheres and cubes, to highly isotropic rods and plates and multifaceted intricate structures. This can provide novel materials, for example, in the study of nanoscale confinement effects in electronic and magnetic properties, or for use as additives in composites, as well as with surface properties tuned for catalysis.

We hope that our collection of examples will promote further research in this fascinating field, which represents an exciting playground for inorganic materials synthesis. The implementation of syntheses for pursuing anisotropy and shape-control in crystal form is particularly appealing, which is relevant for many applications, such as in heterogeneous catalysis, nanocomposite formation and nanotechnology, as well as in processing of powders towards real applications. Hydrothermal and solvothermal methods uniquely allow the direct formation of oxide materials from solution under very mild conditions, without the use of the extreme temperatures needed for classical oxide preparation. While this is highly advantageous for particle growth, this may mean that only certain compositions and structure are accessible since crystallisation is under strictly kinetic control, without forcing high temperatures to reach all possible stoichiometries. This may be a limitation of soft-chemical methods in general, but on the other hand metastable compositions or structures may be accessible that do not survive extreme temperatures, such as the hexagonal $REFeO_3$ perovskites that irreversibly transform on heating to the classical perovskite structure. The occurrence of competing phases from a given reagent mixture as a function if temperature, time or pH is a further complication when exploring new reaction conditions, as was illustrated in the case of $BiFeO_3$.

Predictability of synthetic chemistry and true control of crystal morphology remains in its infancy but as we have illustrated, with the exploration of a wide variety of solvents and solution additives, progress is being made to allow desired particle size and shape in mixed-oxides to be achieved. The examples we have selected from the literature show how particle morphology can be tuned from the nanoscale to the microscale from highly facetted to anisotropic crystals, but for most of these cases the mechanism of crystal engineering is unknown and not even speculated. Much further work is needed to establish crystal growth mechanism, and this must include both experimental and computation approaches. This leads to the possibility of tailor-made materials with desirable functional properties selected by synthetic chemistry in convenient and scalable processes.

Conflicts of interest

There are no conflicts to declare.

References

1 S. Hazra and N. N. Ghosh, Preparation of nanoferrites and their applications, *J. Nanosci. Nanotechnol.*, 2014, **14**, 1983–2000.

2 M. K. Singh, Y. Yang and C. G. Takoudis, Synthesis of multifunctional multiferroic materials from metalorganics, *Coord. Chem. Rev.*, 2009, **253**, 2920–2934.
3 K. K. Kefeni, T. A. M. Msagati and B. B. Mamba, Ferrite nanoparticles: Synthesis, characterisation and applications in electronic device, *Mater. Sci. Eng., B*, 2017, **215**, 37–55.
4 E. Casbeer, V. K. Sharma and X.-Z. Li, Synthesis and photocatalytic activity of ferrites under visible light: A review, *Sep. Purif. Technol.*, 2012, **87**, 1–14.
5 I. H. Gul and A. Maqsood, Structural, magnetic and electrical properties of cobalt ferrites prepared by the sol–gel route, *J. Alloys Compd.*, 2008, **465**, 227–231.
6 S. Jauhar, J. Kaur, A. Goyal and S. Singhal, Tuning the properties of cobalt ferrite: a road towards diverse applications, *RSC Adv.*, 2016, **6**, 97694–97719.
7 Y.-K. Hong and J. Lee, in *Recent Advances in Magnetic Insulators – From Spintronics to Microwave Applications*, ed. M. Wu and A. Hoffmann, Academic Press, 2013, vol. 64, pp. 237–329.
8 I. V. Lisnevskaya, I. A. Bobrova and T. G. Lupeiko, Synthesis of magnetic and multiferroic materials from polyvinyl alcohol-based gels, *J. Magn. Magn. Mater.*, 2016, **397**, 86–95.
9 N. R. Ram, M. Prakash, U. Naresh, N. S. Kumar, T. S. Sarmash, T. Subbarao, R. J. Kumar, G. R. Kumar and K. C. B. Naidu, Review on magnetocaloric effect and materials, *J. Supercond. Novel Magn.*, 2018, **31**, 1971–1979.
10 T. Hyeon, Chemical synthesis of magnetic nanoparticles, *Chem. Commun.*, 2003, 927–934, DOI: 10.1039/B207789B.
11 V. S. R. Kalluri, S. Melad, S. Aanchal and S. Gaddipati, Catalytic activity of functionalized spinels, *Curr. Org. Chem.*, 2017, **21**, 2573–2584.
12 R. Hudson, Y. Feng, R. S. Varma and A. Moores, Bare magnetic nanoparticles: sustainable synthesis and applications in catalytic organic transformations, *Green Chem.*, 2014, **16**, 4493–4505.
13 G. Kaur, P. Devi, S. Thakur, A. Kumar, R. Chandel and B. Banerjee, Magnetically separable transition metal ferrites: Versatile heterogeneous nano-catalysts for the synthesis of diverse bioactive heterocycles, *ChemistrySelect*, 2019, **4**, 2181–2199.
14 O. Vozniuk, T. Tabanelli, N. Tanchoux, M. J.-M. Millet, S. Albonetti, F. Di Renzo and F. Cavani, Mixed-oxide catalysts with spinel structure for the valorization of biomass: The chemical-loop reforming of bioethanol, *Catalysts*, 2018, **8**, 332.
15 A. Antonello, G. Jakob, P. Dolcet, R. Momper, M. Kokkinopoulou, K. Landfester, R. Muñoz-Espí and S. Gross, Synergy of miniemulsion and solvothermal conditions for the low-temperature crystallization of magnetic anostructured transition-metal ferrites, *Chem. Mater.*, 2017, **29**, 985–997.
16 F. de Lira, M. de Souza Farias, A. de Figueiredo, F. dos Santos Gil, M. dos Santos, B. Malheiros, J. Ferreira, J. Pinheiro, O. Treu-Filho and R. Kondo, Quantum chemical modeling of perovskite: An investigation of piezoelectricity in ferrite of yttrium, *J. Mol. Model.*, 2011, **17**, 1621–1624.
17 Q.-H. Jiang, C.-W. Nan and Z.-J. Shen, Synthesis and Properties of Multiferroic La-Modified $BiFeO_3$ Ceramics, *J. Am. Ceram. Soc.*, 2006, **89**, 2123–2127.
18 H. Shokrollahi and L. Avazpour, Influence of intrinsic parameters on the particle size of magnetic spinel nanoparticles synthesized by wet chemical methods, *Particuology*, 2016, **26**, 32–39.
19 R. Masrour, M. Hamedoun and A. Benyoussef, Magnetic properties of B and AB-spinels $Zn_{1-x}M_xFe_2O_4$ (M=Ni, Mg) materials, *J. Alloys Compd.*, 2010, **503**, 299–302.
20 A. H. Latham and M. E. Williams, Controlling transport and chemical functionality of magnetic nanoparticles, *Acc. Chem. Res.*, 2008, **41**, 411–420.
21 D. H. K. Reddy and Y.-S. Yun, Spinel ferrite magnetic adsorbents: Alternative future materials for water purification?, *Coord. Chem. Rev.*, 2016, **315**, 90–111.
22 E. A. Périgo, G. Hemery, O. Sandre, D. Ortega, E. Garaio, F. Plazaola and F. J. Teran, Fundamentals and advances in magnetic hyperthermia, *Appl. Phys. Rev.*, 2015, **2**, 041302.
23 I. Sharifi, H. Shokrollahi and S. Amiri, Ferrite-based magnetic nanofluids used in hyperthermia applications, *J. Magn. Magn. Mater.*, 2012, **324**, 903–915.
24 T. Gao, Z. Chen, Q. Huang, F. Niu, X. Huang, L. Qin and Y. Huang, A review: Preparation of bismuth ferrite nanoparticles and its applications in visible-light induced photocatalyses, *Rev. Adv. Mater. Sci.*, 2015, **40**, 97–109.
25 S. Chandrasekaran, C. Bowen, P. Zhang, Z. Li, Q. Yuan, X. Ren and L. Deng, Spinel photocatalysts for environmental remediation, hydrogen generation, CO_2 reduction and photoelectrochemical water splitting, *J. Mater. Chem. A*, 2018, **6**, 11078–11104.
26 S.-M. Lam, J.-C. Sin and A. R. Mohamed, A newly emerging visible light-responsive $BiFeO_3$ perovskite for photocatalytic applications: A mini review, *Mater. Res. Bull.*, 2017, **90**, 15–30.
27 B. Zhang, J. Zhang and F. Chen, Preparation and characterization of magnetic $TiO_2/ZnFe_2O_4$ photocatalysts by a sol–gel method, *Res. Chem. Intermed.*, 2008, **34**, 375–380.
28 A. Becker, K. Kirchberg and R. Marschall, Magnesium ferrite ($MgFe_2O_4$) nanoparticles for photocatalytic antibiotics degradation, *Z. Phys. Chem.*, 2020, **234**, 645–654.
29 K. Kirchberg, A. Becker, A. Bloesser, T. Weller, J. Timm, C. Suchomski and R. Marschall, Stabilization of monodisperse, phase-pure $MgFe_2O_4$ nanoparticles in aqueous and nonaqueous media and their photocatalytic behavior, *J. Phys. Chem. C*, 2017, **121**, 27126–27138.
30 K. Kirchberg, S. Wang, L. Wang and R. Marschall, Mesoporous $ZnFe_2O_4$ photoanodes with template-tailored mesopores and temperature-dependent photocurrents, *ChemPhysChem*, 2018, **19**, 2313–2320.
31 K. Kirchberg and R. Marschall, Sol–gel synthesis of mesoporous $CaFe_2O_4$ photocathodes with hierarchical pore morphology, *Sustainable Energy Fuels*, 2019, **3**, 1150–1153.

32 R. Tilley, *Understanding Solids - The Science of Materials*, J. Wiley & Sons, Chichester, West Sussex, England, 2004.
33 A. Hajalilou and S. A. Mazlan, A review on preparation techniques for synthesis of nanocrystalline soft magnetic ferrites and investigation on the effects of microstructure features on magnetic properties, *Appl. Phys. A: Mater. Sci. Process.*, 2016, **122**, 680.
34 D. S. Mathew and R.-S. Juang, An overview of the structure and magnetism of spinel ferrite nanoparticles and their synthesis in microemulsions, *Chem. Eng. J.*, 2007, **129**, 51–65.
35 D. Cruickshank, 1–2 GHz dielectrics and ferrites: overview and perspectives, *J. Eur. Ceram. Soc.*, 2003, **23**, 2721–2726.
36 R. C. Pullar, Hexagonal ferrites: A review of the synthesis, properties and applications of hexaferrite ceramics, *Prog. Mater. Sci.*, 2012, **57**, 1191–1334.
37 J. P. Jolivet, C. Chaneac, P. Prene, L. Vayssieres and E. Tronc, Wet chemistry of spinel iron oxide particles, *J. Phys. IV*, 1997, **7**, C1-573–C1-576.
38 R. Kesavamoorthi and C. R. Raja, Studies on the properties of manganese substituted nickel ferrite nanoparticles, *J. Supercond. Novel Magn.*, 2016, **29**, 2729–2734.
39 J.-B. Moussy, From epitaxial growth of ferrite thin films to spin-polarized tunnelling, *J. Phys. D: Appl. Phys.*, 2013, **46**, 143001.
40 T.-D. Nguyen, From formation mechanisms to synthetic methods toward shape-controlled oxide nanoparticles, *Nanoscale*, 2013, **5**, 9455–9482.
41 V. C. B. Pegoretti, P. R. C. Couceiro, C. M. Goncalves, M. d. F. F. Lelis and J. D. Fabris, Preparation and characterization of tin-doped spinel ferrite, *J. Alloys Compd.*, 2010, **505**, 125–129.
42 P. Raju and S. R. Murthy, Preparation and characterization of Ni–Zn ferrite + polymer nanocomposites using mechanical milling method, *Appl. Nanosci.*, 2013, **3**, 469–475.
43 H. H. Sønsteby, H. Fjellvåg and O. Nilsen, Functional perovskites by atomic layer deposition – An overview, *Adv. Mater. Interfaces*, 2017, **4**, 1600903.
44 R. Safi and H. Shokrollahi, Physics, chemistry and synthesis methods of nanostructured bismuth ferrite ($BiFeO_3$) as a ferroelectro-magnetic material, *Prog. Solid State Chem.*, 2012, **40**, 6–15.
45 M. Sugimoto, The past, present, and future of ferrites, *J. Am. Ceram. Soc.*, 1999, **82**, 269–280.
46 V. Mameli, M. S. Angotzi, C. Cara and C. Cannas, Liquid Phase Synthesis of Nanostructured Spinel Ferrites A-Review, *J. Nanosci. Nanotechnol.*, 2019, **19**, 4857–4887.
47 P. T. Anastas and J. C. Warner, *Green Chemistry Theory and Practice*, Oxford University Press, New York, Paperback Ed., 2000.
48 P. A. Cox, *Transition Metal Oxides : Introduction to their Electronic Structure and Properties*, Oxford University Press, Oxford, U.K., 1995.
49 G. F. Dionne, *Magnetic oxides*, Springer, London, 1st edn, 2009.
50 N. N. Greenwood and A. Earnshaw, *Chemistry of the Elements*, Pergamon Press, India, 2nd edn, 1998.
51 A. F. Holleman and E. Wieberg, *Lehrbuch der Anorganischen Chemie*, Walter de Gruyter, New York, 101th edn, 1995.
52 D. Carta, M. F. Casula, A. Falqui, D. Loche, G. Mountjoy, C. Sangregorio and A. Corrias, A Structural and Magnetic Investigation of the Inversion Degree in Ferrite Nanocrystals MFe_2O_4 (M = Mn, Co, Ni), *J. Phys. Chem. C*, 2009, **113**, 8606–8615.
53 V. Blanco-Gutiérrez, M. J. Torralvo, R. Sáez-Puche and P. Bonville, Magnetic properties of solvothermally synthesized $ZnFe_2O_4$ nanoparticles, *J. Phys.: Conf. Ser.*, 2010, **200**, 072013.
54 P. Dolcet, K. Kirchberg, A. Antonello, C. Suchomski, R. Marschall, S. Diodati, R. Muñoz-Espí, K. Landfester and S. Gross, Exploring wet chemistry approaches to $ZnFe_2O_4$ spinel ferrite nanoparticles with different inversion degrees: a comparative study, *Inorg. Chem. Front.*, 2019, **6**, 1527–1534.
55 L. I. Granone, R. Dillert, P. Heitjans and D. W. Bahnemann, Effect of the degree of inversion on the electrical conductivity of spinel $ZnFe_2O_4$, *ChemistrySelect*, 2019, **4**, 1232–1239.
56 L. I. Granone, A. C. Ulpe, L. Robben, S. Klimke, M. Jahns, F. Renz, T. M. Gesing, T. Bredow, R. Dillert and D. W. Bahnemann, Effect of the degree of inversion on optical properties of spinel $ZnFe_2O_4$, *Phys. Chem. Chem. Phys.*, 2018, **20**, 28267–28278.
57 P. Rajagiri, B. N. Sahu, N. Venkataramani, S. Prasad and R. Krishnan, Effect of substrate temperature on magnetic properties of $MnFe_2O_4$ thin films, *AIP Adv.*, 2018, **8**, 056112.
58 J. Jacob and M. A. Khadar, Investigation of mixed spinel structure of nanostructured nickel ferrite, *J. Appl. Phys.*, 2010, **107**, 114310.
59 M. Bastianello, S. Diodati, N. Dengo, L. McCafferty, C. Footer, D. Badocco, P. Pastore, J. Darr and S. Gross, Quaternary ferrites by batch and continuous flow hydrothermal synthesis: a comparison, *CrystEngComm*, 2019, **21**, 6801–6809.
60 M. Bastianello, S. Gross and M. T. Elm, Thermal stability, electrochemical and structural characterization of hydrothermally synthesised cobalt ferrite ($CoFe_2O_4$), *RSC Adv.*, 2019, **9**, 33282–33289.
61 E. Céspedes, J. M. Byrne, N. Farrow, S. Moise, V. S. Coker, M. Bencsik, J. R. Lloyd and N. D. Telling, Bacterially synthesized ferrite nanoparticles for magnetic hyperthermia applications, *Nanoscale*, 2014, **6**, 12958–12970.
62 G. Fan, J. Tong and F. Li, Visible-light-induced photocatalyst based on cobalt-doped zinc ferrite nanocrystals, *Ind. Eng. Chem. Res.*, 2012, **51**, 13639–13647.
63 C. M. B. Henderson, J. M. Charnock and D. A. Plant, Cation occupancies in Mg, Co, Ni, Zn, Al ferrite spinels: a multi-element EXAFS study, *J. Phys.: Condens. Matter*, 2007, **19**, 076214.

64 C.-K. Kim, J.-H. Lee, S. Katoh, R. Murakami and M. Yoshimura, Synthesis of Co-, Co-Zn and Ni-Zn ferrite powders by the microwave-hydrothermal method, *Mater. Res. Bull.*, 2001, **36**, 2241–2250.
65 M. Maletin, E. G. Moshopoulou, A. G. Kontos, E. Devlin, A. Delimitis, V. T. Zaspalis, L. Nalbandian and V. V. Srdic, Synthesis and structural characterization of In-doped $ZnFe_2O_4$ nanoparticles, *J. Eur. Ceram. Soc.*, 2007, **27**, 4391–4394.
66 K. Pemartin, C. Solans, J. Alvarez-Quintana and M. Sanchez-Dominguez, Synthesis of Mn–Zn ferrite nanoparticles by the oil-in-water microemulsion reaction method, *Colloids Surf., A*, 2014, **451**, 161–171.
67 Y. Zhang and D. Wen, Infrared emission properties of RE (RE=La, Ce, Pr, Nd, Sm, Eu, Gd, Tb, and Dy) and Mn co-doped $Co_{0.6}Zn_{0.4}Fe_2O_4$ ferrites, *Mater. Chem. Phys.*, 2012, **131**, 575–580.
68 R. Mohan, M. P. Ghosh and S. Mukherjee, Size dependent exchange bias in single-phase $Zn_{0.3}Ni_{0.7}Fe_2O_4$ ferrite nanoparticles, *J. Magn. Magn. Mater.*, 2018, **458**, 193–199.
69 A. Yadav and D. Varshney, Structural and temperature dependent dielectric behavior of Cr and Zn doped $MnFe_2O_4$ nano ferrites, *Superlattices Microstruct.*, 2018, **113**, 153–159.
70 C. Virlan, F. Tudorache and A. Pui, Increased sensibility of mixed ferrite humidity sensors by subsequent heat treatment, *Int. J. Appl. Ceram. Technol.*, 2017, **14**, 1174–1182.
71 J.-S. Kim, J.-R. Ahn, C. W. Lee, Y. Murakami and D. Shindo, Morphological properties of ultra-fine (Ni,Zn)-ferrites and their ability to decompose CO_2, *J. Mater. Chem.*, 2001, **11**, 3373–3376.
72 I. Ahmad, S. M. Shah, M. N. Ashiq and R. A. Khan, Effect of Nd^{3+} and Cd^{2+} ions co-substitution on the dielectric and electron transport properties of spinel strontium nanoferrites, *Ceram. Int.*, 2016, **42**, 12763–12770.
73 A. K. M. Akther Hossain, M. Seki, T. Kawai and H. Tabata, Colossal magnetoresistance in spinel type $Zn_{1-x}Ni_xFe_2O_4$, *J. Appl. Phys.*, 2004, **96**, 1273–1275.
74 A. S. Albuquerque, J. D. Ardisson, W. A. A. Macedo, J. L. López, R. Paniago and A. I. C. Persiano, Structure and magnetic properties of nanostructured Ni-ferrite, *J. Magn. Magn. Mater.*, 2001, **226–230**(Part 2), 1379–1381.
75 S. Feng, W. Yang and Z. Wang, Synthesis of porous $NiFe_2O_4$ microparticles and its catalytic properties for methane combustion, *Mater. Sci. Eng., B*, 2011, **176**, 1509–1512.
76 K.-S. Lin, C.-L. Chiang, P.-J. Hsu, K. Bat-Erdene, C.-Y. Tang and C.-M. Wu, Magnetic separation and recycling of ferrite nanocatalysts for CO_2 decomposition with CH_4 recovery from steel industrial flyash, *Catal. Today*, 2018, **307**, 260–271.
77 U. Luders, A. Barthelemy, M. Bibes, K. Bouzehouane, S. Fusil, E. Jacquet, J.-P. Contour, J.-F. Bobo, J. Fontcuberta and A. Fert, $NiFe_2O_4$: a versatile spinel material brings new opportunities for spintronics, *Adv. Mater.*, 2006, **18**, 1733–1736.
78 T. Dai Lam, L. Van Hong, P. Hoai Linh, H. Thi My Nhung, N. Thi Quy, L. Thien Tai, H. Phuong Thu and N. Xuan Phuc, Biomedical and environmental applications of magnetic nanoparticles, *Adv. Nat. Sci.: Nanosci. Nanotechnol.*, 2010, **1**, 045013.
79 H.-M. Fan, J.-B. Yi, Y. Yang, K.-W. Kho, H.-R. Tan, Z.-X. Shen, J. Ding, X.-W. Sun, M. C. Olivo and Y.-P. Feng, Single-Crystalline MFe_2O_4 Nanotubes/Nanorings Synthesized by Thermal Transformation Process for Biological Applications, *ACS Nano*, 2009, **3**, 2798–2808.
80 M. R. Phadatare, V. M. Khot, A. B. Salunkhe, N. D. Thorat and S. H. Pawar, Studies on polyethylene glycol coating on $NiFe_2O_4$ nanoparticles for biomedical applications, *J. Magn. Magn. Mater.*, 2012, **324**, 770–772.
81 A. Seyfoori, S. A. S. Ebrahimi, S. Omidian and S. M. Naghib, Multifunctional magnetic $ZnFe_2O_4$-hydroxyapatite nanocomposite particles for local anti-cancer drug delivery and bacterial infection inhibition: An in vitro study, *J. Taiwan Inst. Chem. Eng.*, 2019, **96**, 503–508.
82 C. V. Gopal Reddy, S. V. Manorama and V. J. Rao, Semiconducting gas sensor for chlorine based on inverse spinel nickel ferrite, *Sens. Actuators, B*, 1999, **55**, 90–95.
83 S. Darshane and I. S. Mulla, Influence of palladium on gas-sensing performance of magnesium ferrite nanoparticles, *Mater. Chem. Phys.*, 2010, **119**, 319–323.
84 X. F. Wu, W. Wang, F. Li, S. Khaimanov, N. Tsidaeva and M. Lahoubi, PEG-assisted hydrothermal synthesis of $CoFe_2O_4$ nanoparticles with enhanced selective adsorption properties for different dyes, *Appl. Surf. Sci.*, 2016, **389**, 1003–1011.
85 R. P. Sharma, S. D. Raut, V. V. Jadhav, A. S. Kadam and R. S. Mane, Anti-candida and anti-adhesion efficiencies of zinc ferrite nanoparticles, *Mater. Lett.*, 2019, **237**, 165–167.
86 M. Foerster, J. M. Rebled, S. Estrade, F. Sanchez, F. Peiro and J. Fontcuberta, Distinct magnetism in ultrathin epitaxial $NiFe_2O_4$ films on $MgAl_2O_4$ and $SrTiO_3$ single crystalline substrates, *Phys. Rev. B: Condens. Matter Mater. Phys.*, 2011, **84**, 144422.
87 M. Junaid, M. A. Khan, F. Iqbal, G. Murtaza, M. N. Akhtar, M. Ahmad, I. Shakir and M. F. Warsi, Structural, spectral, dielectric and magnetic properties of Tb–Dy doped Li-Ni nano-ferrites synthesized via micro-emulsion route, *J. Magn. Magn. Mater.*, 2016, **419**, 338–344.
88 S. Sun, H. Zeng, D. B. Robinson, S. Raoux, P. M. Rice, S. X. Wang and G. Li, Monodisperse MFe_2O_4 (M = Fe, Co, Mn) Nanoparticles, *J. Am. Chem. Soc.*, 2004, **126**, 273–279.
89 A. S. Bhalla, R. Y. Guo and R. Roy, The perovskite structure - a review of its role in ceramic science and technology, *Mater. Res. Innovations*, 2000, **4**, 3–26.
90 R. L. White, Review of Recent Work on the Magnetic and Spectroscopic Properties of the Rare-Earth Orthoferrites, *J. Appl. Phys.*, 1969, **40**, 1061–1069.
91 K. K. Bamzai and M. Bhat, Electrical and Magnetic Properties of Some Rare Earth Orthoferrites ($RFeO_3$ where R = Y, Ho, Er) Systems, *Integr. Ferroelectr.*, 2014, **158**, 108–122.

92 J. Silva, A. Reyes, H. Esparza, H. Camacho and L. Fuentes, $BiFeO_3$: A Review on Synthesis, Doping and Crystal Structure, *Integr. Ferroelectr.*, 2011, **126**, 47–59.

93 J. G. Wu, Z. Fan, D. Q. Xiao, J. G. Zhu and J. Wang, Multiferroic bismuth ferrite-based materials for multifunctional applications: Ceramic bulks, thin films and nanostructures, *Prog. Mater. Sci.*, 2016, **84**, 335–402.

94 A. Molak, D. K. Mahato and A. Z. Szeremeta, Synthesis and characterization of electrical features of bismuth manganite and bismuth ferrite: effects of doping in cationic and anionic sublattice: Materials for applications, *Prog. Cryst. Growth Charact. Mater.*, 2018, **64**, 1–22.

95 S. M. Lam, J. C. Sin and A. R. Mohamed, A newly emerging visible light-responsive $BiFeO_3$ perovskite for photocatalytic applications: A mini review, *Mater. Res. Bull.*, 2017, **90**, 15–30.

96 X. S. Xu and W. B. Wang, Multiferroic hexagonal ferrites (h-$RFeO_3$, R = Y, Dy-Lu): a brief experimental review, *Mod. Phys. Lett. B*, 2014, **28**, 27.

97 J. J. Zhu, H. L. Li, L. Y. Zhong, P. Xiao, X. L. Xu, X. G. Yang, Z. Zhao and J. L. Li, Perovskite Oxides: Preparation, Characterizations, and Applications in Heterogeneous Catalysis, *ACS Catal.*, 2014, **4**, 2917–2940.

98 T. Arakawa, S. Tsuchiya and J. Shiokawa, Catalytic activity of rare-earth ortho-ferrites and orthochromites, *Mater. Res. Bull.*, 1981, **16**, 97–103.

99 T. Arakawa, S. Tsuchiya and J. Shiokawa, Catalytic properties and activity of rare-earth ortho-ferrites in oxidation of methanol, *J. Catal.*, 1982, **74**, 317–322.

100 B. P. Barbero, J. A. Gamboa and L. E. Cadus, Synthesis and characterisation of $La_{1-x}Ca_xFeO_3$ perovskite-type oxide catalysts for total oxidation of volatile organic compounds, *Appl. Catal., B*, 2006, **65**, 21–30.

101 P. Ciambelli, S. Cimino, S. De Rossi, L. Lisi, G. Minelli, P. Porta and G. Russo, $AFeO_3$ (A = La, Nd, Sm) and $LaFe_{1-x}Mg_xO_3$ perovskites as methane combustion and CO oxidation catalysts: structural, redox and catalytic properties, *Appl. Catal., B*, 2001, **29**, 239–250.

102 A. Delmastro, D. Mazza, S. Ronchetti, M. Vallino, R. Spinicci, P. Brovetto and M. Salis, Synthesis and characterization of non-stoichiometric $LaFeO_3$ perovskite, *Mater. Sci. Eng., B*, 2001, **79**, 140–145.

103 R. Spinicci, A. Tofanari, A. Delmastro, D. Mazza and S. Ronchetti, Catalytic properties of stoichiometric and non-stoichiometric $LaFeO_3$ perovskite for total oxidation of methane, *Mater. Chem. Phys.*, 2002, **76**, 20–25.

104 G. Pecchi, P. Reyes, R. Zamora, C. Campos, L. E. Caduus and B. P. Barbero, Effect of the preparation method on the catalytic activity of $La_{1-x}Ca_xFeO_3$ perovskite-type oxides, *Catal. Today*, 2008, **133**, 420–427.

105 P. V. Gosavi and R. B. Biniwale, Pure phase $LaFeO_3$ perovskite with improved surface area synthesized using different routes and its characterization, *Mater. Chem. Phys.*, 2010, **119**, 324–329.

106 J. M. Giraudon, A. Elhachimi and G. Leclercq, Catalytic oxidation of chlorobenzene over Pd/perovskites, *Appl. Catal., B*, 2008, **84**, 251–261.

107 Y. C. Wei, J. A. Liu, Z. Zhao, Y. S. Chen, C. M. Xu, A. J. Duan, G. Y. Jiang and H. He, Highly Active Catalysts of Gold Nanoparticles Supported on Three-Dimensionally Ordered Macroporous $LaFeO_3$ for Soot Oxidation, *Angew. Chem., Int. Ed.*, 2011, **50**, 2326–2329.

108 J. Li, J. Miao, X. G. Duan, J. Dai, Q. W. Liu, S. B. Wang, W. Zhou and Z. P. Shao, Fine-Tuning Surface Properties of Perovskites via Nanocompositing with Inert Oxide toward Developing Superior Catalysts for Advanced Oxidation, *Adv. Funct. Mater.*, 2018, **28**, 12.

109 D. Blanck, A. Schon, A. S. Mamede, C. Dujardin, J. P. Dacquin, P. Granger, J. F. Paul and E. Berrier, In situ Raman spectroscopy evidence of an accessible phase potentially involved in the enhanced activity of La -deficient lanthanum orthoferrite in 3-way catalysis (TWC), *Catal. Today*, 2017, **283**, 151–157.

110 Z. X. Li, F. B. Shi and C. H. Yan, Controllable Assembly of Hierarchical Macroporous-Mesoporous $LnFeO_3$ and Their Catalytic Performance in the CO plus NO Reaction, *Langmuir*, 2015, **31**, 8672–8679.

111 P. Garcia-Munoz, C. Lefevre, D. Robert and N. Keller, Ti-substituted $LaFeO_3$ perovskite as photoassisted CWPO catalyst for water treatment, *Appl. Catal., B*, 2019, **248**, 120–128.

112 A. Wattiaux, J. C. Grenier, M. Pouchard and P. Hagenmuller, Electrolytic oxygen evolution in alkaline-medium on $La_{1-x}Sr_xFeO_{3-y}$ perovskite-related ferrites. 1. Electrochemical study, *J. Electrochem. Soc.*, 1987, **134**, 1714–1718.

113 A. Wattiaux, J. C. Grenier, M. Pouchard and P. Hagenmuller, Electrolytic oxygen evolution in alkaline-medium on $La_{1-x}Sr_xFeO_{3-y}$ perovskite-related ferrites. 2. Influence of bulk properties, *J. Electrochem. Soc.*, 1987, **134**, 1718–1724.

114 J. Suntivich, K. J. May, H. A. Gasteiger, J. B. Goodenough and Y. Shao-Horn, A Perovskite Oxide Optimized for Oxygen Evolution Catalysis from Molecular Orbital Principles, *Science*, 2011, **334**, 1383–1385.

115 S. P. Simner, J. R. Bonnett, N. L. Canfield, K. D. Meinhardt, J. P. Shelton, V. L. Sprenkle and J. W. Stevenson, Development of lanthanum ferrite SOFC cathodes, *J. Power Sources*, 2003, **113**, 1–10.

116 A. Mai, V. A. C. Haanappel, S. Uhlenbruck, F. Tietz and D. Stover, Ferrite-based perovskites as cathode materials for anode-supported solid oxide fuel cells Part I. Variation of composition, *Solid State Ionics*, 2005, **176**, 1341–1350.

117 K. Huang, H. Y. Lee and J. B. Goodenough, Sr- and Ni-doped $LaCaO_3$ and $LaFeO_3$ perovskites - New cathode materials for solid-oxide fuel cells, *J. Electrochem. Soc.*, 1998, **145**, 3220–3227.

118 S. P. Jiang, Development of lanthanum strontium cobalt ferrite perovskite electrodes of solid oxide fuel cells - A review, *Int. J. Hydrogen Energy*, 2019, **44**, 7448–7493.

119 J. Lyagaeva, N. Danilov, A. Tarutin, G. Vdovin, D. Medvedev, A. Demin and P. Tsiakaras, Designing a protonic ceramic fuel cell with novel electrochemically active oxygen electrodes based on doped $Nd_{0.5}Ba_{0.5}FeO_{3-\delta}$, *Dalton Trans.*, 2018, **47**, 8149–8157.
120 J. Vieten, B. Bulfin, F. Call, M. Lange, M. Schmucker, A. Francke, M. Roeb and C. Sattler, Perovskite oxides for application in thermochemical air separation and oxygen storage, *J. Mater. Chem. A*, 2016, **4**, 13652–13659.
121 B. Bulfin, J. Lapp, S. Richter, D. Guban, J. Vieten, S. Brendelberger, M. Roeb and C. Sattler, Air separation and selective oxygen pumping via temperature and pressure swing oxygen adsorption using a redox cycle of $SrFeO_3$ perovskite, *Chem. Eng. Sci.*, 2019, **203**, 68–75.
122 S. Hosokawa, Hexagonal Rare Earth-Iron Mixed Oxides ($REFeO_3$): Crystal Structure, Synthesis, and Catalytic Properties, *Front. Chem.*, 2019, **7**, 8.
123 L. Valko, P. Bucek, R. Dosoudil and M. Usakova, Magnetic Properties of Ferrite-Polymer Composites, *J. Electr. Eng.*, 2003, **54**, 100–103.
124 H. Dong, Y. C. Chen and C. Feldmann, Polyol synthesis of nanoparticles: status and options regarding metals, oxides, chalcogenides, and non-metal elements, *Green Chem.*, 2015, **17**, 4107–4132.
125 J. Lin, M. Yu, C. Lin and X. Liu, Multiform oxide optical materials via the versatile Pechini-type sol–gel process: Synthesis and characteristics, *J. Phys. Chem. C*, 2007, **111**, 5835–5845.
126 P. Dolcet, S. Diodati, F. Zorzi, P. Voepel, C. Seitz, B. M. Smarsly, S. Mascotto, F. Nestola and S. Gross, Very fast crystallisation of MFe_2O_4 spinel ferrites (M = Co, Mn, Ni, Zn) under low temperature hydrothermal conditions: a time-resolved structural investigation, *Green Chem.*, 2018, **20**, 2257–2268.
127 S. Diodati, L. Pandolfo, S. Gialanella, A. Caneschi and S. Gross, Green and low temperature synthesis of nanocrystalline transition metal ferrites by simple wet chemistry routes, *Nano Res.*, 2014, **7**, 1027–1042.
128 A. Rabenau, The Role of Hydrothermal Synthesis in Preparative Chemistry, *Angew. Chem., Int. Ed. Engl.*, 1985, **24**, 1026–1040.
129 M. Yoshimura and K. Byrappa, Hydrothermal processing of materials: past, present and future, *J. Mater. Sci.*, 2008, **43**, 2085–2103.
130 G. Demazeau, Solvothermal processes: a route to the stabilization of new materials, *J. Mater. Chem.*, 1999, **9**, 15–18.
131 G. Demazeau, Solvothermal reactions: an original route for the synthesis of novel materials, *J. Mater. Sci.*, 2008, **43**, 2104–2114.
132 G. Demazeau, Solvothermal Processes: Definition, Key Factors Governing the Involved Chemical Reactions and New Trends, *Z. Naturforsch., B: J. Chem. Sci.*, 2010, **65**, 999–1006.
133 C. S. Cundy and P. A. Cox, The Hydrothermal Synthesis of Zeolites: History and Development from the Earliest Days to the Present Time, *Chem. Rev.*, 2003, **103**, 663–701.
134 R. A. Laudise, Hydrothermal synthesis of crystals, *Chem. Eng. News*, 1987, **65**, 30–43.
135 S. Somiya and R. Roy, Hydrothermal synthesis of fine oxide powders, *Bull. Mater. Sci.*, 2000, **23**, 453–460.
136 R. E. Riman, W. L. Suchanek and M. M. Lencka, Hydrothermal crystallization of ceramics, *Ann. Chim.-Sci. Mat.*, 2002, **27**, 15–36.
137 R. I. Walton, Subcritical solvothermal synthesis of condensed inorganic materials, *Chem. Soc. Rev.*, 2002, **31**, 230–238.
138 S. Komarneni, Nanophase materials by hydrothermal, microwave-hydrothermal and microwave-solvothermal methods, *Curr. Sci.*, 2003, **85**, 1730–1734.
139 M. Niederberger, G. Garnweitner, J. H. Ba, J. Polleux and N. Pinna, Nonaqueous synthesis, assembly and formation mechanisms of metal oxide nanocrystals, *Int. J. Nanotechnol.*, 2007, **4**, 263–281.
140 D. R. Modeshia and R. I. Walton, Solvothermal synthesis of perovskites and pyrochlores: crystallisation of functional oxides under mild conditions, *Chem. Soc. Rev.*, 2010, **39**, 4303–4325.
141 S. Hosokawa, Synthesis of metal oxides with improved performance using a solvothermal method, *J. Ceram. Soc. Jpn.*, 2016, **124**, 870–874.
142 S. H. Feng and R. R. Xu, New materials in hydrothermal synthesis, *Acc. Chem. Res.*, 2001, **34**, 239–247.
143 C. I. Hiley and R. I. Walton, Controlling the crystallisation of oxide materials by solvothermal chemistry: tuning composition, substitution and morphology of functional solids, *CrystEngComm*, 2016, **18**, 7656–7670.
144 C. Chen, J. R. Cheng, S. W. Yu, L. J. Che and Z. Y. Meng, Hydrothermal synthesis of perovskite bismuth ferrite crystallites, *J. Cryst. Growth*, 2006, **291**, 135–139.
145 J. T. Han, Y. H. Huang, X. J. Wu, C. L. Wu, W. Wei, B. Peng, W. Huang and J. B. Goodenough, Tunable synthesis of bismuth ferrites with various morphologies, *Adv. Mater.*, 2006, **18**, 2145–2148.
146 S. Li, Y. H. Lin, B. P. Zhang, Y. Wang and C. W. Nan, Controlled Fabrication of $BiFeO_3$ Uniform Microcrystals and Their Magnetic and Photocatalytic Behaviors, *J. Phys. Chem. C*, 2010, **114**, 2903–2908.
147 D. R. Cai, J. M. Li, T. Tong, D. R. Jin, S. W. Yu and J. R. Cheng, Phase evolution of bismuth ferrites in the process of hydrothermal reaction, *Mater. Chem. Phys.*, 2012, **134**, 139–144.
148 A. M. L. Lopes, J. P. Araujo and S. Ferdov, Room temperature synthesis of $Bi_{25}FeO_{39}$ and hydrothermal kinetic relations between sillenite- and distorted perovskite-type bismuth ferrites, *Dalton Trans.*, 2014, **43**, 18010–18016.
149 Z. W. Chen and W. L. Jin, Low-temperature acetone-assisted hydrothermal synthesis and characterization of $BiFeO_3$ powders, *J. Mater. Sci.: Mater. Electron.*, 2014, **25**, 4039–4045.
150 L. Zhang, X. F. Cao, Y. L. Ma, X. T. Chen and Z. L. Xue, Polymer-directed synthesis and magnetic property of nanoparticles-assembled $BiFeO_3$ microrods, *J. Solid State Chem.*, 2010, **183**, 1761–1766.

151 L. Hou, K. H. Zuo, Q. B. Sun, Z. M. Ren, Y. P. Zeng and X. Li, Effects of external magnetic field on the morphology and magnetic property of $BiFeO_3$ particles prepared by hydrothermal synthesis, *Appl. Phys. Lett.*, 2013, **102**, 4.

152 A. Huang, A. D. Handoko, G. K. L. Goh, P. K. Pallathadka and S. Shannigrahi, Hydrothermal synthesis of (001) epitaxial $BiFeO_3$ films on $SrTiO_3$ substrate, *CrystEngComm*, 2010, **12**, 3806–3814.

153 Y. Du, Z. X. Cheng, M. Shahbazi, E. W. Collings, S. X. Dou and X. L. Wang, Enhancement of ferromagnetic and dielectric properties in lanthanum doped $BiFeO_3$ by hydrothermal synthesis, *J. Alloys Compd.*, 2010, **490**, 637–641.

154 A. Chaudhuri and K. Mandal, Enhancement of ferromagnetic and dielectric properties of lanthanum doped bismuth ferrite nanostructures, *Mater. Res. Bull.*, 2012, **47**, 1057–1061.

155 C. Ponzoni, M. Cannio, D. N. Boccaccini, C. R. H. Bahl, K. Agersted and C. Leonelli, Ultrafast microwave hydrothermal synthesis and characterization of $Bi_{1-x}La_xFeO_3$ micronized particles, *Mater. Chem. Phys.*, 2015, **162**, 69–75.

156 A. Chaudhuri and K. Mandal, Study of structural, ferromagnetic and ferroelectric properties of nanostructured barium doped Bismuth Ferrite, *J. Magn. Magn. Mater.*, 2014, **353**, 57–64.

157 K. K. Bharathi, G. Ramesh, L. N. Patro, N. R. C. Raju and D. K. Kim, Enhanced ferromagnetic properties and high temperature dielectric anomalies in $Bi_{0.9}Ca_{0.05}Sm_{0.05}FeO_3$ prepared by hydrothermal method, *Mater. Res. Bull.*, 2015, **62**, 5–10.

158 M. Yoshimura, K. Yamasawa and S. Somiya, Formation of $LaFeO_3$ Crystals under Hydrothermal Conditions, *Nippon. Seram. Kyo. Gak.*, 1982, **90**, 521–527.

159 Y. Abe, I. Satou, T. Aida and T. Adschiri, Formation of La-based perovskite compounds in supercritical water, *Ceram. Int.*, 2018, **44**, 12996–13003.

160 W. J. Zheng, R. H. Liu, D. K. Peng and G. Y. Meng, Hydrothermal synthesis of $LaFeO_3$ under carbonate-containing medium, *Mater. Lett.*, 2000, **43**, 19–22.

161 L. Yuan, K. K. Huang, S. Wang, C. M. Hou, X. F. Wu, B. Zou and S. H. Feng, Crystal Shape Tailoring in Perovskite Structure Rare-Earth Ferrites $REFeO_3$ (RE = La, Pr, Sm, Dy, Er, and Y) and Shape-Dependent Magnetic Properties of YFeO3, *Cryst. Growth Des.*, 2016, **16**, 6522–6530.

162 E. M. Kostyukhin, A. L. Kustov and L. M. Kustov, One-step hydrothermal microwave-assisted synthesis of $LaFeO_3$ nanoparticles, *Ceram. Int.*, 2019, **45**, 14384–14388.

163 S. Thirumalairajan, K. Girija, N. Y. Hebalkar, D. Mangalaraj, C. Viswanathan and N. Ponpandian, Shape evolution of perovskite $LaFeO_3$ nanostructures: a systematic investigation of growth mechanism, properties and morphology dependent photocatalytic activities, *RSC Adv.*, 2013, **3**, 7549–7561.

164 R. D. Kumar and R. Jayavel, in *Solid State Physics: Proceedings of the 58th Dae Solid State Physics Symposium 2013, Pts a & B*, ed. C. Murli, D. Bhattacharyya and S. C. Gadkari, 2014, vol. 1591, pp. 315–317.

165 Y. J. Zhang, A. Zheng, X. Z. Yang, H. M. He, Y. Fan and C. P. Yao, Cubic $GdFeO_3$ particle by a simple hydrothermal synthesis route and its photoluminescence and magnetic properties, *CrystEngComm*, 2012, **14**, 8432–8439.

166 Z. Q. Zhou, L. Guo, H. X. Yang, Q. Liu and F. Ye, Hydrothermal synthesis and magnetic properties of multiferroic rare-earth orthoferrites, *J. Alloys Compd.*, 2014, **583**, 21–31.

167 M. Zhou, H. Yang, T. Xian, J. Y. Ma, H. M. Zhang, W. J. Feng, Z. Q. Wei and J. L. Jiang, Morphology-controlled synthesis of orthorhombic $LuFeO_3$ particles via a hydrothermal route, *J. Alloys Compd.*, 2014, **617**, 855–862.

168 Y. Wang, X. C. Yan, J. Chen, J. X. Deng, R. B. Yu and X. R. Xing, Shape controllable synthesis of $NdFeO_3$ micro single crystals by a hydrothermal route, *CrystEngComm*, 2014, **16**, 858–862.

169 C. Y. Zhang, M. Y. Shang, M. L. Liu, T. S. Zhang, L. Ge, H. M. Yuan and S. H. Feng, Multiferroicity in $SmFeO_3$ synthesized by hydrothermal method, *J. Alloys Compd.*, 2016, **665**, 152–157.

170 J. Q. Zhang, K. K. Huang, L. Yuan and S. H. Feng, Mineralizer effect on facet-controllable hydrothermal crystallization of perovskite structure $YbFeO_3$ crystals, *CrystEngComm*, 2018, **20**, 470–476.

171 W. W. Hu, Y. Chen, H. M. Yuan, G. H. Zhang, G. H. Li, G. S. Pang and S. H. Feng, Hydrothermal synthesis, characterization and composition-dependent magnetic properties of $LaFe_{1-x}Cr_xO_3$ system ($0 \le x \le 1$), *J. Solid State Chem.*, 2010, **183**, 1582–1587.

172 L. Yuan, K. K. Huang, C. M. Hou, W. C. Feng, S. Wang, C. P. Zhou and S. H. Feng, Hydrothermal synthesis and magnetic properties of $REFe_{0.5}Cr_{0.5}O_3$ (RE = La, Tb, Ho, Er, Yb, Lu and Y) perovskite, *New J. Chem.*, 2014, **38**, 1168–1172.

173 Y. Qiao, Y. F. Zhou, S. Wang, L. Yuan, Y. Y. Du, D. Y. Lu, G. B. Che and H. N. Che, Composition dependent magnetic and ferroelectric properties of hydrothermally synthesized $GdFe_{1-x}Cr_xO_3$ ($0.1 \le x \le 0.9$) perovskites, *Dalton Trans.*, 2017, **46**, 5930–5937.

174 V. I. Popkov and O. V. Almjasheva, Formation mechanism of $YFeO_3$ nanoparticles under the hydrothermal conditions, *Nanosyst.: Phys., Chem., Math.*, 2014, **5**, 703–708.

175 A. V. Racu, D. H. Ursu, O. V. Kuliukova, C. Logofatu, A. Leca and M. Miclau, Direct low temperature hydrothermal synthesis of $YFeO_3$ microcrystals, *Mater. Lett.*, 2015, **140**, 107–110.

176 V. I. Popkov, O. V. Almjasheva, A. S. Semenova, D. G. Kellerman, V. N. Nevedomskiy and V. V. Gusarov, Magnetic properties of $YFeO_3$ nanocrystals obtained by different soft-chemical methods, *J. Mater. Sci.: Mater. Electron.*, 2017, **28**, 7163–7170.

177 M. Y. Shang, C. Y. Zhang, T. S. Zhang, L. Yuan, L. Ge, H. M. Yuan and S. H. Feng, The multiferroic perovskite $YFeO_3$, *Appl. Phys. Lett.*, 2013, **102**, 3.

178 C. M. Hou, W. C. Feng, L. Yuan, K. K. Huang and S. H. Feng, Crystal facet control of $LaFeO_3$, $LaCrO_3$, and $La_{0.75}Sr_{0.25}MnO_3$, *CrystEngComm*, 2014, **16**, 2874–2877.
179 K. K. Huang, L. Yuan and S. H. Feng, Crystal facet tailoring arts in perovskite oxides, *Inorg. Chem. Front.*, 2015, **2**, 965–981.
180 M. Inoue, T. Nishikawa, T. Nakamura and T. Inui, Glycothermal reaction of rare-earth acetate and iron acetylacetonate: Formation of hexagonal $REFeO_3$, *J. Am. Ceram. Soc.*, 1997, **80**, 2157–2160.
181 S. Hosokawa, H. J. Jeon, S. Iwamoto and M. Inoue, Synthesis of Rare Earth Iron-Mixed Oxide Nanoparticles by Solvothermal Methods, *J. Am. Ceram. Soc.*, 2009, **92**, 2847–2853.
182 S. Hosokawa, H. J. Jeon and M. Inoue, Thermal stabilities of hexagonal and orthorhombic $YbFeO_3$ synthesized by solvothermal method and their catalytic activities for methane combustion, *Res. Chem. Intermed.*, 2011, **37**, 291–296.
183 X. F. Guan, J. Zheng, M. L. Zhao, L. P. Li and G. S. Li, Synthesis of $FeTiO_3$ nanosheets with {0001} facets exposed: enhanced electrochemical performance and catalytic activity, *RSC Adv.*, 2013, **3**, 13635–13641.
184 F. Zhang, C. Wei, Y. Hu and H. Wu, Zinc ferrite catalysts for ozonation of aqueous organic contaminants: phenol and bio-treated coking wastewater, *Sep. Purif. Technol.*, 2015, **156**(Part 2), 625–635.
185 T. K. Aparna and R. Sivasubramanian, $FeTiO_3$ nanohexagons based electrochemical sensor for the detection of dopamine in presence of uric acid, *Mater. Chem. Phys.*, 2019, **233**, 319–328.
186 S. Palanisamy, S. Srinivasan, A. P. Shyma, N. Rajendhran, K. Subramani, V. Murugan and R. Venkatachalam, Influence of nanoflower $FeTiO_3$ in carbon dioxide reduction, *SN Appl. Sci.*, 2019, **1**, 10.
187 T. Tao, A. M. Glushenkov, H. W. Liu, Z. W. Liu, X. J. J. Dai, H. Chen, S. P. Ringer and Y. Chen, Ilmenite $FeTiO_3$ Nanoflowers and Their Pseudocapacitance, *J. Phys. Chem. C*, 2011, **115**, 17297–17302.
188 T. Tao, Y. Chen, Y. H. Chen, D. S. Fox, H. Z. Zhang, M. Q. Zhou, M. Raveggi, A. J. Barlow and A. M. Glushenkov, Two-Dimensional Metal Oxide Nanoflower-Like Architectures: A General Growth Method and Their Applications in Energy Storage and as Model Materials for Nanofabrication, *ChemPlusChem*, 2017, **82**, 295–302.
189 A. R. Gainsford, M. J. Sisley, T. W. Swaddle and P. Bayliss, Hydrothermal formation of ferrite spinels, *Can. J. Chem.*, 1975, **53**, 12–19.
190 Y. Xie, Y. T. Qian, J. Li, Z. Y. Chen and Y. Li, Hydrothermal preparation and characterization of ultrafine powders of ferrite spinels MFe_2O_4 (M=Fe, Zn and Ni), *Mater. Sci. Eng., B*, 1995, **34**, L1–L3.
191 C. Rath, K. K. Sahu, S. Anand, S. K. Date, N. C. Mishra and R. P. Das, Preparation and characterization of nanosize Mn-Zn ferrite, *J. Magn. Magn. Mater.*, 1999, **202**, 77–84.
192 C. Rath, S. Anand, R. P. Das, K. K. Sahu, S. D. Kulkarni, S. K. Date and N. C. Mishra, Dependence on cation distribution of particle size, lattice parameter, and magnetic properties in nanosize Mn-Zn ferrite, *J. Appl. Phys.*, 2002, **91**, 2211–2215.
193 A. L. Xia, S. K. Liu, C. G. Jin, L. Chen and Y. H. Lv, Hydrothermal $Mg_{1-x}Zn_xFe_2O_4$ spinel ferrites: Phase formation and mechanism of saturation magnetization, *Mater. Lett.*, 2013, **105**, 199–201.
194 L. Nalbandian, A. Delimitis, V. T. Zaspalis, E. A. Deliyanni, D. N. Bakoyannakis and E. N. Peleka, Hydrothermally prepared nanocrystalline Mn-Zn ferrites: Synthesis and characterization, *Microporous Mesoporous Mater.*, 2008, **114**, 465–473.
195 H. W. Wang and S. C. Kung, Crystallization of nanosized Ni-Zn ferrite powders prepared by hydrothermal method, *J. Magn. Magn. Mater.*, 2004, **270**, 230–236.
196 X. Y. Hou, J. Feng, X. D. Xu and M. L. Zhang, Synthesis and characterizations of spinel $MnFe_2O_4$ nanorod by seed-hydrothermal route, *J. Alloys Compd.*, 2010, **491**, 258–263.
197 J. Wang, Q. W. Chen, B. Y. Hou and Z. M. Peng, Synthesis and magnetic properties of single-crystals of $MnFe_2O_4$ nanorods, *Eur. J. Inorg. Chem.*, 2004, 1165–1168, DOI: 10.1002/ejic.200300555.
198 R. Fareghi-Alamdari, F. Zandi and M. H. Keshavarz, Copper-cobalt synergy in $Cu_{1-x}Co_xFe_2O_4$ spinel ferrite as a highly efficient and regioselective nanocatalyst for the synthesis of 2,4-dinitrotoluene, *RSC Adv.*, 2015, **5**, 71911–71921.
199 A. L. Tiano, G. C. Papaefthymiou, C. S. Lewis, J. Han, C. Zhang, Q. Li, C. Y. Shi, A. M. M. Abeykoon, S. J. L. Billinge, E. Stach, J. Thomas, K. Guerrero, P. Munayco, J. Munayco, R. B. Scorzelli, P. Burnham, A. J. Viescas and S. S. Wong, Correlating Size and Composition-Dependent Effects with Magnetic, Mossbauer, and Pair Distribution Function Measurements in a Family of Catalytically Active Ferrite Nanoparticles, *Chem. Mater.*, 2015, **27**, 3572–3592.
200 A. Sheoran, M. Dhiman, S. Bhukal, R. Malik, J. Agarwal, B. Chudasama and S. Singhal, Development of magnetically retrievable spinel nanoferrites as efficient catalysts for aminolysis of epoxides with amines, *Mater. Chem. Phys.*, 2019, **222**, 207–216.
201 L. Satyanarayana, K. M. Reddy and S. V. Manorama, Synthesis of nanocrystalline $Ni_{1-x}Co_xMn_xFe_{2-x}O_4$: a material for liquefied petroleum gas sensing, *Sens. Actuators, B*, 2003, **89**, 62–67.
202 X. Shen, Y. X. Wang, X. Yang, L. Q. Lu and L. Huang, 0.3–3 GHz magneto-dielectric properties of nanostructured NiZnCo ferrite from hydrothermal process, *J. Mater. Sci.: Mater. Electron.*, 2010, **21**, 630–634.
203 Y. A. Pu, X. Tao, J. Zhai and J. F. Chen, Synthesis and electromagnetic properties of microwave absorbing material: $Co_x(Cu_{0.5}Zn_{0.5})_{1-x}Fe_2O_4$ ($0 < x < 1$) nanoparticles, *Mater. Sci. Eng., B*, 2011, **176**, 163–166.

204 L. X. Wang, J. C. Li, Y. Q. Wang, L. J. Zhao and Q. Jiang, Adsorption capability for Congo red on nanocrystalline MFe_2O_4 (M = Mn, Fe, Co, Ni) spinel ferrites, *Chem. Eng. J.*, 2012, **181**, 72–79.

205 X. Wang, L. S. Gao, L. Li, H. G. Zheng, Z. D. Zhang, W. C. Yu and Y. T. Qian, Low temperature synthesis of metastable lithium ferrite: magnetic and electrochemical properties, *Nanotechnology*, 2005, **16**, 2677–2680.

206 Z. T. Chen and L. Gao, Synthesis and magnetic properties of $CoFe_2O_4$ nanoparticles by using PEG as surfactant additive, *Mater. Sci. Eng., B*, 2007, **141**, 82–86.

207 H. Kavas, A. Baykal, M. S. Toprak, Y. Koseoglu, M. Sertkol and B. Aktas, Cation distribution and magnetic properties of Zn doped $NiFe_2O_4$ nanoparticles synthesized by PEG-assisted hydrothermal route, *J. Alloys Compd.*, 2009, **479**, 49–55.

208 F. Gozuak, Y. Koseoglu, A. Baykal and H. Kavas, Synthesis and characterization of $Co_xZn_{1-x}Fe_2O_4$ magnetic nanoparticles via a PEG-assisted route, *J. Magn. Magn. Mater.*, 2009, **321**, 2170–2177.

209 Y. Koseoglu, M. Bay, M. Tan, A. Baykal, H. Sozeri, R. Topkaya and N. Akdogan, Magnetic and dielectric properties of $Mn_{0.2}Ni_{0.8}Fe_2O_4$ nanoparticles synthesized by PEG-assisted hydrothermal method, *J. Nanopart. Res.*, 2011, **13**, 2235–2244.

210 M. Tan, Y. Koseoglu, F. Alan and E. Senturk, Overlapping large polaron tunneling conductivity and giant dielectric constant in $Ni_{0.5}Zn_{0.5}Fe_{1.5}Cr_{0.5}O_4$ nanoparticles (NPs), *J. Alloys Compd.*, 2011, **509**, 9399–9405.

211 Y. Koseoglu, F. Alan, M. Tan, R. Yilgin and M. Ozturk, Low temperature hydrothermal synthesis and characterization of Mn doped cobalt ferrite nanoparticles, *Ceram. Int.*, 2012, **38**, 3625–3634.

212 T. R. Bastami, M. H. Entezari, Q. H. Hu, S. B. Hartono and S. Z. Qiao, Role of polymeric surfactants on the growth of manganese ferrite nanoparticles, *Chem. Eng. J.*, 2012, **210**, 157–165.

213 Y. Koseoglu, M. I. O. Oleiwi, R. Yilgin and A. N. Kocbay, Effect of chromium addition on the structural, morphological and magnetic properties of nano-crystalline cobalt ferrite system, *Ceram. Int.*, 2012, **38**, 6671–6676.

214 Y. Koseoglu, Structural, magnetic, electrical and dielectric properties of $Mn_xNi_{1-x}Fe_2O_4$ spinel nanoferrites prepared by PEG assisted hydrothermal method, *Ceram. Int.*, 2013, **39**, 4221–4230.

215 B. Paul, D. D. Purkayastha and S. S. Dhar, Size-controlled synthesis of $NiFe_2O_4$ nanospheres via a PEG assisted hydrothermal route and their catalytic properties in oxidation of alcohols by periodic acid, *Appl. Surf. Sci.*, 2016, **370**, 469–475.

216 J. L. Zhang, J. X. Shi and M. L. Gong, Synthesis of magnetic nickel spinel ferrite nanospheres by a reverse emulsion-assisted hydrothermal process, *J. Solid State Chem.*, 2009, **182**, 2135–2140.

217 B. Bateer, C. G. Tian, Y. Qu, S. C. Du, Y. Yang, Z. Y. Ren, K. Pan and H. G. Fu, Synthesis, size and magnetic properties of controllable $MnFe_2O_4$ nanoparticles with versatile surface functionalities, *Dalton Trans.*, 2014, **43**, 9885–9891.

218 M. Fantauzzi, F. Secci, M. S. Angotzi, C. Passiu, C. Cannas and A. Rossi, Nanostructured spinel cobalt ferrites: Fe and Co chemical state, cation distribution and size effects by X-ray photoelectron spectroscopy, *RSC Adv.*, 2019, **9**, 19171–19179.

219 L. Wang, J. W. Ren, Y. G. Wang, X. H. Liu and Y. Q. Wang, Controlled synthesis of magnetic spinel-type nickel ferrite nanoparticles by the interface reaction and hydrothermal crystallization, *J. Alloys Compd.*, 2010, **490**, 656–660.

220 A. Repko, J. Vejpravova, T. Vackova, D. Zakutna and D. Niznansky, Oleate-based hydrothermal preparation of $CoFe_2O_4$ nanoparticles, and their magnetic properties with respect to particle size and surface coating, *J. Magn. Magn. Mater.*, 2015, **390**, 142–151.

221 M. S. Angotzi, A. Musinu, V. Mameli, A. Ardu, C. Cara, D. Niznansky, H. L. Xin and C. Cannas, Spinel Ferrite Core-Shell Nanostructures by a Versatile Solvothermal Seed-Mediated Growth Approach and Study of Their Nanointerfaces, *ACS Nano*, 2017, **11**, 7889–7900.

222 S. Phumying, S. Labuayai, E. Swatsitang, V. Amornkitbamrung and S. Maensiri, Nanocrystalline spinel ferrite (MFe_2O_4, M = Ni, Co, Mn, Mg, Zn) powders prepared by a simple aloe vera plant-extracted solution hydrothermal route, *Mater. Res. Bull.*, 2013, **48**, 2060–2065.

223 K. Vamvakidis, M. Katsikini, D. Sakellari, E. C. Paloura, O. Kalogirou and C. Dendrinou-Samara, Reducing the inversion degree of $MnFe_2O_4$ nanoparticles through synthesis to enhance magnetization: evaluation of their H-1 NMR relaxation and heating efficiency, *Dalton Trans.*, 2014, **43**, 12754–12765.

224 D. S. Cook, R. J. Kashtiban, K. Krambrock, G. M. de Lima, H. O. Stumpf, L. R. S. Lara, J. D. Ardisson and R. I. Walton, Nanocrystalline Transition-Metal Gallium Oxide Spinels from Acetylacetonate Precursors via Solvothermal Synthesis, *Materials*, 2019, **12**, 838.

225 K. Vamvakidis, M. Katsikini, G. Vourlias, M. Angelakeris, E. C. Paloura and C. Dendrinou-Samara, Composition and hydrophilicity control of Mn-doped ferrite ($Mn_xFe_{3-x}O_4$) nanoparticles induced by polyol differentiation, *Dalton Trans.*, 2015, **44**, 5396–5406.

226 C. Jolley, V. Pool, Y. Idzerda and T. Douglas, All in the Packaging: Structural and Electronic Effects of Nanoconfinement on Metal Oxide Nanoparticles, *Chem. Mater.*, 2011, **23**, 3921–3929.

227 L. Y. Chen, Y. M. Shen and J. F. Bai, Large-scale synthesis of uniform spinel ferrite nanoparticles from hydrothermal decomposition of trinuclear heterometallic oxo-centered acetate clusters, *Mater. Lett.*, 2009, **63**, 1099–1101.

228 K. O. Abdulwahab, M. A. Malik, P. O'Brien, G. A. Timco, F. Tuna, C. A. Muryn, R. E. P. Winpenny, R. A. D. Pattrick, V. S. Coker and E. Arenholz, A One-Pot Synthesis of Monodispersed Iron Cobalt Oxide and Iron Manganese

Oxide Nanoparticles from Bimetallic Pivalate Clusters, *Chem. Mater.*, 2014, **26**, 999–1013.

229 K. O. Abdulwahab, M. A. Malik, P. O'Brien, G. A. Timco, F. Tuna, R. E. P. Winpenny, R. A. D. Pattrick, V. S. Coker and E. Arenholz, Hot injection thermolysis of heterometallic pivalate clusters for the synthesis of monodisperse zinc and nickel ferrite nanoparticles, *J. Mater. Chem. C*, 2014, **2**, 6781–6789.

230 H. Deng, X. L. Li, Q. Peng, X. Wang, J. P. Chen and Y. D. Li, Monodisperse magnetic single-crystal ferrite microspheres, *Angew. Chem., Int. Ed.*, 2005, **44**, 2782–2785.

231 C. Y. Hou, H. Yu, Q. H. Zhang, Y. G. Li and H. Z. Wang, Preparation and magnetic property analysis of monodisperse Co-Zn ferrite nanospheres, *J. Alloys Compd.*, 2010, **491**, 431–435.

232 Y. Wang, D. W. Su, A. Ung, J. H. Ahn and G. X. Wang, Hollow $CoFe_2O_4$ nanospheres as a high capacity anode material for lithium ion batteries, *Nanotechnology*, 2012, **23**, 055402.

233 R. Otero-Lorenzo, M. A. Ramos-Docarripo, B. Rodriguez-Gonzalez, M. Comesana-Hermo and V. Salgueirino, Solvothermal Clustering of Magnetic Spinel Ferrite Nanocrystals: A Raman Perspective, *Chem. Mater.*, 2017, **29**, 8729–8736.

234 H. Hayashi and Y. Hakuta, Hydrothermal synthesis of metal oxide nanoparticles in supercritical water, *Materials*, 2010, **3**, 3794–3817.

235 B. Stieberova, M. Zilka, M. Ticha, F. Freiberg, P. Caramazana-Gonzalez, J. McKechnie and E. Lester, Sustainability assessment of continuous-flow hydrothermal synthesis of nanomaterials in the context of other production technologies, *J. Cleaner Prod.*, 2019, **241**, 10.

236 A. Cabañas and M. Poliakoff, The continuous hydrothermal synthesis of nano-particulate ferrites in near critical and supercritical water, *J. Mater. Chem.*, 2001, **11**, 1408–1416.

237 T. Sato, K. Sue, W. Suzuki, M. Suzuki, K. Matsui, Y. Hakuta, H. Hayashi, K. Arai, S. I. Kawasaki, A. Kawai-Nakamura and T. Hiaki, Rapid and continuous production of ferrite nanoparticles by hydrothermal synthesis at 673 K and 30 MPa, *Ind. Eng. Chem. Res.*, 2008, **47**, 1855–1860.

238 M. Stingaciu, H. L. Andersen, C. Granados-Miralles, A. Mamakhel and M. Christensen, Magnetism in $CoFe_2O_4$ nanoparticles produced at sub- and near-supercritical conditions of water, *CrystEngComm*, 2017, **19**, 3986–3996.

239 Y. Xu, F. Ozcan, P. Zielke, S. Becker, M. Heimann, J. Heese, K. Chakrapani, M. Behrens, S. B. Simonsen, P. Norby, P. V. Hendriksen and R. Kiebach, Continuous Hydrothermal Flow Synthesis of $Co_{1-x}Ni_xFe_2O_4$ (x = 0–0.8) Nanoparticles and Their Catalytic Properties for CO Oxidation and Oxygen Evolution Reaction, *Z. Anorg. Allg. Chem.*, 2018, **644**, 1727–1733.

240 H. Tumazawa, Y. Maeda and E. Sada, Further consideration of hydrothermal synthesis of barium ferrite fine particles, *J. Mater. Sci. Lett.*, 1995, **14**, 68–70.

241 X. Y. Liu, J. Wang, L. M. Gan and S. C. Ng, Improving the magnetic properties of hydrothermally synthesized barium ferrite, *J. Magn. Magn. Mater.*, 1999, **195**, 452–459.

242 S. Che, J. Wang and Q. W. Chen, Soft magnetic nanoparticles of $BaFe_{12}O_{19}$ fabricated under mild conditions, *J. Phys.: Condens. Matter*, 2003, **15**, L335–L339.

243 G. V. Duong, R. S. Turtelli, B. D. Thuan, D. V. Linh, N. Hanh and R. Groessinger, Magnetic properties of nanocrystalline $BaFe_{12}O_{19}$ prepared by hydrothermal method, *J. Non-Cryst. Solids*, 2007, **353**, 811–813.

244 T. Yamauchi, Y. Tsukahara, T. Sakata, H. Mori, T. Chikata, S. Katoh and Y. Wada, Barium ferrite powders prepared by microwave-induced hydrothermal reaction and magnetic property, *J. Magn. Magn. Mater.*, 2009, **321**, 8–11.

245 Y. Liu, M. G. B. Drew, J. P. Wang, M. L. Zhang and Y. Liu, Efficiency and purity control in the preparation of pure and/or aluminum-doped barium ferrites by hydrothermal methods using ferrous ions as reactants, *J. Magn. Magn. Mater.*, 2010, **322**, 366–374.

246 A. L. Xia, C. H. Zuo, L. Chen, C. G. Jin and Y. H. Lv, Hexagonal $SrFe_{12}O_{19}$ ferrites: Hydrothermal synthesis and their sintering properties, *J. Magn. Magn. Mater.*, 2013, **332**, 186–191.

247 H. Mocuta, L. Lechevallier, J. M. Le Breton, J. F. Wang and I. R. Harris, Structural and magnetic properties of hydrothermally synthesised $Sr_{1-x}Nd_xFe_{12}O_{19}$ hexagonal ferrites, *J. Alloys Compd.*, 2004, **364**, 48–52.

248 L. Lechevallier, J. M. Le Breton, J. F. Wang and I. R. Harris, Structural analysis of hydrothermally synthesized $Sr_{1-x}Sm_xFe_{12}O_{19}$ hexagonal ferrites, *J. Magn. Magn. Mater.*, 2004, **269**, 192–196.

249 Y. Jing, L. Jia, Y. Zheng and H. Zhang, Hydrothermal synthesis and competitive growth of flake-like M-type strontium hexaferrite, *RSC Adv.*, 2019, **9**, 33388–33394.

250 G. D. Soria, P. Jenus, J. F. Marco, A. Mandziak, M. Sanchez-Arenillas, F. Moutinho, J. E. Prieto, P. Prieto, J. Cerdá, C. Tejera-Centeno, S. Gallego, M. Foerster, L. Aballe, M. Valvidares, H. B. Vasili, E. Pereiro, A. Quesada and J. de la Figuera, Strontium hexaferrite platelets: a comprehensive soft X-ray absorption and Mössbauer spectroscopy study, *Sci. Rep.*, 2019, **9**, 11777.

251 S. Dong, C. Lin and X. Meng, One-pot synthesis and microwave absorbing properties of ultrathin $SrFe_{12}O_{19}$ nanosheets, *J. Alloys Compd.*, 2019, **783**, 779–784.

252 W. Shen, B. Y. Ren, W. Wang and J. P. Liu, Formation of Samarium Ferrites With Controllable Morphology by Changing the Addition of KOH, *IEEE Trans. Magn.*, 2019, **55**, 5.

253 K. S. Suslick, M. Fang and T. Hyeon, Sonochemical synthesis of iron colloids, *J. Am. Chem. Soc.*, 1996, **118**, 11960–11961.

254 L. H. Thompson and L. K. Doraiswamy, Sonochemistry: Science and engineering, *Ind. Eng. Chem. Res.*, 1999, **38**, 1215–1249.

255 T. J. Mason and J. P. Lorimal, *Applied sonochemistry*, Wiley, New York, 2002.

256 M. Abbas, B. Parvatheeswara Rao, M. Nazrul Islam, K. W. Kim, S. M. Naga, M. Takahashi and C. Kim, Size-controlled high magnetization $CoFe_2O_4$ nanospheres and nanocubes using rapid one-pot sonochemical technique, *Ceram. Int.*, 2014, **40**, 3269–3276.

257 T.-W. Chen, U. Rajaji, S.-M. Chen, M. M. Al Mogren, M. Hochlaf, S. D. A. Al Harbi and R. J. Ramalingam, A novel nanocomposite with superior electrocatalytic activity: A magnetic property based $ZnFe_2O_4$ nanocubes embellished with reduced graphene oxide by facile ultrasonic approach, *Ultrason. Sonochem.*, 2019, **57**, 116–124.

258 H. A. Choudhury, A. Choudhary, M. Sivakumar and V. S. Moholkar, Mechanistic investigation of the sonochemical synthesis of zinc ferrite, *Ultrason. Sonochem.*, 2013, **20**, 294–302.

259 K. S. Suslick, Sonochemistry, *Science*, 1990, **247**, 1439.

260 J. H. Bang and K. S. Suslick, Applications of Ultrasound to the Synthesis of Nanostructured Materials, *Adv. Mater.*, 2010, **22**, 1039–1059.

261 P. R. Gogate and A. B. Pandit, Sonochemical reactors: scale up aspects, *Ultrason. Sonochem.*, 2004, **11**, 105–117.

262 N. Das, R. Majumdar, A. Sen and H. S. Maiti, Nanosized bismuth ferrite powder prepared through sonochemical and microemulsion techniques, *Mater. Lett.*, 2007, **61**, 2100–2104.

263 D. P. Dutta, B. P. Mandal, R. Naik, G. Lawes and A. K. Tyagi, Magnetic, ferroelectric, and magnetocapacitive properties of sonochemically synthesized Sc-doped $BiFeO_3$ nanoparticles, *J. Phys. Chem. C*, 2013, **117**, 2382–2389.

264 M. Abbas, B. Parvatheeswara Rao and C. Kim, Shape and size-controlled synthesis of Ni Zn ferrite nanoparticles by two different routes, *Mater. Chem. Phys.*, 2014, **147**, 443–451.

265 B. R. Reddy, T. Sivasankar, M. Sivakumar and V. S. Moholkar, Physical facets of ultrasonic cavitational synthesis of zinc ferrite particles, *Ultrason. Sonochem.*, 2010, **17**, 416–426.

266 H. Harzali, F. Saida, A. Marzouki, A. Megriche, F. Baillon, F. Espitalier and A. Mgaidi, Structural and magnetic properties of nano-sized NiCuZn ferrites synthesized by co-precipitation method with ultrasound irradiation, *J. Magn. Magn. Mater.*, 2016, **419**, 50–56.

267 R. S. Yadav, I. Kuřitka, J. Vilcakova, J. Havlica, L. Kalina, P. Urbánek, M. Machovsky, D. Skoda, M. Masař and M. Holek, Sonochemical synthesis of Gd^{3+} doped $CoFe_2O_4$ spinel ferrite nanoparticles and its physical properties, *Ultrason. Sonochem.*, 2018, **40**, 773–783.

268 K. K. Senapati, C. Borgohain and P. Phukan, Synthesis of highly stable $CoFe_2O_4$ nanoparticles and their use as magnetically separable catalyst for Knoevenagel reaction in aqueous medium, *J. Mol. Catal. A: Chem.*, 2011, **339**, 24–31.

269 K. V. P. M. Shafi, A. Gedanken, R. Prozorov and J. Balogh, Sonochemical preparation and size-dependent properties of nanostructured $CoFe_2O_4$ particles, *Chem. Mater.*, 1998, **10**, 3445–3450.

270 K. V. P. M. Shafi, Y. Koltypin, A. Gedanken, R. Prozorov, J. Balogh, J. Lendvai and I. Felner, Sonochemical preparation of nanosized amorphous $NiFe_2O_4$ particles, *J. Phys. Chem. B*, 1997, **101**, 6409–6414.

271 W. Wu, Q. He and C. Jiang, Magnetic iron oxide nanoparticles: synthesis and surface functionalization strategies, *Nanoscale Res. Lett.*, 2008, **3**, 397–415.

272 R. Muñoz-Espì, Y. Mastai, S. Gross and K. Landfester, Colloidal systems for crystallization processes from liquid phase, *CrystEngComm*, 2013, **15**, 2175–2191.

273 P. Dolcet, F. Latini, M. Casarin, A. Speghini, E. Tondello, C. Foss, S. Diodati, L. Verin, A. Motta and S. Gross, Inorganic Chemistry in a Nanoreactor: Doped ZnO Nanostructures by Miniemulsion, *Eur. J. Inorg. Chem.*, 2013, **2013**, 2291–2300.

274 N. A. Heutz, P. Dolcet, A. Birkner, M. Casarin, K. Merz, S. Gialanella and S. Gross, Inorganic chemistry in a nanoreactor: Au/TiO_2 nanocomposites by photolysis of a single-source precursor in miniemulsion, *Nanoscale*, 2013, **5**, 10534–10541.

275 P. Dolcet, M. Casarin, C. Maccato, L. Bovo, G. Ischia, S. Gialanella, F. Mancin, E. Tondello and S. Gross, Miniemulsions as chemical nanoreactors for the room temperature synthesis of inorganic crystalline nanostructures: ZnO colloids, *J. Mater. Chem.*, 2012, **22**, 1620–1626.

276 M. Fanun, *Microemulsions: Properties and Applications*, CRC Press, Boca Raton, 1st edn, 2019.

277 M. Sanchez-Dominguez, K. Pemartin and M. Boutonnet, Preparation of inorganic nanoparticles in oil-in-water microemulsions: A soft and versatile approach, *Curr. Opin. Colloid Interface Sci.*, 2012, **17**, 297–305.

278 I. Danielsson and B. Lindman, The definition of microemulsion, *Colloids Surf.*, 1981, **3**, 391–392.

279 K. Landfester, Synthesis of colloidal particles in miniemulsions, *Annu. Rev. Mater. Res.*, 2006, **36**, 231–279.

280 K. Landfester, The generation of nanoparticles in miniemulsions, *Adv. Mater.*, 2001, **13**, 765–768.

281 K. Landfester, in *Colloid Chemistry II*, ed. M. Antonietti, Springer Berlin Heidelberg, Berlin, Heidelberg, 2003, pp. 75–123, DOI: 10.1007/3-40-36412-9_4.

282 Z. Cao and U. Ziener, Synthesis of nanostructured materials in inverse miniemulsions and their applications, *Nanoscale*, 2013, **5**, 10093–10107.

283 M. A. López-Quintela, C. Tojo, M. C. Blanco, L. García Rio and J. R. Leis, Microemulsion dynamics and reactions in microemulsions, *Curr. Opin. Colloid Interface Sci.*, 2004, **9**, 264–278.

284 K. Landfester, Recent developments in miniemulsions — formation and stability mechanisms, *Macromol. Symp.*, 2000, **150**, 171–178.

285 A. Scano, V. Cabras, M. Pilloni and G. Ennas, Microemulsions: The Renaissance of Ferrite Nanoparticle Synthesis, *J. Nanosci. Nanotechnol.*, 2019, **19**, 4824–4838.

286 V. Uskokovic and M. Drofenik, A mechanism for the formation of nanostructured NiZn ferrites via a micro-

emulsion-assisted precipitation method, *Colloids Surf., A*, 2005, **266**, 168–174.

287 V. Uskokovic and M. Drofenik, Synthesis of materials within reverse micelles, *Surf. Rev. Lett.*, 2005, **12**, 239–277.

288 C. Aubery, C. Solans, S. Prevost, M. Gradzielski and M. Sanchez-Dominguez, Microemulsions as reaction media for the synthesis of mixed oxide nanoparticles: Relationships between microemulsion structure, reactivity, and nanoparticle characteristics, *Langmuir*, 2013, **29**, 1779–1789.

289 C. Aubery, C. Solans and M. Sanchez-Dominguez, Tuning high aqueous phase uptake in nonionic water-in-oil microemulsions for the synthesis of Mn–Zn ferrite nanoparticles: Phase behavior, characterization, and nanoparticle synthesis, *Langmuir*, 2011, **27**, 14005–14013.

290 M. Bellusci, S. Canepari, G. Ennas, A. La Barbera, F. Padella, A. Santini, A. Scano, L. Seralessandri and F. Varsano, Phase evolution in synthesis of manganese ferrite nanoparticles, *J. Am. Ceram. Soc.*, 2007, **90**, 3977–3983.

291 J. Chandradass, A. H. Jadhav and H. Kim, Surfactant modified $MgFe_2O_4$ nanopowders by reverse micelle processing: Effect of water to surfactant ratio (R) on the particle size and magnetic property, *Appl. Surf. Sci.*, 2012, **258**, 3315–3320.

292 J. Chandradass and K. H. Kim, Solvent effects in the synthesis of $MgFe_2O_4$ nanopowders by reverse micelle processing, *J. Alloys Compd.*, 2011, **509**, L59–L62.

293 P. Holec, J. Plocek, D. Niznansky and J. P. Vejpravova, Preparation of $MgFe_2O_4$ nanoparticles by microemulsion method and their characterization, *J. Sol-Gel Sci. Technol.*, 2009, **51**, 301–305.

294 E. J. Choi, Y. Ahn and Y. D. Her, Size dependence of magnetic properties of Co-ferrite nanoparticles, *J. Korean Phys. Soc.*, 2007, **50**, 460–463.

295 A. J. Rondinone, A. C. S. Samia and Z. J. Zhang, Superparamagnetic Relaxation and Magnetic Anisotropy Energy Distribution in $CoFe_2O_4$ Spinel Ferrite Nanocrystallites, *J. Phys. Chem. B*, 1999, **103**, 6876–6880.

296 A. J. Rondinone, A. C. S. Samia and Z. J. Zhang, A chemometric approach for predicting the size of magnetic spinel ferrite nanoparticles from the synthesis conditions, *J. Phys. Chem. B*, 2000, **104**, 7919–7922.

297 R. D. K. Misra, A. Kale, B. J. Kooi and J. T. M. De Hosson, Some aspects of nanocrystalline nickel and zinc ferrites processed using microemulsion technique, *Mater. Sci. Technol.*, 2003, **19**, 1617–1621.

298 R. D. K. Misra, A. Kale, R. S. Srivastava and O. N. Senkov, Synthesis of nanocrystalline nickel and zinc ferrites by microemulsion technique, *Mater. Sci. Technol.*, 2003, **19**, 826–830.

299 M. A. Dar, J. Shah, W. A. Siddiqui and R. K. Kotnala, Influence of synthesis approach on structural and magnetic properties of lithium ferrite nanoparticles, *J. Alloys Compd.*, 2012, **523**, 36–42.

300 M. Hashim, S. E. Shirsath, S. S. Meena, M. L. Mane, S. Kumar, P. Bhatt, R. Kumar, N. K. Prasad, S. K. Alla, J. Shah, R. K. Kotnala, K. A. Mohammed, E. Senturk and Alimuddin, Manganese ferrite prepared using reverse micelle process: Structural and magnetic properties characterization, *J. Alloys Compd.*, 2015, **642**, 70–77.

301 S. Kumar, P. Kumar, V. Singh, U. K. Mandal and R. K. Kotnala, Synthesischaracterization and magnetic properties of monodisperse Ni, Zn-ferrite nanocrystals, *J. Magn. Magn. Mater.*, 2015, **379**, 50–57.

302 S. Kumar, V. Singh, S. Aggarwal, U. K. Mandal and R. K. Kotnala, Synthesis of nanocrystalline $Ni_{0.5}Zn_{0.5}Fe_2O_4$ ferrite and study of its magnetic behavior at different temperatures, *Mater. Sci. Eng., B*, 2010, **166**, 76–82.

303 A. Parveen, H. Asghar, M. Khalid, Z. A. Gilani, S. Aslam, M. Saleem, F. A. Shaikh and J. Rehman, Dielectric, impedance and modulus spectroscopic studies of $Co_{0.3}Cd_{0.7}Zn_{1.5x}Fe_{2-x}O_4$ nanoparticles, *Appl. Phys. A: Mater. Sci. Process.*, 2019, **125**, 731.

304 C. Singh, A. Goyal and S. Singhal, Nickel-doped cobalt ferrite nanoparticles: efficient catalysts for the reduction of nitroaromatic compounds and photo-oxidative degradation of toxic dyes, *Nanoscale*, 2014, **6**, 7959–7970.

305 C. R. Vestal and Z. J. Zhang, Synthesis of $CoCrFeO_4$ nanoparticles using microemulsion methods and size-dependent studies of their magnetic properties, *Chem. Mater.*, 2002, **14**, 3817–3822.

306 C. R. Vestal and Z. J. Zhang, Magnetic spinel ferrite nanoparticles from microemulsions, *Int. J. Nanotechnol.*, 2004, **1**, 240–263.

307 M. M. Baig, M. A. Yousuf, M. F. Warsi, P. O. Agboola, M. Sher and I. Shakir, Surfactant assisted synthesis of rare earth Dy^{3+} substituted $MnFe_2O_4$ nanoparticles, *Ceram. Int.*, 2019, **45**, 18014–18022.

308 S. Tajik and S. Khodabakhshi, Novel and feasible synthetic routes to copper ferrite nanoparticles: Taguchi optimization and photocatalytic application, *J. Mater. Sci.: Mater. Electron.*, 2016, **27**, 5175–5182.

309 R. Ali, M. A. Khan, A. Manzoor, M. Shahid, S. Haider, A. S. Malik, M. Sher, I. Shakir and M. FarooqWarsi, Investigation of structural and magnetic properties of Zr-Co doped nickel ferrite nanomaterials, *J. Magn. Magn. Mater.*, 2017, **429**, 142–147.

310 I. Ali, M. U. Islam, M. N. Ashiq, M. A. Iqbal, N. Karamat, M. S. Awan and S. Naseem, Role of Tb-Mn substitution on the magnetic properties of Y-type hexaferrites, *J. Alloys Compd.*, 2014, **599**, 131–138.

311 T. Koutzarova, S. Kolev, C. Ghelev, I. Nedkov, B. Vertruen, R. Cloots, C. Henrist and A. Zaleski, Differences in the structural and magnetic properties of nanosized barium hexaferrite powders prepared by single and double microemulsion techniques, *J. Alloys Compd.*, 2013, **579**, 174–180.

312 T. Koutzarova, S. Kolev, K. Grigorov, C. Ghelev, A. Zaleski, R. E. Vandenberghe, M. Ausloos, C. Henrist, R. Cloots and I. Nedkov, in *Nanostructured Materials, Thin Films and*

Hard Coatings for Advanced Applications, ed. L. Kolakieva and R. Kakanakov, 2010, vol. 159, pp. 57–62.

313 V. Pillai, P. Kumar, M. S. Multani and D. O. Shah, Structure and magnetic-properties of nanoparticles of barium ferrite synthesized using microemulsion processing, *Colloids Surf., A*, 1993, **80**, 69–75.

314 G. Murtaza, R. Ahmad, T. Hussain, R. Ayub, I. Ali, M. A. Khan and M. N. Akhtar, Structural and magnetic properties of Nd-Mn substituted Y-type hexaferrites synthesized by microemulsion method, *J. Alloys Compd.*, 2014, **602**, 122–129.

315 M. Baghbanzadeh, L. Carbone, P. D. Cozzoli and C. O. Kappe, Microwave-assisted synthesis of colloidal inorganic nanocrystals, *Angew. Chem., Int. Ed.*, 2011, **50**, 11312–11359.

316 Y. Li and W. Yang, Microwave synthesis of zeolite membranes: A review, *J. Membr. Sci.*, 2008, **316**, 3–17.

317 C. O. Kappe, Controlled microwave heating in modern organic synthesis, *Angew. Chem., Int. Ed. Engl.*, 2004, **43**, 6250–6284.

318 S. A. Galema, Microwave chemistry, *Chem. Soc. Rev.*, 1997, **26**, 233–238.

319 L. Perreux and A. Loupy, A tentative rationalization of microwave effects in organic synthesis according to the reaction medium, and mechanistic considerations, *Tetrahedron*, 2001, **57**, 9199–9223.

320 A. de la Hoz, A. Diaz-Ortiz and A. Moreno, Microwaves in organic synthesis. Thermal and non-thermal microwave effects, *Chem. Soc. Rev.*, 2005, **34**, 164–178.

321 C. Gabriel, S. Gabriel, E. H. Grant, B. S. J. Halstead, P. Michael and D. Mingos, Dielectric parameters relevant to microwave dielectric heating, *Chem. Soc. Rev.*, 1998, **27**, 213–223.

322 S. Horikoshi, F. Sakai, M. Kajitani, M. Abe and N. Serpone, Microwave frequency effects on the photoactivity of TiO_2: Dielectric properties and the degradation of 4-chlorophenol, bisphenol A and methylene blue, *Chem. Phys. Lett.*, 2009, **470**, 304–307.

323 Y. J. Zhu and F. Chen, Microwave-assisted preparation of inorganic nanostructures in liquid phase, *Chem. Rev.*, 2014, **114**, 6462–6555.

324 M. B. Schütz, L. Xiao, T. Lehnen, T. Fischer and S. Mathur, Microwave-assisted synthesis of nanocrystalline binary and ternary metal oxides, *Int. Mater. Rev.*, 2017, **63**, 341–374.

325 S. Komarneni, M. C. D'Arrigo, C. Leonelli, G. C. Pellacani and H. Katsuki, Microwave-Hydrothermal Synthesis of Nanophase Ferrites, *J. Am. Ceram. Soc.*, 1998, **81**, 3041–3043.

326 S. W. Cao, Y. J. Zhu, G. F. Cheng and Y. H. Huang, $ZnFe_2O_4$ nanoparticles: microwave-hydrothermal ionic liquid synthesis and photocatalytic property over phenol, *J. Hazard. Mater.*, 2009, **171**, 431–435.

327 Y. H. Choi, E. C. Ra, E. H. Kim, K. Y. Kim, Y. J. Jang, K. N. Kang, S. H. Choi, J. H. Jang and J. S. Lee, Sodium-Containing Spinel Zinc Ferrite as a Catalyst Precursor for the Selective Synthesis of Liquid Hydrocarbon Fuels, *ChemSusChem*, 2017, **10**, 4764–4770.

328 L. Wu, H. Yao, B. Hu and S.-H. Yu, Unique Lamellar Sodium/Potassium Iron Oxide Nanosheets: Facile Microwave-Assisted Synthesis and Magnetic and Electrochemical Properties, *Chem. Mater.*, 2011, **23**, 3946–3952.

329 M. J. Williams, E. Sánchez, E. R. Aluri, F. J. Douglas, D. A. MacLaren, O. M. Collins, E. J. Cussen, J. D. Budge, L. C. Sanders, M. Michaelis, C. M. Smales, J. Cinatl, S. Lorrio, D. Krueger, R. T. M. de Rosales and S. A. Corr, Microwave-assisted synthesis of highly crystalline, multifunctional iron oxide nanocomposites for imaging applications, *RSC Adv.*, 2016, **6**, 83520–83528.

330 T. Caillot, D. Aymes, D. Stuerga, N. Viart and G. Pourroy, Microwave flash synthesis of iron and magnetite particles by disproportionation of ferrous alcoholic solutions, *J. Mater. Sci.*, 2002, **37**, 5153–5158.

331 E. Solano, C. Frontera, T. Puig, X. Obradors, S. Ricart and J. Ros, Neutron and X-ray diffraction study of ferrite nanocrystals obtained by microwave-assisted growth. A structural comparison with the thermal synthetic route, *J. Appl. Crystallogr.*, 2014, **47**, 414–420.

332 R. Sai, S. D. Kulkarni, K. J. Vinoy, N. Bhat and S. A. Shivashankar, $ZnFe_2O_4$: Rapid and sub-100 °C synthesis and anneal-tuned magnetic properties, *J. Mater. Chem.*, 2012, **22**, 2149–2156.

333 F. Bensebaa, F. Zavaliche, P. L'Ecuyer, R. W. Cochrane and T. Veres, Microwave synthesis and characterization of Co-ferrite nanoparticles, *J. Colloid Interface Sci.*, 2004, **277**, 104–110.

334 J. Giri, T. Sriharsha and D. Bahadur, Optimization of parameters for the synthesis of nano-sized $Co_{1-x}Zn_xFe2O4$, ($0 \leq x \leq 0.8$) by microwave refluxing, *J. Mater. Chem.*, 2004, **14**, 875–880.

335 Z. Kozakova, I. Kuritka, N. E. Kazantseva, V. Babayan, M. Pastorek, M. Machovsky, P. Bazant and P. Saha, The formation mechanism of iron oxide nanoparticles within the microwave-assisted solvothermal synthesis and its correlation with the structural and magnetic properties, *Dalton Trans.*, 2015, **44**, 21099–21108.

336 A. Garzón-Manjón, E. Solano, M. de la Mata, R. Guzmán, J. Arbiol, T. Puig, X. Obradors, R. Yáñez, S. Ricart and J. Ros, Induced shape controllability by tailored precursor design in thermal and microwave-assisted synthesis of Fe_3O_4 nanoparticles, *J. Nanopart. Res.*, 2015, **17**, 291.

337 E. Bartolomé, P. Cayado, E. Solano, S. Ricart, J. Gázquez, B. Mundet, M. Coll, T. Puig, X. Obradors, M. Valvidares, J. Herrero-Martín, P. Gargiani and E. Pellegrin, Magnetic stability against calcining of microwave-synthesized $CoFe_2O_4$ nanoparticles, *New J. Chem.*, 2016, **40**, 6890–6898.

338 E. Solano, L. Perez-Mirabet, F. Martinez-Julian, R. Guzmán, J. Arbiol, T. Puig, X. Obradors, R. Yañez, A. Pomar, S. Ricart and J. Ros, Facile and efficient one-pot solvothermal and microwave-assisted synthesis of stable

colloidal solutions of MFe_2O_4 spinel magnetic nanoparticles, *J. Nanopart. Res.*, 2012, **14**, 1034.

339 T. Schneider, A. Löwa, S. Karagiozov, L. Sprenger, L. Gutiérrez, T. Esposito, G. Marten, K. Saatchi and U. O. Häfeli, Facile microwave synthesis of uniform magnetic nanoparticles with minimal sample processing, *J. Magn. Magn. Mater.*, 2017, **421**, 283–291.

340 J. Nandhini, P. Neeraja, S. Rex Jeya Rajkumar, V. Umapathy and S. Suresh, Comparative Studies of Microwave and Sol–Gel-Assisted Combustion Methods of $NiFe_2O_4$ Nanostructures: Synthesis, Structural, Morphological, Opto-magnetic, and Antimicrobial Activity, *J. Supercond. Novel Magn.*, 2016, **30**, 1213–1220.

341 S. Javadi, S. M. Masoudpanah and A. Zakeri, Conventional versus microwave combustion synthesis of $CoFe_2O_4$ nanoparticles, *J. Sol-Gel Sci. Technol.*, 2016, **79**, 176–183.

342 I. Bilecka, M. Kubli, E. Amstad and M. Niederberger, Simultaneous formation of ferrite nanocrystals and deposition of thin films via a microwave-assisted nonaqueous sol–gel process, *J. Sol-Gel Sci. Technol.*, 2010, **57**, 313–322.

343 C. Suchomski, B. Breitung, R. Witte, M. Knapp, S. Bauer, T. Baumbach, C. Reitz and T. Brezesinski, Microwave synthesis of high-quality and uniform 4 nm $ZnFe_2O_4$ nanocrystals for application in energy storage and nanomagnetics, *Beilstein J. Nanotechnol.*, 2016, **7**, 1350–1360.

344 O. Pascu, M. Gich, G. Herranz and A. Roig, 2D Magnetic Frames Obtained by the Microwave-Assisted Chemistry Approach, *Eur. J. Inorg. Chem.*, 2012, **2012**, 2656–2660.

345 L. F. da Silva, W. Avansi, M. L. Moreira, J. Andrés, E. Longo and V. R. Mastelaro, Novel $SrTi_{1-x}Fe_xO_3$ nanocubes synthesized by microwave-assisted hydrothermal method, *CrystEngComm*, 2012, **14**, 4068–4073.

346 J. Martynczuk, M. Arnold, H. Wang, J. Caro and A. Feldhoff, How $(Ba_{0.5}Sr_{0.5})(Fe_{0.8}Zn_{0.2})O_{3-\delta}$ and $(Ba_{0.5}Sr_{0.5})(Co_{0.8}Fe_{0.2})O_{3-\delta}$ perovskites form via an EDTA/citric acid complexing method, *Adv. Mater.*, 2007, **19**, 2134–2140.

347 K. Chybczynska, M. Blaszyk, B. Hilczer, T. Lucinski, M. Matczak and B. Andrzejewski, PEG-controlled thickness of $BiFeO_3$ crystallites in microwave hydrothermal synthesis, *Mater. Res. Bull.*, 2017, **86**, 178–185.

348 S. Li, G. Zhang, H. Zheng, N. Wang, Y. Zheng and P. Wang, Microwave-assisted synthesis of $BiFeO_3$ nanoparticles with high catalytic performance in microwave-enhanced Fenton-like process, *RSC Adv.*, 2016, **6**, 82439–82446.

349 J. Huang, G. Tan, W. Yang, L. Zhang, H. Ren and A. Xia, Microwave hydrothermal synthesis of $BiFeO_3$: Impact of different surfactants on the morphology and photocatalytic properties, *Mater. Sci. Semicond. Process.*, 2014, **25**, 84–88.

350 G. Kolhatkar, F. Ambriz-Vargas, B. Huber, R. Thomas and A. Ruediger, Thermionic Emission Based Resistive Memory with Ultrathin Ferroelectric $BiFe_{1-x}Cr_xO_3$ Films Deposited by Mineralizer-Free Microwave-Assisted Hydrothermal Synthesis, *Cryst. Growth Des.*, 2018, **18**, 1864–1872.

351 J. M. Byrne, V. S. Coker, E. Cespedes, P. L. Wincott, D. J. Vaughan, R. A. D. Pattrick, G. van der Laan, E. Arenholz, F. Tuna, M. Bencsik, J. R. Lloyd and N. D. Telling, Biosynthesis of zinc substituted magnetite nanoparticles with enhanced magnetic properties, *Adv. Funct. Mater.*, 2014, **24**, 2518–2529.

352 S. H. Xiao, W. F. Jiang, L. Y. Li and X. J. Li, Low-temperature auto-combustion synthesis and magnetic properties of cobalt ferrite nanopowder, *Mater. Chem. Phys.*, 2007, **106**, 82–87.

353 S. Diodati, L. Nodari, M. M. Natile, A. Caneschi, C. de Julián Fernández, C. Hoffmann, S. Kaskel, A. Lieb, V. Di Noto, S. Mascotto, R. Saini and S. Gross, Coprecipitation of oxalates: an easy and reproducible wet-chemistry synthesis route for transition metal ferrites., *Eur. J. Inorg. Chem.*, 2014, 875–887.

354 J. Gass, H. Srikanth, N. Kislov, S. S. Srinivasan and Y. Emirov, Magnetization and magnetocaloric effect in ball-milled zinc ferrite powder, *J. Appl. Phys.*, 2008, **103**, 07B309.

355 M. Ghaffari, P. Y. Tan, M. E. Oruc, O. K. Tan, M. S. Tse and M. Shannon, Effect of ball milling on the characteristics of nanostructure $SrFeO_3$ powder for photocatalytic degradation of methylene blue under visible light irradiation and its reaction kinetics, *Catal. Today*, 2011, **161**, 70–77.

356 R. M. Glaister, N. A. Allen and N. J. Hellicar, Comparison of methods for preparing fine ferrite powders, *Proc. Br. Ceram. Soc.*, 1965, (3), 67–80.

357 V. G. Harris, D. J. Fatemi, J. O. Cross, E. E. Carpenter, V. M. Browning, J. P. Kirkland, A. Mohan and G. J. Long, One-step processing of spinel ferrites via the high-energy ball milling of binary oxides, *J. Appl. Phys.*, 2003, **94**, 496–501.

358 D. Chen and H.-y. Liu, One-step synthesis of nickel ferrite nanoparticles by ultrasonic wave-assisted ball milling technology, *Mater. Lett.*, 2012, **72**, 95–97.

359 D. Chen, H. y. Liu and L. Li, One-step synthesis of manganese ferrite nanoparticles by ultrasonic wave-assisted ball milling technology, *Mater. Chem. Phys.*, 2012, **134**, 921–924.

360 M. A. Gabal, A. A. Al-Juaid, S. M. Al-Rashed, M. A. Hussein and F. Al-Marzouki, Synthesis, characterization and electromagnetic properties of Zn-substituted $CoFe_2O_4$ via sucrose assisted combustion route, *J. Magn. Magn. Mater.*, 2017, **426**, 670–679.

361 S. A. Saafan, S. T. Assar and S. F. Mansour, Magnetic and electrical properties of $Co_{1-x}Ca_xFe_2O_4$ nanoparticles synthesized by the auto combustion method, *J. Alloys Compd.*, 2012, **542**, 192–198.

362 A. Sutka and G. Mezinskis, Sol-gel auto-combustion synthesis of spinel-type ferrite nanomaterials, *Front. Mater. Sci.*, 2012, **6**, 128–141.

363 F. Deganello, L. F. Liotta, A. Longo, M. P. Casaletto and M. Scopelliti, Cerium effect on the phase structure, phase stability and redox properties of Ce-doped strontium ferrates, *J. Solid State Chem.*, 2006, **179**, 3406–3419.

